People's Democratic Republic of Algeria

Ministry of Higher Education and Scientific Research

Université SAAD DAHLEB Blida 01

Institute of Aeronautics and Space Studies
Aircraft Construction Department

Graduation thesis

In order to obtain the diploma of

Master's Degree in Aeronautics

Option: Propulsion

THEME

CFD Simulation of Von Kármán Vortex Street Formation Around Different Geometric Bodies

Proposed by:

Promoter Mr. ABADA Omar

Co- Promoter Mr. BENTRAD Houcine

Directed by:

DABOU Taha Yacine

Promotion 2023/2024

Acknowledgement

I would like to take this opportunity to express our sincere gratitude and appreciation to our esteemed Research Director, **Mr. Abada Omar**, for his invaluable guidance and support throughout the entire thesis process. His expertise, dedication, and unwavering commitment to our research were instrumental in the successful completion of this project. His insightful comments, constructive criticism, and willingness to go above and beyond have greatly enriched the quality of our work. Dear Professor, successes are people who appreciate their meaning, and creativity has people who reap it. Therefore, we appreciate your strenuous efforts. You are worthy of thanks and appreciation, so we must appreciate you. You have all our praise and appreciation.

I am truly grateful for his guidance and the opportunity to learn from his extensive knowledge and experience.

We would also like to express our sincere thanks to our Associate Research Director, **Mr**. **Bentrad Houcine**, for his unwavering support and assistance during the various challenges faced throughout our research journey. His steady presence and willingness to lend a helping hand were invaluable in overcoming obstacles and finding innovative solutions. His commitment to our project and insightful suggestions played a pivotal role in shaping the direction and results of my research. I am extremely grateful for his dedication and the spirit of cooperation that he brought with him.

Also, let us not forget the two distinguished professors, **Sbaa laazeb and Bekhti Ahmed** who did not spare me any information they had in the CFD, and their dedication and great mastery of this equipment. I extend my sincere thanks to you both.

I would like to express my sincere thanks to the commandant of higher school of aeronautics techniques and the colonel **BelKalouche**, who facilitated the use of the laboratory on aerodynamics and heat transfer in order to complete my research.

Finally, to the director of the Institute, Professor **Benkhedda Amina**, and all the professors and doctors who did not spare us any information, I would like to thank you for your great efforts. You have the most beautiful bouquets of thanks scented with roses.

الاهداء

الحمد لله على تمام الرحله لم تكن الرحلة قصيرة ولا ينبغي لها أن تكون لم يكن الحلم قريبا ولا الطريق محفوفاً بالتسهيلات لكنني فعلتها ونلتها وارفع قبع التخرج لمرارة الرحلة

"من قال أنا لها "نالها
.وإن أبت رغماً عنها أتيت بها
(و آخر دَعْوَاهُمْ أَنِ الحَمْدُ للهِ رَبِّ الْعَالَمِينَ)

إلى "والداي رفقاء الرحله عبدوا الطريق إلي بهم استندت وحاولت الوصول إلى من كانوا دواء قبل أن يكون لي داء ... والي من جمل أسمي بأجمل الألقاب ذالك الرجل العظيم الذي علمني أن الدنيا كفاح وسلاحها العلم والتعلم، إلى من كلل العرق جبينه و وعلمني ان النجاح لا يأتي إلا بالصبر والإصرار ... إلى شمعتي في الليالي المظلمات ، إلى ملاكي الطاهر إلى من أحتضنت اسمي بين كفيها وفرشت لي الطريق للوصول ها أنا الآن وصلت ويضيق الكلام عند شكركم لم يفي الكلام فعلكم إلى من بهم أسقيت حتى أثمرت وهديكم ثمره سقياكم "والداي " لطالما تمنيت أن اقرن
عينكم بنجاحي
كنتم أرضي الصلبة وجداري المتين ... مشاجعيني الذي لطالما أوفحمتم لا أجلي وقطعتم المسافات

لأعطاني جرعه الأمل لم تكن جرعه داء... الذين لا يحبطوني ويؤمنون بقدراتي مهما ضعفت

وأرتخيت واقفين خلفي مثل ظلاً مهما كثرت تخبطاتي
***

رفيقة الدرب أختي الحبيبة إلى

من بها ازالت عقبات الطريق ... ضماد الروح

دواء الجروح ضحكتي الدائمة سندي ومتكاي
(اختي هبة الرحمان)

***

رفقاء السنين وأصحاب الشدائد

والأزمات ... بهم أتشفى وأنسى الطريق

وبهم أكتمل لذة الوصول
(اخواني هيثم وعبد المهيمن)

Abstract

the flow around seven shapes (circle, semi -circle, rectangle, triangle, flat plate and two airfoils) and a circle with slits has been investigated numerically (using OpenFOAM and fluent). The main purpose of this study is to show the effect of the geometer and slits respectively on the vortex detachment behind a smooth shape, and stationary using the finite element approach to solve the fluid governing equations system at Re = 20,100,200 and 1000 The variation of the contact surface, the geometer and the spacing ratio (D/S) of the slit is strongly influence both the various physical parameters and the vortex detachment behind a circle.

The second part in this study is to determine the drag coefficient for four shapes (circle ,semi-circle ,flat plate and NACA0040) has been investigated numerically (using fluent) and compare the numerical results with the experimental one (wind tunnel) and we can talk about the electric power generation by the VIV phenomenon we get that their creation depends on the number of frequency and the amplitude of the vibration, which gave us the smooth circle with larger vibrations and larger amplitudes. There is no doubt that it is one of the new solutions in light of the exhaustion of non-renewable energies.

ملخص

تم دراسة تدفق الرياح حول سبعة أشكال (دائرة، نصف دائرة، مستطيل، مثلث، لوح مسطح وجنيحين) ودائرة بها شقوق (باستخدام OpenFOAM وfluent). الغرض الرئيسي من هذه الدراسة هو إظهار تأثير السطح والشقوق على التوالي على انفصال الدوامة خلف شكل أملس وثابت باستخدام نهج العناصر المحدودة لحل نظام معادلات التحكم في السوائل عند Re = 20،100،200 و1000.

يؤثر تغير سطح التلامس والهندسة ونسبة التباعد (D/S) للشق بشكل كبير على كل من المعلمات الفيزيائية المختلفة وانفصال الدوامة خلف الدائرة.

الجزء الثاني في هذه الدراسة هو تحديد معامل السحب لاربعة اشكال (الدائرة ونصف الدائرة واللوح المسطح وNACA0040) وقد تم دراستها عدديا (باستخدام Fluent) ومقارنة النتائج العددية مع النتائج التجريبية (نفق الرياح) ويمكننا الحديث عن توليد الطاقة الكهربائية بواسطة ظاهرة VIV فنجد ان انشائها يعتمد على عدد الترددات وسعة الاهتزاز مما اعطانا الدائرة الملساء ذات الاهتزازات الاكبر والسعة الاكبر ولا شك انها من الحلول الجديدة في ظل استنفاد الطاقات غير المتجددة.

Summary

Figures list

Tables list

Nomenclature

Notations Usual:

m : mass of the fluid (Kg)

P:: time(s)

f : frequencies (HZ)

$\vec{v}$: velocity vector

$\vec{n}$unit vector normal to a surface element s : elementary surface (m2)

P: local fluid pressure (Kg/ms2)

u : axial component of the velocity vector (m/s)

V : vertical component of the velocity (m/s)

x, y : the Cartesian coordinates

X, Y: dimensionless coordinates

V : the volume of the control volume

$\vec{A}$: the vector the area of the surface

SΦ : the source term (the source of Φ per unit volume)

Nfaces : The number of faces (interfaces) in the control volume

νf : the mass flow through the interface f

Af : l'aire de l'interface f

μ: dynamic viscosity (N.s/m2)

Φ : viscous dissipation (N/s.m2)

ΓΦ **:** the diffusion coefficient of the quantity Φ

Φf **:** the value of Φ transferred by convection through the interface f

$(\vec{\nabla}\Phi)_n$ **:** the value of normal $\vec{\nabla}\Phi$ (perpendicular) to the interface f

Symbol Grecque :

ρ: Density (Kg/m3) Ω: Control volume (m3) Σ: Control area (m2)

μ: dynamic viscosity (N.s/m2)

Φ : viscous dissipation (N/s.m2)

ΓΦ **:** the diffusion coefficient of the quantity Φ

Φf **:** the value of Φ transferred by convection through the interface f

$(\vec{\nabla}\Phi)_n$ **:** the value of normal $\vec{\nabla}\Phi$ (perpendicular) to the interface *f*

Dimensionless numbers :

Re: Reynolds number

Cd : drag coefficients

Cl : coefficient de portance

St : numbers de Strouhal

Abbreviations

CFD	computational fluid dynamics
PIV	particle image velocimetry
2D	bidimensional
3D	Tridimensional
CAD	Computer-aided design

General introduction and bibliographical study

1. General Introduction

Fluid mechanics is a science that studies the behavior of fluids at rest and in motion. It is a science that has applications in several fields such as astrophysics, biomedicine, meteorology, geophysics, plasma physics, aerodynamics, hydraulics, turbomachinery and thermal equipment. Fluid mechanics is subdivided into several branches that are defined by the properties of fluids [1].

The development of aerodynamics followed that of other sciences such as computer science with the appearance of increasingly powerful computers, despite their cost, experimental techniques (wind tunnel tests) and of course, mathematics with their great progress and contribution in numerical techniques for the solution in fluid mechanics of generalized NAVIER STOKES equations [2].

In fact, all these advances are due to aerodynamics. This branch of fluid dynamics primarily involves the understanding and analysis of airflows, and about their effect on surrounding solid elements.

Its behavior is completely predicted by the Navier-Stokes equations for a compressible fluid. These partial differential equations are now numerically solved. As air is the seat of turbulent phenomena, the solution sought can only be unsteady, but the scales of the geometric structures encountered are so numerous that theoretical and numerical models must be imagined to capture these unsteady phenomena. including frictional force, lift force, torque and their distinctive properties.

Le travail effectué dans le cadre de mémoire de fin d'études porte justement sur l'écoulement autour de sphère avec comme objectif principal la réduction du coefficient de trainée. Différentes sphères ont été usinées puis soumises à des essais en soufflerie pour la détermination des coefficients de trainée et de pression à plusieurs nombres de Reynolds.

The objective of the present work is to study with a numerical simulation the aerodynamic behavior and the experimental work is then completed by a numerical simulation by ANSYS and OpenFOAM software of the flow around a sphere and several geometric shapes. One of the results obtained is compared to those obtained experimentally and the others with numerical results [41] and very small part on the problems of VIV and one of the solution to get it well

efficiency in the generation of electricity.

Chapter 1

In the first chapter, we reviewed and recalled the basic principles of aerodynamics and VIV in order to study the forces affected by geometric shapes, including frictional force, lift force, and their distinctive properties.

Chapter 2

Chapter two presents the mathematical modeling of the problem we have. Simplifying assumptions are cited, accompanied by a detailed study of the equations governing a viscous incompressible flow in steady state to measure fluid motions under boundary conditions.

Chapter 3

In the third chapter we mention the geometries studied and the method of numerical resolution of the airflow, from the creation of the geometry in ANSYS fluent and OpenFOAM and the generation of the mesh in CFD (ANSYS.24), through the parameterization of "Fluent" (ANSYS) to the simulation on OpenFOAM and after the resolution. The results of the numerical simulation will be interpreted and discussed. These will be represented in the form of graphs and contours.

Chapter 4

The fourth chapter concerns the designation of the parts and the printing according to the 3D printer for the design in SolidWorks software and smoothing it to obtain very good and close results with the experimental

Chapter 5

The fifth chapter concerns the aerodynamic study of our profile (numerical simulation on different bodies to determine the numerical coefficients and the St); and structural geometric shapes. Finally, we moved on to the comparison of the results. Numerical with the experimental results.

We ended our work with a general conclusion.

2. Bibliographic research

Research is directly linked to the evolution of technology; And this is what pushes researchers to move forward in very complicated and topical cases that can be treated with the help of a very powerful computer tool and with the most sophisticated and efficient experimental means. In order to broaden our knowledge in this field, we have made a reading of the other authors which can be summarized as follows:

P. ARDONCEAU, in (2009) developed a nodal procedure for numerical resolution of the Laplace equation applied to velocity-potential flows around load-bearing bodies. This method is based on the internal Direchlet conditions expressed at the nodes of the mesh rather than on smooth parts of the surface. Then an original Neumann-type formulation of the Kutta conditions is proposed. Expressed as a minimization of the velocity wall flux, it leads to a significant reduction in the impact of discretization on the estimation of overall forces compared to local formulations. The method is applicable to two- or three-dimensional, stationary or non-stationary flows.

F. Meddane et al (2007) studied the flow of fluid around an obstacle, such as a NACA 0021 profile wing. They showed that the use of the flap has a direct influence on the pressure distribution and thus on the aerodynamic forces of the profile

D.LIU et al, en (2012) numerically studied a two-dimensional viscous flow around a supercritical wing profile of type RAE2822 for different Reynolds numbers. The solution was passed on the solution of the two-dimensional Navier–Stokes equation with the use of the Spalart – Allmaras (SA) turbulence model. The results of the calculations on the RAE2822 wing are compared with the experimental results of the wind tunnel. The numerical processing performed for a Reynolds number range between 2 〖7〗^6 up to 2. 〖7〗^6, and for Mach number cases: 0.74 and 0.8 with a variable angle of incidence from 2° to 6°. The results show that the distribution of the upper surface pressure including the location and intensity of the shock waves and the pressure, apparently changed with Reynolds numbers, The numerical results obtained show that the effect of the Reynolds number must be considered when designing and optimizing the jumbo jets applied to the airfoils.

Madani and Abidat (2002) proposed an algorithm for solving the Navier-stokes equations, which uses a combination of two finite-difference schemes of order 0(h2) and 0(h4), to study unsteady flows around profiled bodies. The advantages in terms of computation time and accuracy of the proposed method have been highlighted.

Dal Jae Park et al (2007) experimentally investigated the effects of different obstructions formed on flame spread in a rectangular entrapment. Four different simple obstacles were used: rectangular, cylindrical, triangular and square cross-sections with clogging ratios of 5 and 10%. They used a high-speed video camera to study the interaction between a propagation flame and the obstacle. Time-resolved images of flame were observed.

The flame movement speeds, which are a function of the probability density, were obtained for the different obstacles. As the propagation flame encroaches on the obstacle, an increase in local velocity of propagation due to the expansion of the burned gas and the clogging of the obstacle was obtained.

This local increase in speed becomes greater as it goes from a circular obstacle to a triangular or square one. They found that the velocities measured with different clogging ratios for the same obstacle and reduced to an average flame displacement were not appreciably different from those studied in this work. However, they observed the increase in the fastest speed reduced to an average of flame.

Madani et Abidat (2002) Ont proposé un algorithme pour la résolution des équations de Navier-stokes, qui utilise une combinaison de deux schémas aux différences finies d'ordre 0(h2) et 0(h4), afin d'étudier les écoulements in stationnaires autour des corps profilés. Les Avantages en temps de calcul et en précision de la méthode proposée ont été mis en évidence.

F. Meddane et al (2007) Ont étudié l'écoulement de fluide autour d'un obstacle, telle une aile de profil NACA 0021. Ils ont montré que l'utilisation du volet a une la fluence directe sur la distribution de pression et donc sur les forces aérodynamiques du profil.

Ankur Bajoria (2008) A effectué un travail sur le flux de vent autour d'une plaque carrée. Le

logiciel ADINA qui utilise la méthode des éléments finis a été utilisé pour la simulation. Le modèle

De turbulence K-ε a été utilisé. Dans ce projet, il a augmenté le nombre de Reynolds pour diminuer la viscosité de 0,01 à 0,0001 N.s /m2 dans trois modèles différents. Cela aide à étudier l'effet de la non-linéarité et les différentes mesures requises pour que la solution converge.

Il a constaté que ces techniques utilisées par le logiciel ADINA permettent d'évaluer le débit en aval de la plaque. Cette analyse peut être appliquée pendant la phase de conception pour améliorer la structure aérodynamique et réduire les forces. Parmi les résultats obtenus, il a constaté qu'avec l'augmentation du nombre de Reynolds, les vortices en aval de la plaque augmentent parallèlement.

Merouane Salhi1 : The flow around a circle with slits has been investigated numerically. The main purpose of this study is to show the effect of the slits on the vortex detachment behind circle smooth, and
stationary using the finite element approach to solve the fluid governing equations system at Re = 200.The variation of the spacing ratio (D/S) of the slit is strongly influenced both the various physical parameters and the vortex detachment behind a circle. We found that the drag coefficient varies between 1.43 and 1.24 in the case of the horizontal slit and between 1.45 and 1.39 in the case of the vertical slit. In the case of the double horizontal-vertical slit, the values vary between 1.47 and 1.38. We also found that the values of the Strouhal number vary between 0.201 and 0.268 according to the spacing ratio (D/S) of the slit. A comparison was made with experimental works for the Strouhal number. The results are very important, and the error found is less than 7%.

Atul Kumar Sotia, Mark C. Thompsonb, John Sheridanb, Rajneesh Bhardwajc

Renewable energy sources are likely to become essential due to continuously increasing energy demands together with the depletion of natural resources that are currently used for power generation, such as coal and gas. They are also advantageous in terms of their reduced environmental impact. Here, the generation of electrical power from Vortex-Induced Vibration (VIV) of a circle is investigated numerically. The circle is free to oscillate in the direction transverse to the incoming flow.

Purpose of work

The aim of this work is to numerically study the phenomena of the stationary and two-dimensional turbulent flow, of the incompressible fluid on different bodies to determine all the aerodynamic parameters necessary to have the aerodynamic performance of each part.

In the two-dimensional case, a numerical simulation was made using the ANSYS calculation code. And OpenFoam to compare the different velocity and pressure fields as well as the Navier-Stokes phenomenon and observe the Van-Karman wake phenomenon between the flow around sphere, half-sphere and plate-plate obstacles (Trapezoidal shape). Flat plate, profile (NACA 0040), triangle and rectangle.

The experimental study was carried out at the level of the ECOLE SUPERIEUR TECHNIQUE DE L'AÉRONAUTIQUE. The thesis theme: CFD simulation on Von Karman vortex street of on different bodies geometric"

Department of Aeronautics (INSTITUTE OF AERONOTICS AND SPACE STUDIES). The numerical simulation was done using the SOLIWORKS 23 calculation code. The steady-state effect on flow was taken into account using Navier-Stokes.

In all the cases considered, satisfactory pressure and velocity fields, physical phenomena such as boundary layer development, friction coefficient variation and viscous model production area were all captured by this simulation.

The exploitation of the future of aerodynamics to do a little research on the phenomenon of VIV

Study design:

This work consists of five chapters as follows:

- the first chapter, we reviewed and recalled the basic principles of aerodynamics

- In the second chapter, we set out the mathematical equations that govern the physical phenomenon to be studied.

- The third chapter interprets the description of the problem and the procedure for solving the problem by software (ANSYS and OPENFOAM) with the choice of adequate meshes to simulate the flow in turbulent regimes for the seven geometric shapes at the base and high regimes.
- In the fourth chapter we talked about the wind tunnel and the experimental study of this piece and all the stages of this work
- In the fifth chapter, we present our numerical and experimental results and discuss the results found, then concluded with a general conclusion.

CHAPTER 1
GENERALS AERODYNAMICS

1.1. Introduction

Aerodynamics is the science of studying the movements of air around bodies. In other words, phenomena that come into play whenever there is a relative motion between a body and the air that surrounds it. The body can move in the stationary fluid (airplane in flight) or be fixed in the moving fluid (realization of geometric shapes for measurement in a wind tunnel).

A branch of fluid dynamics that deals with the understanding and analysis of airflows, as well as their effects on solid elements in the environment, these effects can naturally be caused by a stationary body subjected to a velocity of air flow or by a body moving through the atmosphere or by a combination of the two preceding propositions. The field of study can be subdivided into incompressible and compressible aerodynamics as a function of Mach number. [3].

There are also other branches related to fluid mechanics: hydraulics, hydrodynamics, aerodynamics, etc. A new approach has emerged in recent decades: Computational Fluid Dynamics (CFD), which simulates the flow of fluids by solving the equations that govern them using very powerful computers: supercomputers.

Fluid mechanics has many applications in various fields such as marine engineering, biomedicine, meteorology, hydraulics, geophysics, turbomachinery and aerodynamics [7].

1.2 Simplifying assumptions

We assume the flow is viscous, stationary (permanent) and turbulent (Navier-Stokes) and the (Von-Karman) phenomenon in (subcritical and critical), two-dimensional, criterion of (k-epsilon .2eqn), Newtonian

CHAPTER 1 GENERALITIES OF AERODYNAMICS

1.3. General information on aerodynamics

Aerodynamics is the science that studies the different aspects of the action of air in forces, pressures and moments that result from the placement of bodies in the atmosphere. Aerodynamics is mainly involved in the design of aircraft and missiles, defining their optimal shapes. However, studies conducted in aerodynamics on fluid recoil around airfoils are the subject of a very large development within NASA (National Aeronautics and Space Administration, USA) and ONERA (Office d'Etude et de Recherche Aerospatiale, France). At the current stage of research, the majority of the experimental resources deployed in these laboratories are computer-assisted, which leads to more precise and concrete results. [4].

1.3.1. Air

When a fluid moves around an object, it causes different phenomena of friction and turbulence, and to study these phenomena we call aerodynamics which is the "science of air movement". [5]

1.3.1.1. Existence

Air is the gaseous mixture that makes up the Earth's atmosphere. Like all gases, it is composed of molecules that are extremely mobile in relation to each other. It is invisible, which makes it easier to understand the phenomena related to the flight of the aircraft.

1.3.1.2 Physical Properties

-Air is compressible: it is possible to reduce its volume by compressing it

-Air is expandable: it tends to occupy an ever-increasing volume

-Air is elastic: resulting from the previous 2. That is to say, the air returns exactly to its original volume when it is placed back in the conditions that preceded compression or expansion. [6]

-Air is heavy: compared to other bodies, the weight of air remains low, however, it is already possible to determine the state of the ambient air by knowing the density, (denoted ρ, and expressed in kg.m3).

1.4. Flow

An umbrella term for the movement of air. In general, there are three types of flow, classified according to the behavior of the air particles

I.4.1 Laminar Flow

A flow is laminar when the movement of fluid particles occurs in a regular and orderly manner. The air streams follow straight and parallel paths with each other. They slide over each other, like blades of fluid. [7]

Figure 1. 1 : Laminar flow.

The air particles glide perfectly over each other without exchanging particles with each other. They follow a rectilinear and parallel movement.

1.4.1 Turbulent flow

A flow is turbulent when the displacement is irregular and random fluctuations in velocity are superimposed on the average motion of the fluid.

Figure 1. 2 : Turbulent flow

The air particles have trajectories that are almost parallel to each other, but which are no longer straight, while moving roughly in the same direction at the same speed.

I.4.2. Whirlpool flow

Turbulence disperses and mixes the environment in which it develops. Then it fades

away and disappears once the unity and homogeneity it has fostered has been produced.

Turbulence is present in many areas. In aeronautics, it is considered harmful since it is responsible for increasing drag and decreasing lift. [8]

The first characterizations of turbulence appeared at the end of the 19th century thanks to the scientist Osborne Reynolds. His work on flows in pipes allowed him to define a dimensionless number to which he gave his name.

He showed that above a critical value of this number, the flow radically changed its topology and dynamics. [4]. This number is defined in the following paragraph.

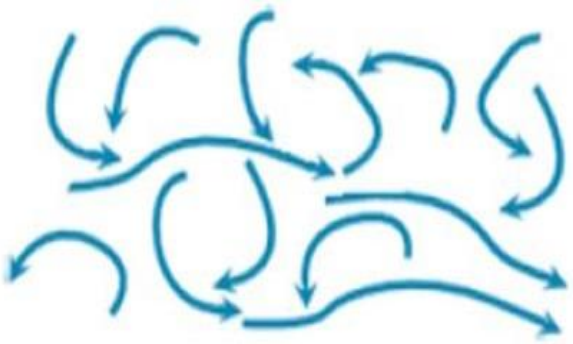

Figure 1. 3 : Whirlpool flow.

The flow is very disordered, the particles mix together and do not follow a straight or parallel path, and some particles can move up the current and thus form vortices. [9]

1.5. Aerodynamic forces

To be able to compare and test the capabilities, efficiency and aerodynamic quality of a wing airfoil

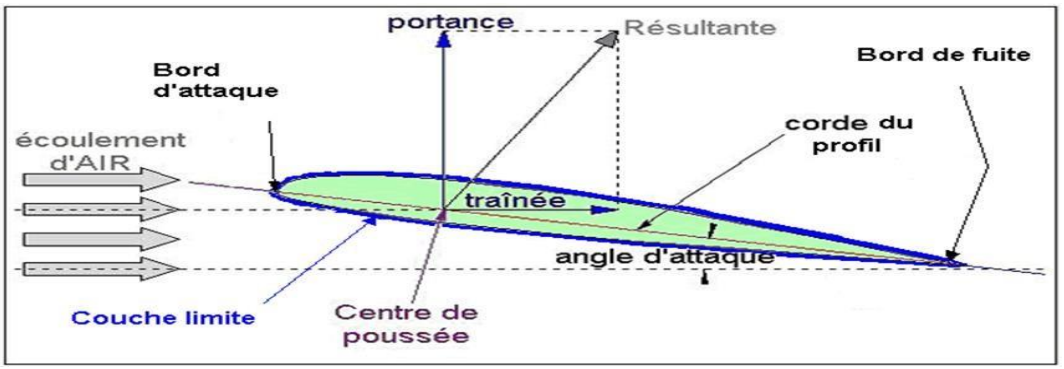

Figure 1. 4 : The resultant of aerodynamic forces.

Scientists have defined 2 vectors (lift and drag) that give the resultant of aerodynamic forces [10].

1.5.1 Lift force

The effect is that when a (usually asymmetrical) wing profile is placed in the direction and direction of the airflow, the airflow splits in half after touching the compression point (stop). Part of the airflow passes through the part above the wing and another part under the airfoil (lead-out). The airflow above the wing must be accelerated as it must cover a longer distance than the airflow under the wing. [14].

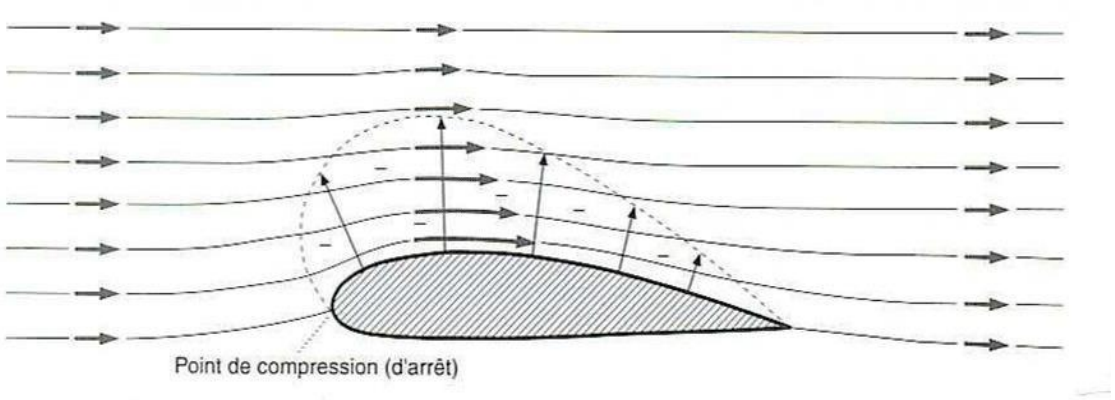

Figure 1. 5 : The flow of fluid around a wing profile.

According to Bernoulli's equation, an increase in velocity (dynamic pressure) leads to a decrease in static pressure. A pressure lower than the pressure of the surrounding air (static pressure) then occurs on the upper surface of the airfoil (upper surface), which then creates an upward force called lift.

Lift is defined by the following formula:

$$F_z = \frac{1}{2}\rho V^2 S C_z$$

ρ is the density of the air (in kg/m³)

S is the surface area of the wing. This is the total area of one of the surfaces. (In m²).

V is the velocity of the flow of air over the solid, and consequently the velocity of the solid. (m/s)

Cz is the lift coefficient.

1.5.2 Drag force

If the viscosity of the air did not exist, there would be no frictional force, there would only be pressure and vacuum forces, and the aerodynamic resultant would be perpendicular to

the relative wind. However, there is always a trail of out the expression and as follows

$$F_x = \frac{1}{2}\rho S C_x V^2$$

ρ: density of Pair in kg/m3.

S: wing area in m².

V: velocity in m/s.

Cx: airfoil lift coefficient.

1.5.2.1 Drag Type

Several categories of drag can be distinguished, but in reality, only the greatest contribution is that of friction, form and induced

1.5.2.2 Frictional drag

Frictional drag is caused by the viscosity of the air. Air molecules in contact with the surface of a body are slowed down by frictional forces. These forces are such that the velocity of the air streams is zero when in contact with the body. Frictional drag affects all parts of the aircraft. Its size varies with:

- the total surface area of the aircraft skin (wing, fuselage, empennage, etc.)
- boundary layer (laminar, turbulent)
- the roughness of the walls
- Relative wind speed
- the shape and thickness of the profile
- the angle of attack.

1.5.2.3 Form Trail (Airfoil)

As its name suggests, it is related to the shape of the profile, in fact, the flows are different depending on the profiles, and therefore the pressure differences between the leading edge and the trailing edge are not identical. The leading-edge pressure is higher than the trailing edge pressure due to slight detachment of the air threads at this level. [15].

To increase the drag force, we can add small wingtips, called Winglets Figure 1.6

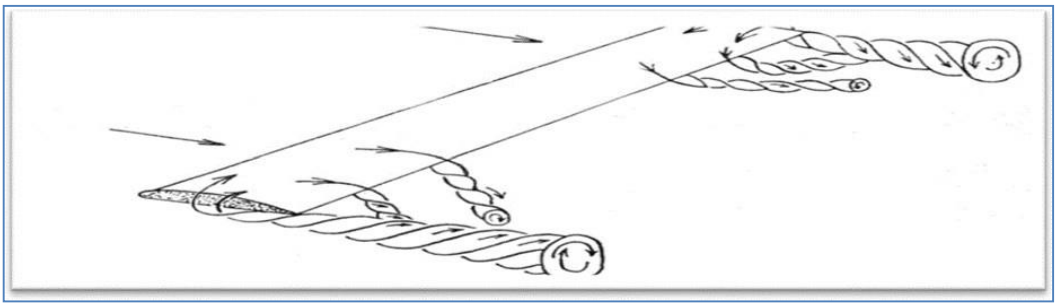

Figure 1. 6 : Marginal vortices.

1.5.2.4 Drag coefficient

The drag coefficient Cd is defined as a dimensionless number that provides information about the overall drag of any object, i.e. its ability to generate as little resistance as possible as it moves through the air. It is given by the following equation equivalent to the relation [11].

$$C_x = \frac{F_x}{\frac{1}{2}\rho v^2 S}$$

1.5.2.5 Pressure Coefficient

The distribution of pressure on a body is characterized by the dimensionless coefficient *Cx* defined by the relation

$$C_p = \frac{p - p_\infty}{\frac{1}{2}\rho_\infty v_\infty^2}$$

P is the static pressure and the index ∞ refers to the upstream infinity characteristics of the flow before it is disturbed by the presence of the obstacle.

1.6. Aerodynamic Moments

A force F exerted at the center of gravity of any solid body does not cause that body to rotate. If the point of application is moved away by a distance d, the aforementioned force produces an effect which will tend to cause the body to rotate: it is said to apply a moment (F x d) to the body in question.

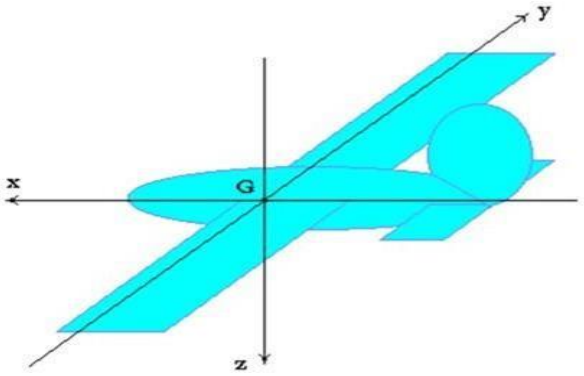

Figure 1. 7 : aerodynamic moments.

1.7 Air Resistance

1.7.1 Causes

Everybody in motion in the air is subjected by it to a resistance which tends to oppose this movement. This resistance has its origin in the properties of the air, but also depends on the characteristics of the body concerned (surface, shape, etc.). The pressure forces depend on the shape of the body and the position it occupies in relation to the direction of the relative velocity of the airflow. This action of the air results at each point on the surface of the body by:

- an elementary force of pressure perpendicular to the surface
- an elementary frictional force tangent to the surface

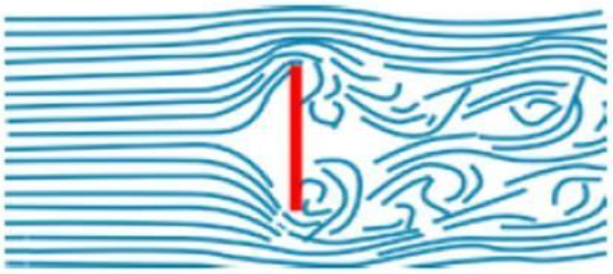

Figure 1. 8 : Air Resistance Flat Plate.

The frictional forces, due to the viscosity of the air, have an effect directly related to the extent of the surface of the body and also to the condition of this surface. By placing a flat plate perpendicular to the airflow, we find that the air exerts a strong pressure at the front, while at the back a depression is formed.

By installing a device (dynamometer) connected to the plate, we can measure this force exerted by the air and what are the factors that will cause it to vary. [16].

1.7.2. Factors Influencing Air Resistance

I.7.2.1 Area

If the area of the flat plate is doubled, the force measured by the dynamometer also doubles: The air resistance is proportional to the area.

I.7.2.2 Speed

By increasing the velocity of the flow, the force exerted by the air also increases: The air resistance is proportional to the square of the velocity

I.7.2.3 Density

The density of the air decreases with altitude, the air resistance will also decrease.
We can therefore deduce that: The air resistance is proportional to the density of the air.

1.7.2.4 Body Shape

By installing a device (dynamometer) connected to the plate, we can measure this force exerted by the air and what are the factors that will make it.
Air flow on a thin flat disc arranged parallel to the air threads is the seat of minimal resistance due simply to the friction of the air on both walls of the plate. [16]

Figure 1. 9 : Almost Zero Resistance Horizontal Cockroach Plate

By placing a flat disc perpendicular to the airflow of a wind tunnel, we find that the airflow struggles to get around the obstacle and that an overpressure is formed at the front and a depression at the rear with a vortex effect.

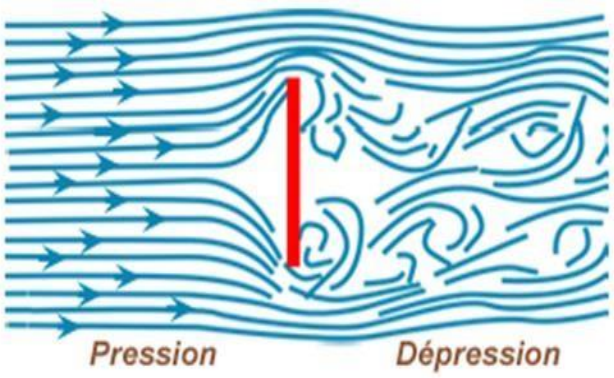

Figure 1. 10 : Air Resistance Flat Plate.

By adding a half-sphere to the front of the disc, we find that the air goes around the object better.

The overpressure decreases but there is still a depression and a vortex zone at the back.

Figure 1. 11 : Half-sphere resistance 75%.

If this half-sphere is completed to form a complete sphere, the flow is improved, the rear vortex zone is reduced, but not completely resorbed.

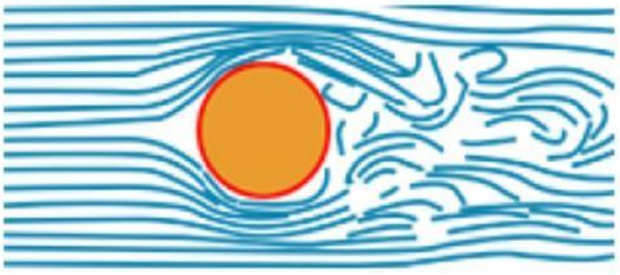

Figure 1. 12 : Resistance of the sphere 50

By stretching the back part of the sphere to substantially obtain the shape of an egg, we can see that the air threads meet at the back without creating vortices. The result is a tapered body.

Figure 1. 13 : Resistance in the form of NACA 15%.

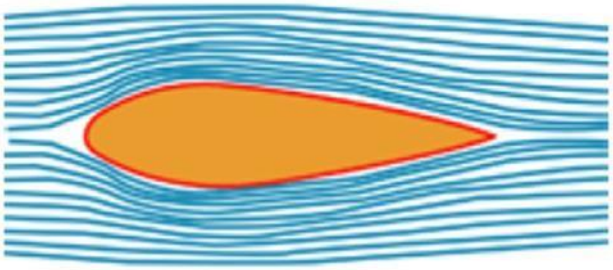

Figure 1. 14 : Profile shape resistance 5%.

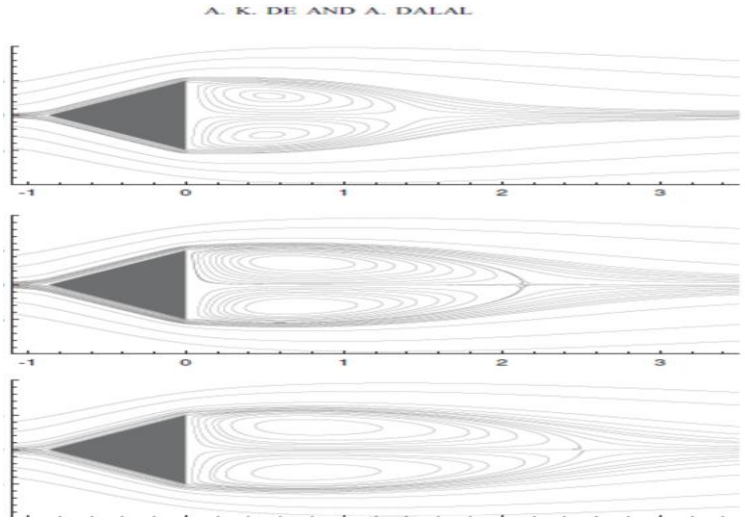

Figure 1. 15 : Streamlines on a Triangle in Transient Regime

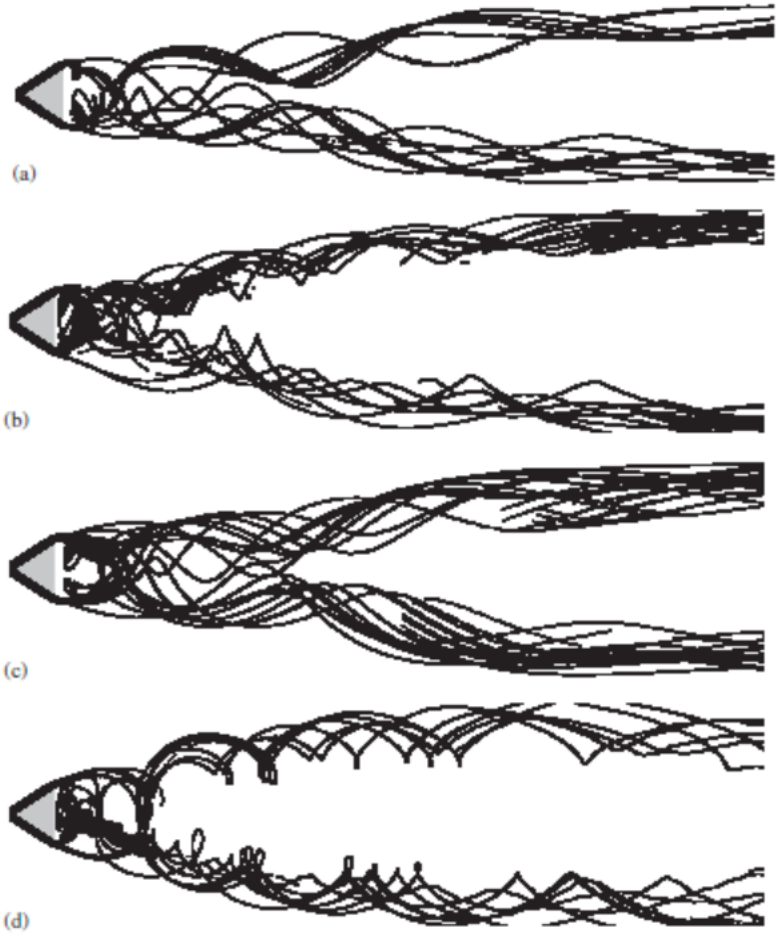

Figure 1. 16 : Van Karman effects on a Triangle in different Reynolds number

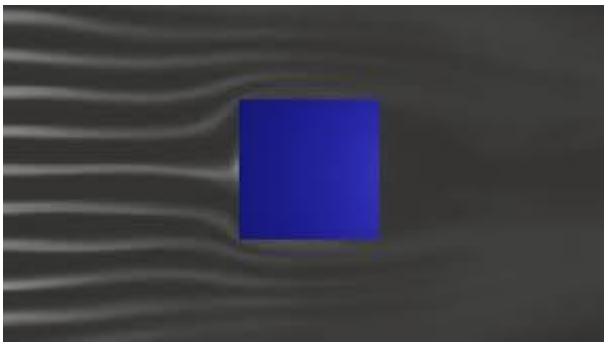

Figure 1. 17 : Streamlines on rectangle

1.8. Lift Coefficient

The lift coefficient represents the ratio of the lift force to the dynamic force of the flow, which is denoted Cd, and which depends on the angle of attack and the shape of the wing, as shown in the formula:

$$Rz = \frac{1}{2}\rho V^2 S Cz$$

The greater the angle of attack, the greater the Cd (see figure below). This coefficient increases to a maximum limit, the Cd max, after exceeding this value, i.e. the flow is no longer laminar but turbulent, this state is extremely dangerous.

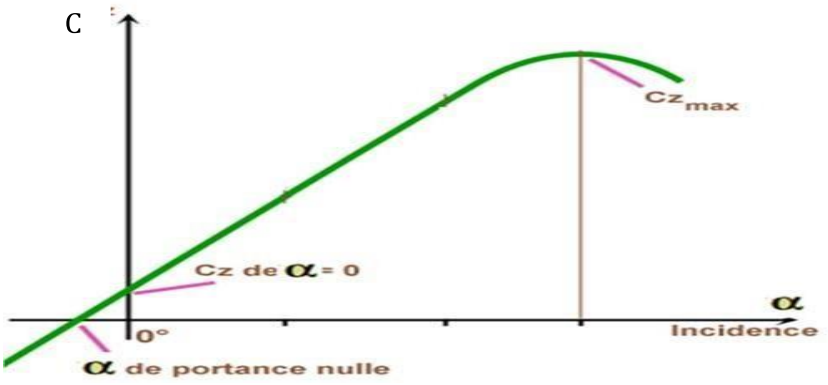

Figure 1. 18 : Lift coefficient

1.9 Reynolds number

This number characterizes a flow. It represents the ratio of inertial forces to viscous forces. It is the largest dimensionless number in fluid dynamics. It is proportional to the speed and length of the depth of the profile, but also to the density of the air. [17].

Here's the formula:

$$\mathrm{Re} = \frac{\rho V L}{\eta}$$

Or

$$\mathrm{Re} = \frac{LV}{\nu}$$

With

V - fluid velocity, [m/s]

L- Characteristic Dimension [m]

ν - kinematic viscosity of the fluid: ν , [m2/s]

ρ - density of fluid, [kg/m3]

1.10 Boundary layer around obstacles

1.10.1 Definition

When a fluid flow encounters an obstacle, due to friction on the surface of the obstacle and the viscosity of the flow, the velocity of the flow is equal to zero on the surface of the obstacle. Above this surface, the velocity of the flow gradually increases to a certain height where the velocity of the undisturbed flow is regained. This area of velocity gradient is called the boundary layer. The Figure shows an illustration of the boundary layer, which grows over an obstacle. [17]

There are two types of boundary layers: The laminar boundary layer is characterized by the fact that all velocities are parallel to the same plane, the flow is

then present in the form of air gaps sliding over each other. These blades remain straight for a certain length and then fade. Such a boundary layer is observed towards the leading edge of a profile.

The δ thickness of the boundary layer is conventionally called the distance from the wall from which the velocity V is such that: V = 0.99 Vo (Vo being the velocity that would exist if the air were non-viscosity). [18].

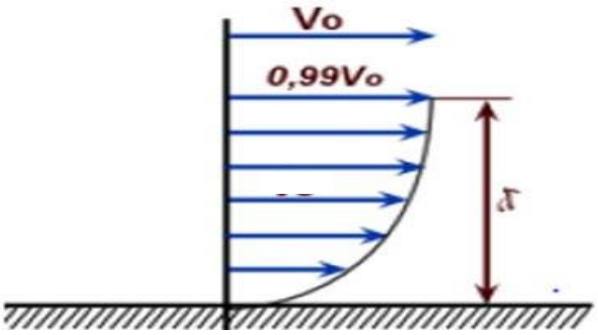

Figure 1. 19 : Boundary layer.

In fact, the blades disappear quite quickly and the flow is disorderly, partly due to the rough edges that still exist on the wall. The boundary layer becomes turbulent and the velocity vectors are no longer parallel to each other.

1.10.2 Laminar-Turbulent Boundary Layer Transition

In general, the mechanism of transition from laminar to turbulent state is the result of a nonlinear boundary layer response to perturbations.

The latter have different origins which can be the rate of turbulence of the free flow, the surface finish (roughness) or vibrations. Since Reynolds' experiments in 1883, the phenomena of laminar flow instability and the transition to turbulence have maintained a constant interest in fluid mechanics.

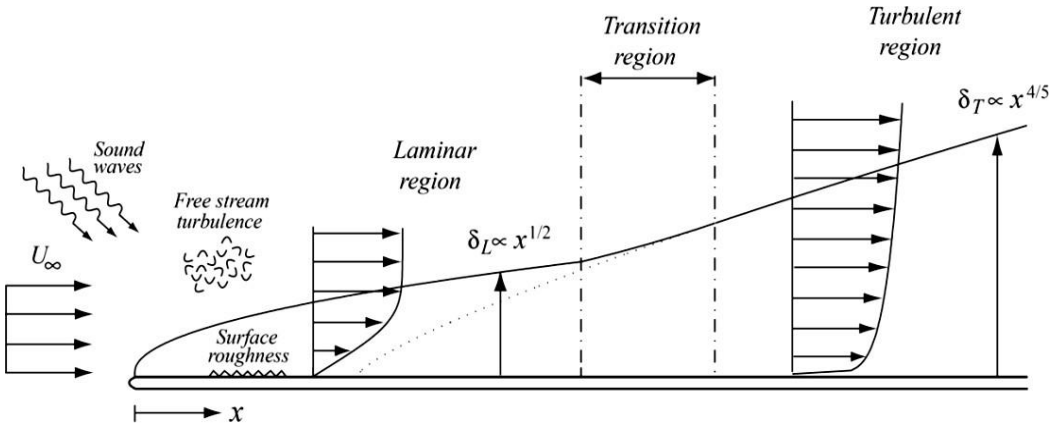

Figure 1. 20 : Boundary layer developing on a flat plate: transition from laminar to turbulent state. [5]

1.10.3 Boundary Layer Control

There are several different ways to classify detachment control methods to achieve desired results.

Gad-El-Hak [19] presents a classification of control based on the mode of operation of the actuator. The actuator is the mechanical, pneumatic, electrical, or acoustic device intended to interact with the flow to give it the desired behavior .

Figure 1. 21 : Régimes as a function of the experimental results of Rynolds.

Nombre de Reynolds	Régime d'écoulement	Forme de l'écoulement
Re→0	Ecoulement rampant	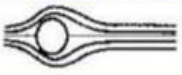
3-4<Re<30-40	Paire de vortex dans le sillage	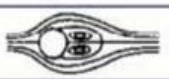
30-40<Re<80-90	Début de vortex de Karman	
80-90<Re<150-300	Purs vortex de Karman	
150-300<Re<10^5-1.3.10^5	Régime sub-critique	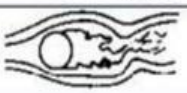

1.10.3.1 Active Control Systems

Active control works on the principle of velocity variation due to the porous layer compared to a surface boundary layer in the fluid domain.

At the boundary between the porous medium and a fluid, the local flow velocity is not zero. Thus, a porous medium acting as a wall on an object of study makes it possible to disturb the establishment of the boundary layer in the near wall, inducing a modification of the resulting downstream flow.

1.10.3.2 Passive Control Systems

The passive control system is a simple solution that takes the form of more or less discreet appendages, which allow a modification of the aerodynamic torso to be obtained. In automobiles, the best-known application is the rear aileron, in the shape of an inverted airplane wing profile, allowing an increase in downforce as speed increases. In this case, it is a question of increasing the lift of the vehicle to improve these handling characteristics.

The VG control then of small appendages in relation to the lengths of the object of study and arranged in a regular space, transversely to the reference flow. [20].

1.10.4 Boundary layer detachment

A detached flow is characterized by the presence of a recirculation zone in which velocities are low and energy losses are significant. That's why aerodynamicists try to limit its development.

In general, when an object is placed in a flow, the fluid threads follow the surface of the body: they "stick" to the wall. Under certain circumstances, these threads can detach from the wall, this is called detachment. This detachment, caused by a positive pressure gradient or by a geometric break in the wall, strongly influences aerodynamic performance. As a source of unsteady power, it can cause noise pollution or be the cause of structural vibrations: it has overall penalizing effects on the aerodynamic efficiency of vehicles.

In fact, detachment is a phenomenon that is sought to be avoided except in specific cases, such as the use of speed brakes on aircraft wings.

But in most cases, the goal is to reduce or even eliminate detachment. [21].

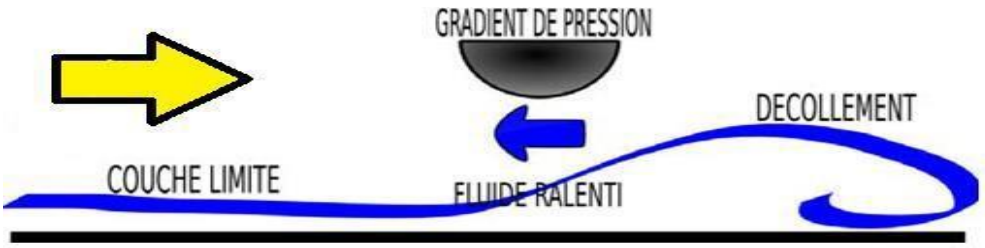

Figure 1. 22 : Boundary layer detachment

For example, when the boundary layer takes off, the pressure drag becomes high (Figure I.9.a) and the pour point of the small turbulent boundary layer is also the pressure drag is lower when the separation region is smaller. (Figure. I.19)

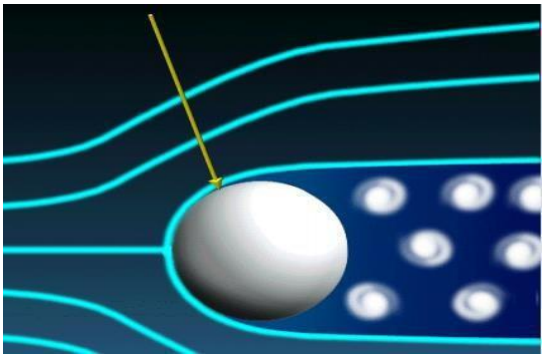

Figure 1. 23 : Detachment point for a laminar boundary layer

1.11 Vortex Shedding

One of the first to describe the vortex shedding phenomenon was Leonardo da Vinci by drawn some rather accurate sketches of the vortex formation in the flow behind bluff bodies. The formation of vortices in body wakes is described by Theodore von Karman (Ausoni, 2009). In fluid dynamics, vortex is district, in a fluid medium, where the flow, most of which revolve on the vortical flow axis, occurring either direct-axis or curved axis. In other words, vortex shedding occurs when the current flow of a water body is impaired by an obstruction, in this case a bluff body. Vortex or vortices are rotating or swirl, often turbulent fluid flow. Examples of a vortex or vortices appear in Figure 2.1. Speed is the largest at the center, and reduces graduallywith distance from the center

Figure 1. 24 24 Vortex created by the passage of aircraft wing, which is exposed by the colored smoke (Rafiuddin, 2008)

Vortex shedding has become a fundamental issue in fluid mechanics since shedding frequency Strouhal's measurement in 1878 and analysis of stability of the Von Karman vortex Street in 1911 (Chen & Shao, 2013). The phenomenon of vortex formation and shedding has been deeply study by many researchers included (Gandhiet al., 2004; Ausoni, 2009; Azman, 2008). In the natural vortex shedding and vortex- street appears established when stream flow cross a bluff body can be seen in Figure. 1.21. It has been observed that vortex shedding is unsteady flow which creates a separate stream throughout most of the surface and generally have three types of flow instability namely, boundary layer instability and separated shear layer instability (Gandhi et al., 2004).

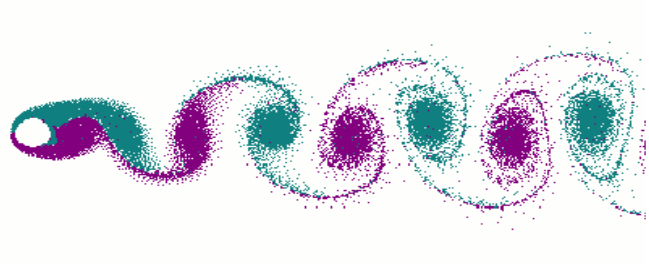

Figure 1. 25 Vortex spill evolving into a vortex street.

1.12 Von Karman Vortex Street

Von Karman Vortex is a term defining the periodic detachment of alternating pairs of vortices that bluff a body immersed in a flow of fluid, generating an upward sway, or Vortex Street, behind it, and causing fluctuating forces felt by the object. When a fluid flows over a two-dimensional, blunt body, vortices are created and spread alternately over the upper and lower body (Graebel, 2007; Bjswe et al., 2010). This phenomenon was initially symmetrical, but it later turned into a classic alternating pattern because the body is symmetrical. The Figure.

I.21 is a good representation of a common von Karman vortex street. This behavior was named Theodore Von Karman for his studies in the field. The Von Karman vortex street is a typical example of fluid dynamics of natural instabilities during the transition from laminar flow conditions to turbulent flow conditions. The Von Karman Vortex is a typical example of the dynamic fluid instability inherent in the transition from laminar flow to turbulent flow conditions.

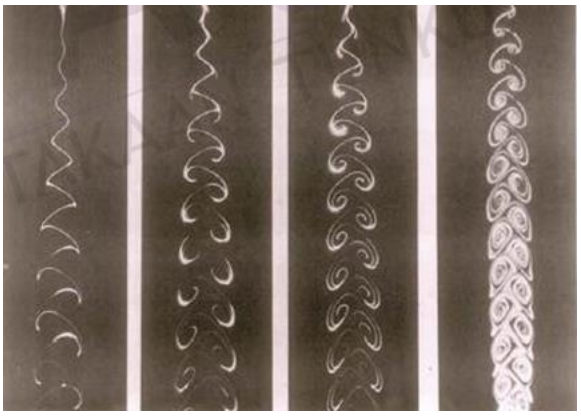

Figure 1. 26 Von Karman Vortex Street at increasing Reynolds Numbers

Vortex Street will only be considered in a given range of Reynolds numbers, usually above the Re limit of about 90. When the flow reaches Reynolds numbers between 40 and 200 in the wake of the circle, alternating vortices are emitted from the edges behind the circle. and slowly dissipates along the wake, as shown in the Figure. 1.22.

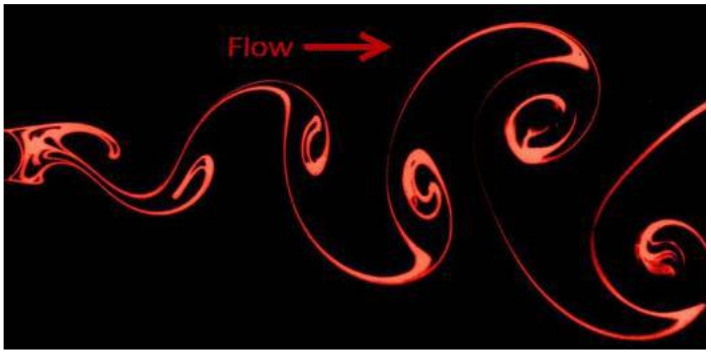

Figure 1. 27 Von Karman Vortex Street, the wake pattern behind a circle oscillating in Re = 140 (Aref et al., 2006; Azman, 200

1.12.1 Vortex shedding Frequency

After experimental Strouhal's introduced to determine the vortex shedding frequency, some appropriate methods that have been proposed in the technical literature. Shedding frequency, *f*, have been identified from the peak in the power spectrum and lift coefficients used to calculate the Strouhal number (Gonçalves et al., 1999). The frequency of vortex shedding becomes constant at lock-in and the free-stream velocity changes the value of the Strouhal number. Vortex shedding frequency is perpendicular to the direction of flow and has a period equal to the lift. Since the vortices are shed periodically, resulting in lift on the body also vary from time to time.

The Strouhal number (St) is a dimensionless proportionality constant between the main frequency vortex shedding and the free stream velocity divided by bluff-body dimensions. It is also often approximated by a constant value

1.13. The VIV (Vortex-Induced Vibration) as a source of generation electric power

Generating electric power using the vortex-induced vibration (VIV) phenomenon is an innovative approach that harnesses the energy from fluid flow, such as wind or water, interacting with a structure. Vortex shedding occurs when a fluid flows past a bluff body, creating alternating low-pressure vortices on the downstream side, causing the body to oscillate. And we have like example when we can use this important source like:

- ❖ Bluff Body: A cylindrical structure placed in a fluid flow.
- ❖ Mounting System: Flexible supports or springs allowing for oscillation.
- ❖ Energy Harvesting:

Magnets attached to the circle.

Coils positioned around the magnets.

- ❖ Power Electronics:

Rectifier to convert AC to DC.

Power management system to regulate the output.

- ❖ Storage: Battery system to store the harvested energy.

Also, we can note some application for this power like:

- ✓ Underwater Power Generation: Utilizing ocean currents to generate electricity for underwater sensors or remote systems.
- ✓ Wind Power: Small-scale wind energy harvesters for urban environments where traditional turbines are impractical

CHAPTER 2

Mathematical Model Equation

2.1 Introduction

Aerodynamics is the science which aims to study the movements of air around solid bodies. In other words, these are the phenomena brought into play whenever there is a relative movement between a body and the air which surrounds it.

In this chapter, we recall different basic notions on aerodynamics such as efforts or even aerodynamic coefficients which are of interest to the work carried out within the framework of this dissertation. An overview of the boundary layer and the phenomena that arise from it is also given.

2.1.1. Simplifying hypotheses

We assume the flow is: transient, two -dimensional, turbulent, Newtonian and incompressible.

2.2. Mathematical Modeling

In the present work, the flows considered are two-dimensional, and transient, without heat transfer.

In what follows, the equations reflecting the transport of mass and momentum governing such flows will be described with the necessary simplifications which are made in the ANSYS and OPENFOAM codes.

In what follows, the continuity and momentum equations (Navier Stokes) governing such flows will be described with the necessary simplifications which are made in the ANSYS and OPENFOAM codes according to the cases studied.

2.3 Transport equations

The equations that govern the flow of a Newtonian incompressible fluid are the continuity equation as well as the momentum conservation equations:

2.3.1. Energy Equation

The energy equation is based on the thermodynamic equation, it is used under the

The following form [23-4]

$$\frac{\partial(\rho.h_t)}{\partial t}+\frac{\partial(\rho.h_t.u_j)}{\partial x_j}=\frac{\partial \rho}{\partial t}+\frac{\partial}{\partial x_j}.\left(K.\frac{\partial T}{\partial x_J}\right)+\frac{\partial}{\partial x_J}(t_{ij}.u_j)+S_E \qquad (2.1)$$

h_t : Total energy

S_E : Energy source term.

μ : Molecular viscosity depends on temperature

Where: Ω is the dissipation function, representing the thermal equivalent of energy Mechanics related to viscous dissipation and shear forces.

In the case of a moving Newtonian fluid, the relationship between the shear stress, τ, and the velocity gradient is linear (the direction of the y-axis is perpendicular and the velocity of the flow

$$\rho C_p \frac{Dh}{Dt}=\gamma T\frac{Dp}{Dt}+\tilde{\nabla}\,(\lambda \nabla T)+\emptyset \qquad (2.2)$$

Dh/Dt: represents the change in enthalpy (particulate derivative)

Dp/Dt: the working rate of the pressure forces.

μ: is the coefficient of thermal conductivity.

2.3.2. Total energy

$$\varepsilon = e+\frac{V^2}{2} \qquad (2.3)$$

A fluid can be considered to be formed of a large number of material particles, very small and free to move relative to each other, a fluid is therefore a continuous, deformable medium, without rigidity and which can flow. Among fluids, a distinction is often made between liquid and gas. A fluid can be real (viscous), perfect (non-viscous).[7]

The viscosity of a fluid and the property that expresses its resistance to a tangential force of friction. Its effect is mainly manifested in the vicinity of the walls. In the case of a moving Newtonian fluid, the relationship between the shear stress, τ, and the velocity gradient is linear (the direction of the y-axis is perpendicular and the velocity of the flow.

It is only at rest that it will be assumed that the real fluid behaves like a perfect fluid, and that the contact forces are perpendicular to the surface elements on which they are exerted. The statics of real fluids merge with the statics of perfect fluids [7].

Knowing the distribution of parietal pressure, it is quite easy to integrate it in order to obtain

global forces. However, these forces can also be measured directly using aerodynamic scales. In this case, it is essential to first define the reference frame in which the torso is represented.

2.3.3. Continuity equation

The equation of continuity must reflect the principle of conservation of mass. That is, the change in mass over a time of an element of fluid volume must be equal to the sum of the masses of incoming fluid minus that of outgoing fluid.

We consider a material volume Ω. Its mass can be expressed as:

$$\frac{\partial \rho}{\partial t} + \frac{\partial (\rho . u_i)}{\partial} = 0 \tag{2.5}$$

2.3.4. The equation for conservation of momentum:

$$\frac{\partial (\rho . u_i)}{\partial t} + \frac{\partial (\rho . u_i . u_j)}{\partial t} = -\frac{\partial \rho}{\partial x_i} + \frac{\partial t_{ij}}{\partial x_j} + s_i \tag{2.6}$$

s_i : Source term for all the forces of volume (gravity, centrifugal forces, Coriolis force).

$$S_i = S_{i,cor} + S_{i,cent} = -2.\varepsilon_{ijk}.\rho.\omega_j.u_k - \varepsilon_{klm}.\rho.\omega_j.\omega_l.r_m \tag{2.7}$$

t_{ij} : The viscous stress tensor is expressed by the following equation:

$$t_{ij=}\delta_{ij}.\lambda.\frac{\partial u_k}{\partial x_k} + u.\left(\frac{\partial u_i}{\partial x_j} + \frac{\partial u_j}{\partial x_i}\right) = \delta_{ij}.\lambda.\frac{\partial u_k}{\partial x_k} + 2.\mu.\delta_{ij} \tag{2.8}$$

δ_{ij} : is the Kronecker symbol.

2.3.5. *k - epsilon* model equation

is one of the most common models used in computational fluid dynamics (CFD) to simulate mean flow characteristics for turbulent flow conditions. It is a two equation model that gives a general description of turbulence by means of two transport equations (partial differential equations, PDEs). The original impetus for the K-epsilon model was to improve the mixing-length model, as well as to find an alternative to algebraically prescribing turbulent length scales in moderate to high complexity flows.

$$\frac{\partial(\overline{\rho}.k)}{\partial t}+\frac{\partial}{\partial x_j}(\overline{\rho}.\widetilde{u_j}.k)=\frac{\partial}{\partial x_j}\left[(\mu+\frac{\mu_T}{\sigma_k})\frac{\partial k}{\partial x_j}\right]+P_K-\overline{\rho}.\varepsilon \qquad (2.10)$$

The dissipation rate equation:

$$\frac{\partial(\overline{\rho}.\varepsilon)}{\partial t}+\frac{\partial}{\partial x_j}(\overline{\rho}.\widetilde{u_j}.\varepsilon)=\frac{\partial}{\partial x_j}\left[(\mu+\frac{\mu_T}{\sigma_\varepsilon})\frac{\partial \varepsilon}{\partial x_j}\right]+\frac{\varepsilon}{k}(C_{\varepsilon 1}.P_K.C_{\varepsilon 2}.\overline{\rho}.\varepsilon) \qquad (2.11)$$

With:

P_K : The production of turbulence due to viscous forces and buoyancy.

k - $epsilon$ model constants in ANSYS CFX and OPENFOAM

C_μ	C_{S1}	$C_{\varepsilon 2}$	σ_k	σ_ε
0.09	1.44	1.92	1.0	1.3

2.3.6. The k-ω model equation:

In computational fluid dynamics, the k–omega (k–ω) turbulence model is a common two-equation turbulence model, that is used as an approximation for the Reynolds-averaged Navier–Stokes equations (RANS equations). The model attempts to predict turbulence by two partial differential equations for two variables, k and ω, with the first variable being the turbulence kinetic energy (k) while the second (ω) is the specific rate of dissipation (of the turbulence kinetic energy k into internal thermal energy).

$$\frac{\partial(\overline{\rho}.k)}{\partial t}+\frac{\partial}{\partial x_j}(\overline{\rho}.\widetilde{u_j}.k)=\frac{\partial}{\partial x_j}\left[(\mu+\frac{\mu_T}{\sigma_{k1}})\frac{\partial k}{\partial x_j}\right]+P_K-\beta.\overline{\rho}.k.\omega \qquad (2.12)$$

The turbulent frequency equation:

$$\frac{\partial(\overline{\rho}.\omega)}{\partial t}+\frac{\partial}{\partial x_j}(\overline{\rho}.\widetilde{u_j}.\omega)=\frac{\partial}{\partial x_j}\left[(\mu+\frac{\mu_T}{\sigma_{\omega 1}})\frac{\partial \omega}{\partial x_j}\right]+\alpha_1.\frac{\omega}{k}.P_k-\beta_1.\overline{\rho}.\omega^2 \qquad (2.13)$$

k-ω model constants in ANSYS CFX and OPENFOAM

β’	α_1	β_1	σ_k	σ_ω
0.09	5*9	0.075	2.0	2.0

2.3.7. The S.S.T model equation:

The SST k-ω turbulence model [Menter 1993] is a two-equation eddy-viscosity model which has become very popular. The shear stress transport (SST) formulation combines the best of two worlds. The use of a k-ω formulation in the inner parts of the boundary layer makes the model directly usable all the way down to the wall through the viscous sub-layer, hence the SST k-ω model can be used as a Low-Re turbulence model without any extra damping functions. The SST formulation also switches to a k-ε behavior in the free-stream and thereby avoids the common k-ω problem that the model is too sensitive to the inlet free-stream turbulence properties. Authors who use the SST k-ω model often merit it for its good behavior in adverse pressure gradients and separating flow. The SST k-ω model does produce a bit too large turbulence levels in regions with large normal strain, like stagnation regions and regions with strong acceleration. This tendency is much less pronounced than with a normal k-ε model though.

$$S.S.T = F(k-\omega) + (1-F)(k-\varepsilon)$$

➢

$$\frac{\partial(\overline{\rho}.\omega)}{\partial t}\frac{\partial}{\partial x_j}(\overline{\rho}.\overline{u_j}.\omega) = \frac{\partial}{\partial x_j}\left[(\mu+\frac{\mu_T}{\sigma_{\omega 2}})\frac{\partial \omega}{\partial x_j}\right] + (1-F_1).2.\overline{\rho}.\frac{\partial k}{\sigma_{\omega 2}.\omega.\partial x_j}.\frac{\partial \omega}{\partial x_j} + \alpha_3.\frac{\omega}{k}.P_k - \beta_3.\overline{\rho}.\omega^2$$

The frequency transport equation:

$$\frac{\partial(\overline{\rho}.k)}{\partial t} + \frac{\partial}{\partial x_j}(\overline{\rho}.\widetilde{u_j}.k) = \frac{\partial}{\partial x_j}\left[(\mu+\frac{\mu_T}{\sigma_{k2}})\frac{\partial k}{\partial x_j}\right] + P_K - \beta'.\overline{\rho}.k.\omega \qquad (2.14)$$

The constants used by the S.S.T model are determined in the same way as the constants in the BSL model.

-For k-ω model

k-ω model constants in ANSYS CFX and OPENFOAM

α_1	β_1	β’	$\sigma_{\omega 1}$	σ_{k1}
0.5	0.075	0.09	2	2

-For k - $epsilon$ model

k - $epsilon$ model constants in ANSYS CFX and OPENFOAM

α_2	β_2	β’	$\sigma_{\omega 2}$	σ_{k2}
0.44	0.0828	0.09	1/0.856	1

2.4 Conclusion

The role of the aerodynamicist is therefore to determine the aerodynamic coefficients, a function of all the parameters previously defined.

•We also have to analyses the origin of this aerodynamic result.

•Similarly, the role of certain key parameters must be precisely determined.

•the Navier-Stokes equations when the viscous effects are not negligible. The main parameter quantifying these effects is the Reynolds number.

• Observation of the wake phenomenon (Von-Karman).

•Euler's equations or perfect fluid equations, when viscous effects are negligible.

•Stokes' equations when viscous effects are preponderant.

• the equation of state of the gas (ideal gas for air).

Experience always remains the effective means of predicting and explaining complex physical phenomena of any analytical solutions that are difficult to achieve

CHAPTER III

Numerical Simulation

3.1. Introduction

Simulation is defined as the use or analysis of models relating to a certain system in order to study the behavior of the latter in a given situation. This is the first simulation method and the logical continuation of the modelling. As a result, the system studied becomes more adaptable. Parametric studies are simple to perform.

Numerical simulation tools occupy a prominent place in fluid mechanics studies. The laws of physics can be written in different ways, some of which are more efficient than others and they are represented by a system of partial differential equations. It is not always possible to find analytical solutions to this system of equations. This is why the continuous system should be replaced by a discrete system whose behavior is described by algebraic equations that can be solved with numerical methods.

Simulation is defined as the use or resolution of models corresponding to a given system to study the behavior of the latter in a specific context. It is the logical continuation of modelling, which is the first approach to a simulation.

In this chapter, we used the different software (OPENFOAM, ANSYS) to do the simulation and get results that concern the aerodynamic study of our model.

3.2. Definition of SOLIDWORKS Software

SOLIDWORKS Parametric Mechanical Design Software is a function-based, parametric, solid-based modeling design tool that takes advantage of the Windows graphical user interface, which is known for its user-friendliness, you can create fully integrated 3D solid models with or without constraints while using automatic or user-defined relationships to capture design intent

CHAPTER 3 NUMERICAL SIMULATION

3.3. Geometric formulation of the problem

3.3.1. Geometry

The seven geometric configurations covered are presented below:

Table3. 1 : details technics of our shapes

Circle	75 mm diameter sphere Approx. 660 mm long X 175 mm X 75 mm
Semi -circle	75 mm diameter hemisphere Approx. 660 mm long x 155 mm x 75 mm
rectangle	75 mm Length with 70 mm Width Approx. 660 mm long X 175 mm X 75 mm
triangle	75 mm base with 75-millimeter height Approx. 660 mm long X 175 mm X 75 mm
Flat plat	75 mm maximum diameter flat beveled plate 670 g Approx. 660 mm long X 145 mm X 75 mm
NACA4412	75 mm Diameter Teardrop Approx. 660 mm long X 188 mm X 75 mm Based on turned NACA0040 wing
NACA0040	75 mm Diameter Teardrop Approx. 660 mm long X 188 mm X 75 mm Based on turned NACA0040 wing

3.4. ANSYS Software Presentation

Is a computer-aided design (CAD) tool that allows the design and generation of 2D/3D geometries and applies simulations. It allows you to construct surfaces and volumes from a series of points that define the basic geometry. Once the geometry is built,

It can be exported in different formats to the mesh generator and solvers for analysis or simulation.

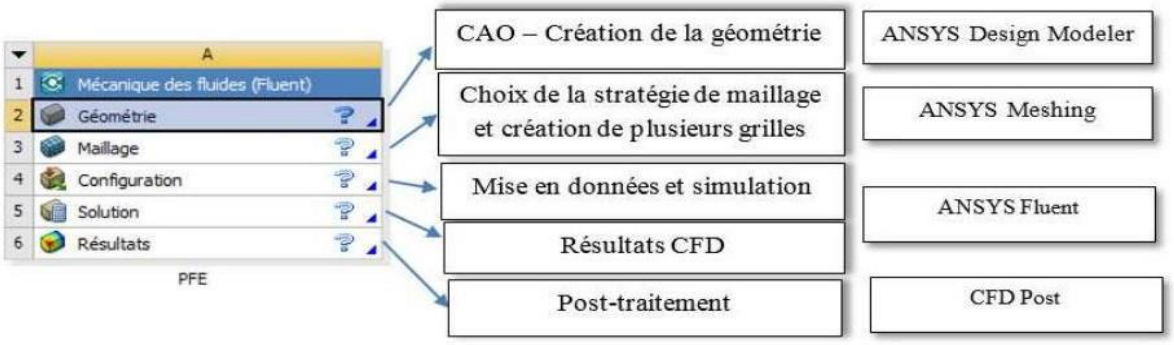

Figure3. 1 : ANSYS fluid mechanics simulation software.

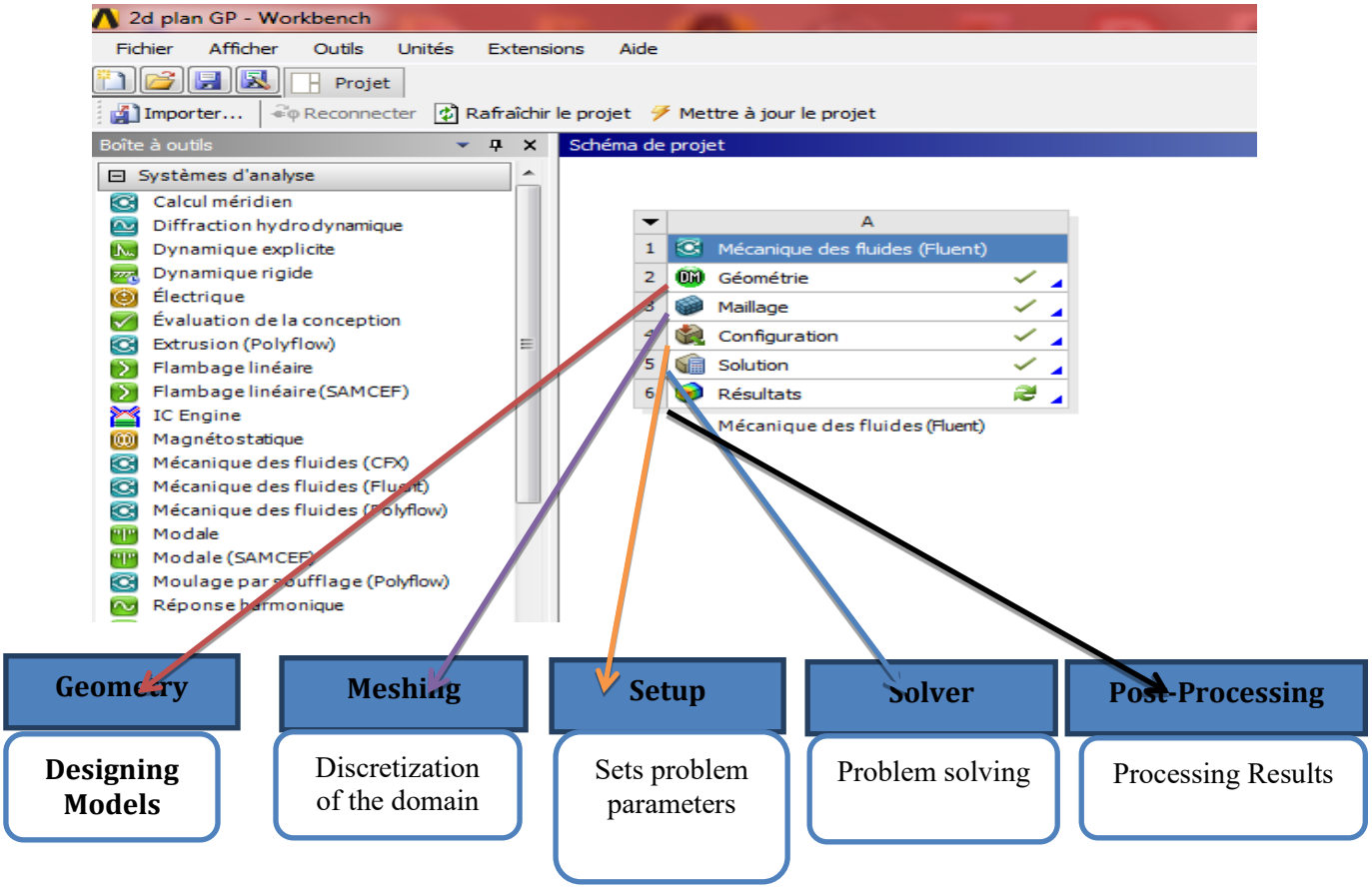

Figure3. 2 : the main steps of ANSYS Fluent

3.4.1. Numerical Fluent Solving Procedure

Once the geometry is created and the boundaries are defined, the mesh is exported to be able to perform a numerical resolution and discretize integral equations that translate the conservation of mass, momentum and energy.

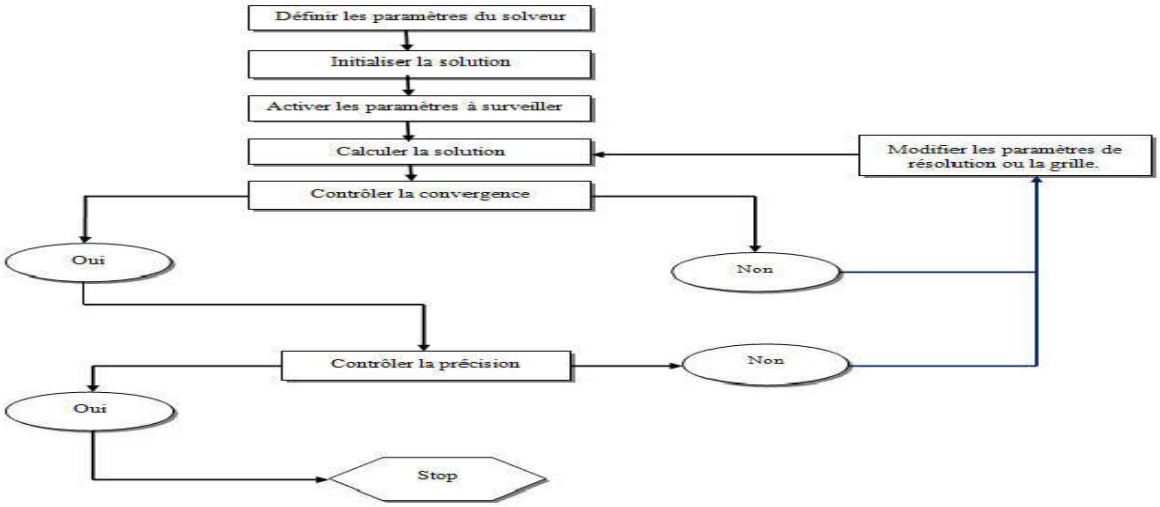

Figure3. 3 : Fluent Digital Resolution Step

3.4.2 Simulation Condition

3.4.2.1 Physical model and boundary conditions

It is well known that the entire simulation relies on how the computational domain is transformed into small elements (control volumes). We will start with the presentation of the results concerning a first test case which is the flow around a sphere with a circular cross-section. Subsequently, we will discuss the behavior of fluid flows around other six geometric shapes arranged in a half-sphere shape, (Trapezoidal), triangle, rectangle and profile (NACA 4412, 0040).

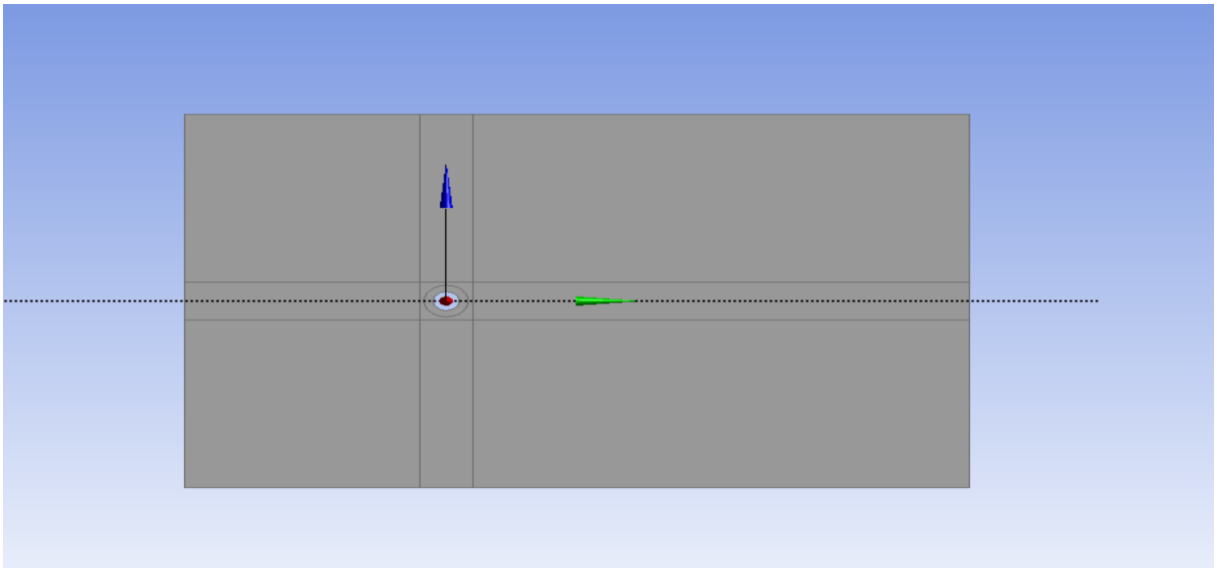

Figure3. 4 : Create control volume and contour lines.

Indeed, the use of numerical methods will be practically necessary for the solution of balance equations. For our problem, we used the software (ANSYS) based on the finite volume method.

3.4.3 Creating the Mesh

3.4.3.1 Choice of mesh type

Knowing that the mesh used considerably influences the accuracy of the results, several meshes were tested. As a result, structured and unstructured meshes are condensed in the vicinity of the walls (geometric shapes).

3.4.3.2 Structured mesh (quadra/hexa)

It is much easier to generate using multi-block geometry, it has the following advantages:

• Economical in number of elements, has a lower number of cells compared to an equivalent unstructured mesh.

• Reduces the chance of numerical errors as the flow is aligned with the mesh.

Its disadvantages are:

• Difficult to generate in the case of complex geometry

• Difficult to obtain good mesh quality for some complex geometries

3.4.3.3 Generation of a boundary layer mesh

The notion of resolution concerns more particularly the areas that have a strong gradient. Thus, a good resolution makes it possible to better describe the physical phenomena that occur in these areas.

L'écoulement Mauvaise résolution Meilleure résolution

3.4.4 Mesh of ANSYS

3.4.4.1 Mesh creation and volume control and Creation and refined mesh

The meshing of the computational domain is made with "Ansys-Meshing". We tested several structured and unstructured meshes in order to choose the optimal mesh with which we will have a good result and a computation time that is not too exaggerated.

The first step is therefore to create an adequate network. Having no more constraints in relation to the number of cells, we set out to adapt our mesh to regions with strong velocity and pressure gradients on the sphere. To fully capture these phenomena, it is essential to have a very refined mesh in these areas (Figure 16). Therefore, we proceeded with the simulation campaign for different flow velocities.

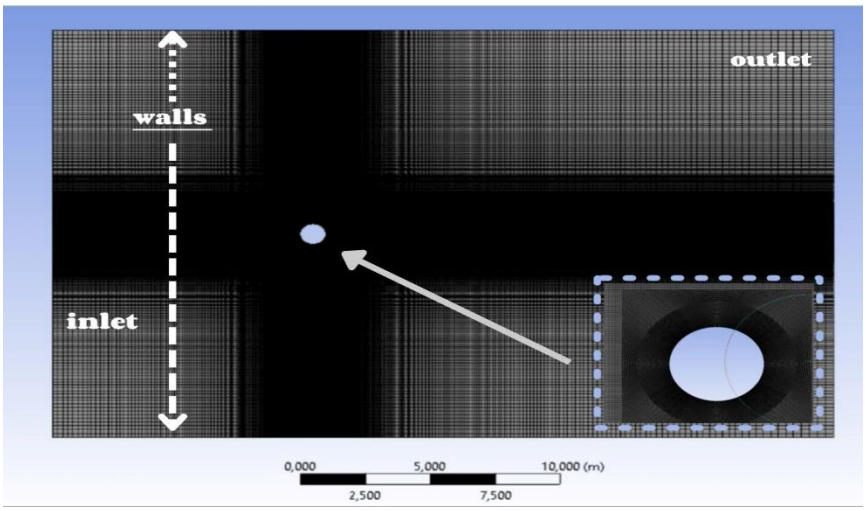

Figure3. 5 circle Mesh

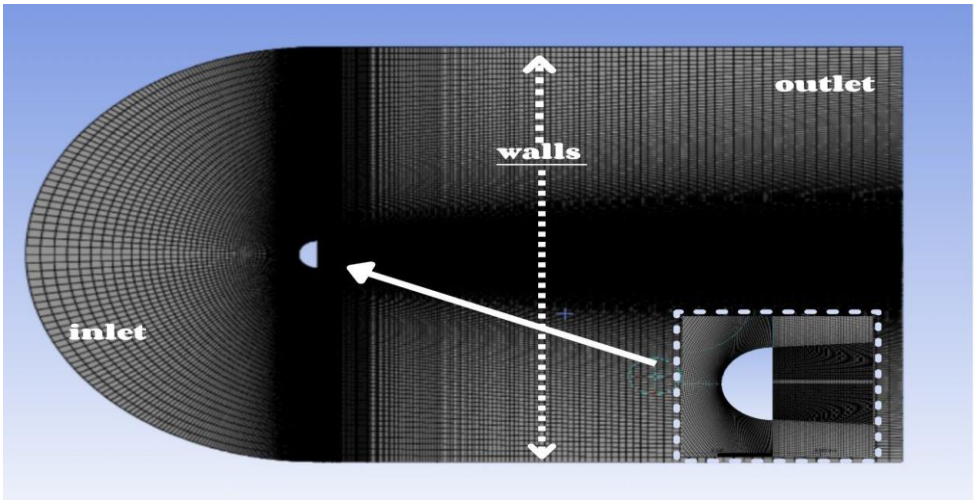

Figure3. 6 circle Mesh

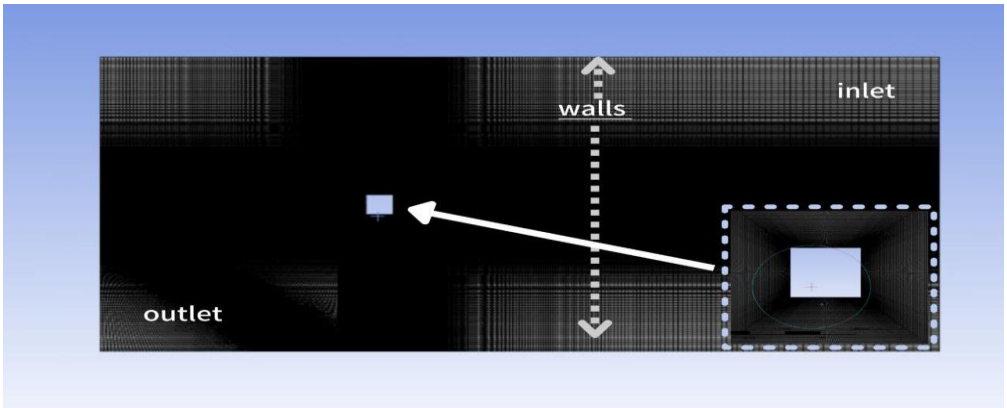

Figure3. 7 circle Mesh

3.4.5 Orthogonality Quality Mesh Parameters

The purpose of the geometry construction is to define the computational domains that are faces in a 2D problem and dimensioning. The geometry considered is of a spherical shape, generated through the software (ANSYS). The geometries were modeled on (ANSYS) and then the field of study was meshed on the ANSYSR1software, for mesh inflation.

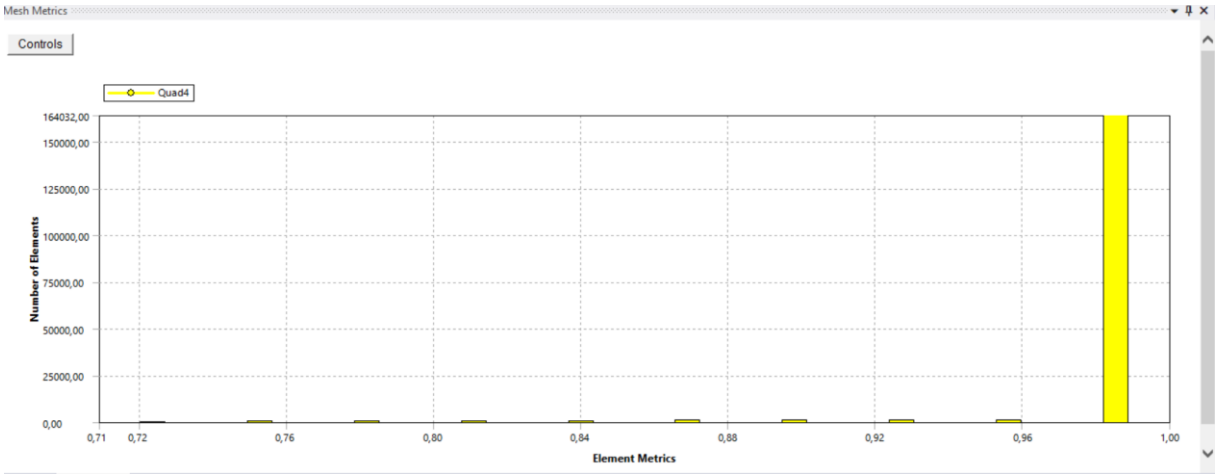

Figure3. 8 circle Mesh

3.4.6 Steps in Numerical Simulation on ANSYS

The choice of 2D double precision seems the most appropriate for our simulation, In this step, we will define an analyzer and define the physical models, the properties of the materials, the conditions of the simulated area "ANSYS" is used through a very simple graphical interface. The advanced user can adapt or augment the interface by writing macros and menu functions to automate certain procedures. Thus, it has the ability to model:

• 2D or 3D flows.

• Permanent or transitory states

• Incompressible or compressible flows including any speed of revs

• Non-viscous, viscous, laminar or turbulent flows in Portus media

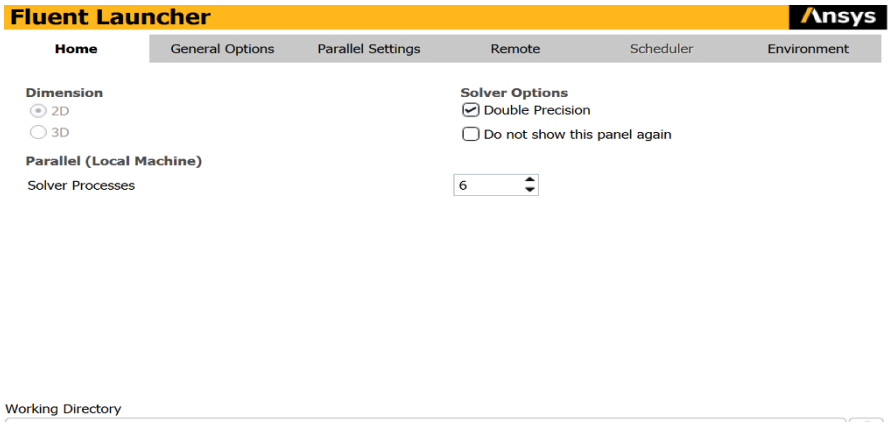

Figure3. 9 : ANSYS Fluent Launcher.•

3.4.7 Boundary Conditions and Objective

This step consists of defining the type of the different boundaries of the system as well as the nature of the domain(s) described globally.

Type incompressible

Steady state

*For the seven geometric shapes:

1) circle.

2) Semi-Circle.

3) rectangle.

4) triangle.

5) Flat-plate (Trapezoidal Shape).

6)profile de NACA4412.

7) profile de (NACA 0040).

For the big velocities we choose the steady time but if we want to use the base velocities, we have to choose the transient time for we can see our phenomenon.

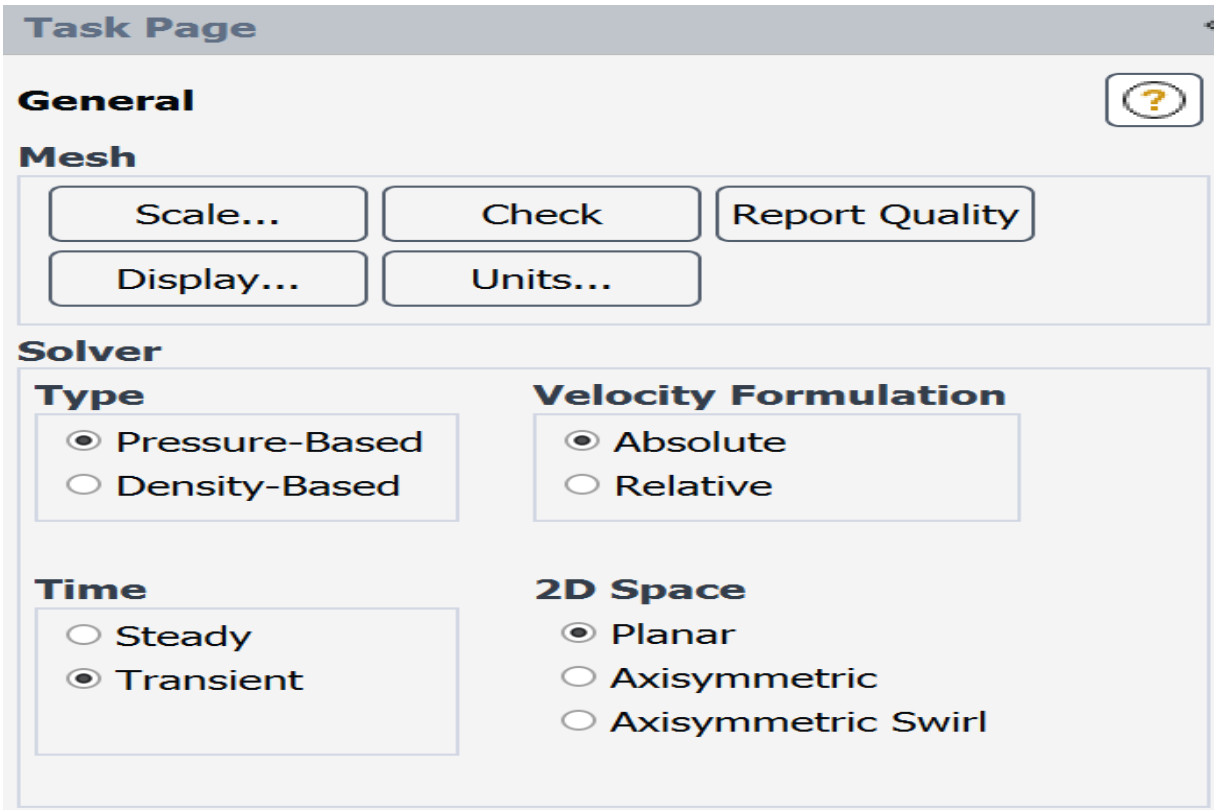

Figure3. 10 : General Window.

3.4.8 Slime Model Dialog Box

The dialog box

Viscous model

Allows you to define the parameters of a turbulent flow

K-epsilon criterion (2 equations)

*For the seven geometric shapes:

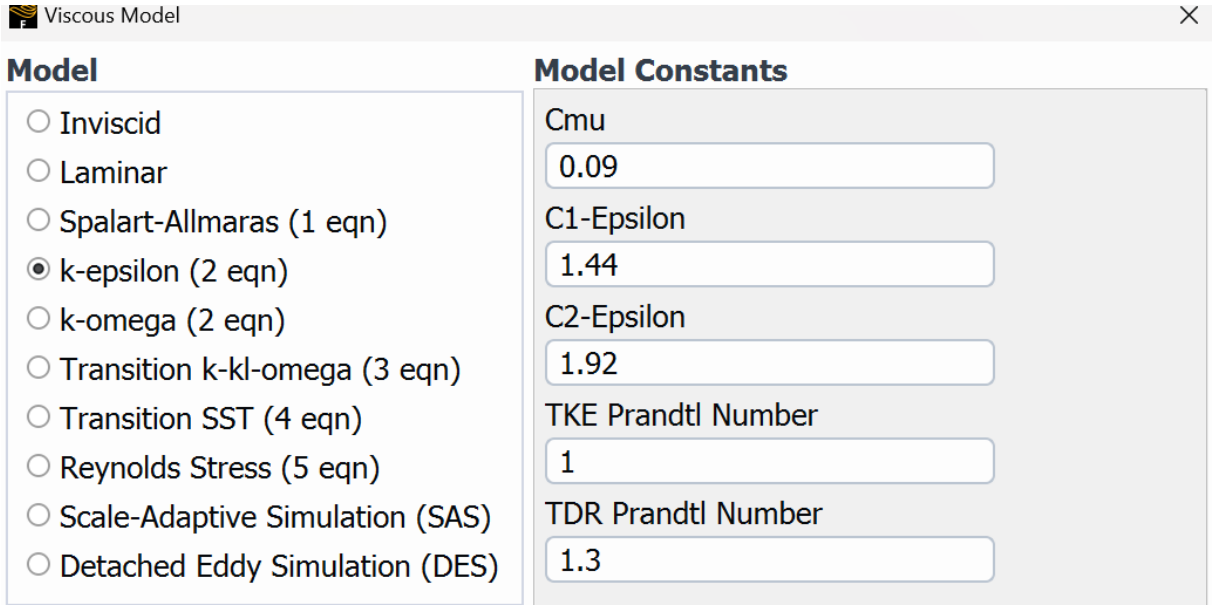

Figure3. 11 Slime Model dialog box.

3.4.9 Inlet Conditions

The boundary conditions for each boundary will be defined with the Boundary Conditions window. We then select the edge concerned and introduce the associated edge conditions

Re	20	100	200	1000
Velocity (m/s)	0.0039	0.02	0.04	0.2

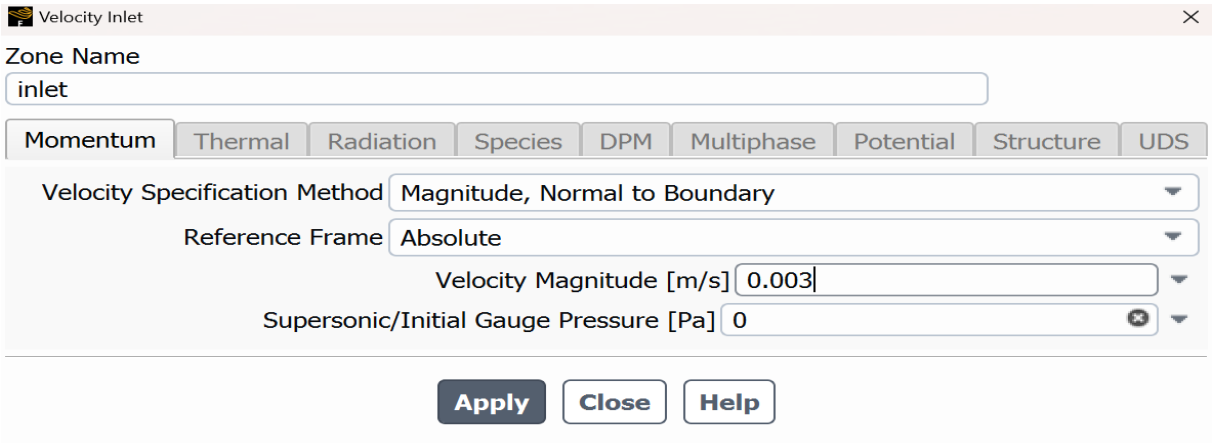

Figure3. 12 : Boundary Conditions.

3.4.10 Reference Values

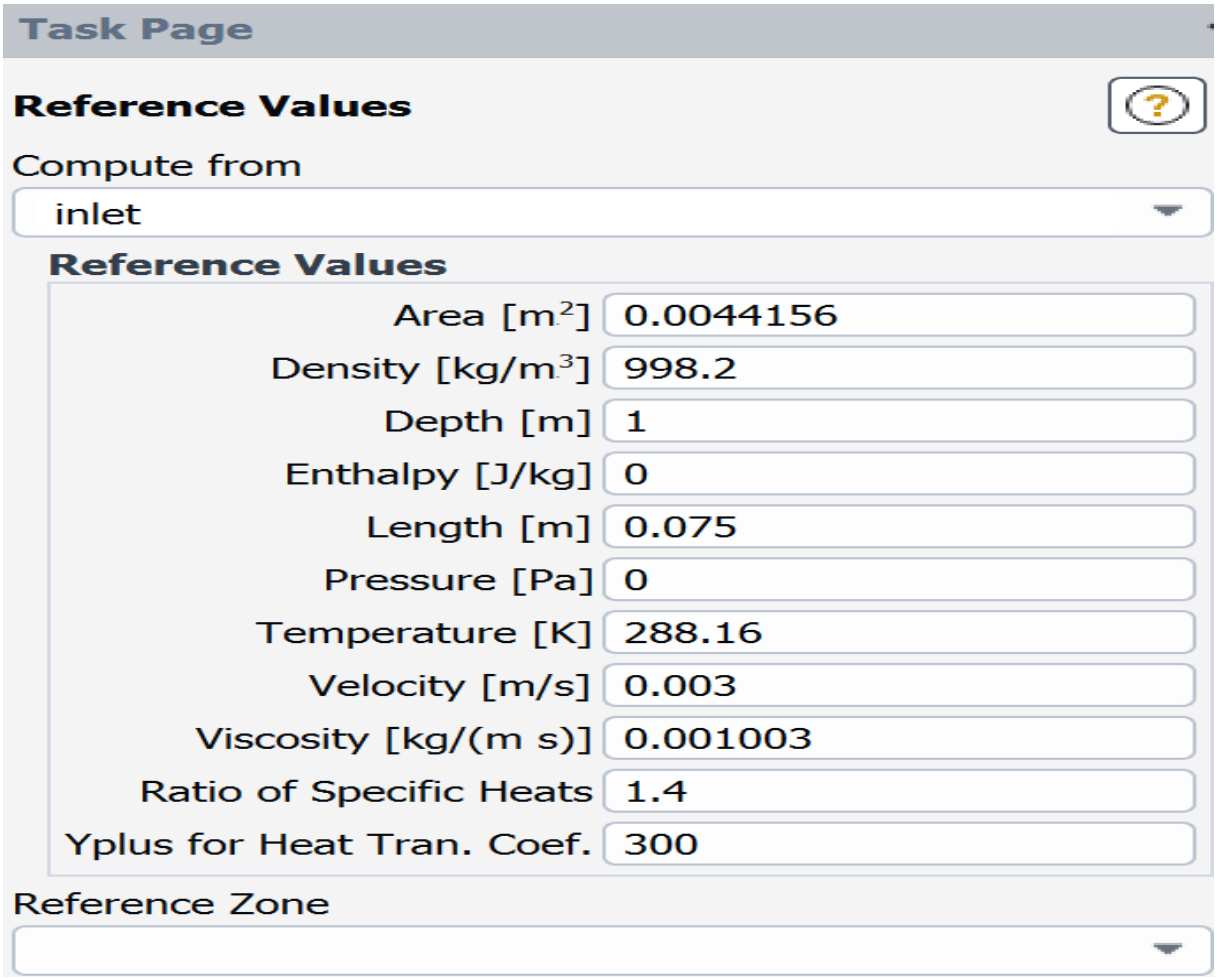

Figure3. 13 : Reference values.

3.4.11 Solutions

3.4.11.1 Solution Methods

The Fluent code allows us to choose the discretization scheme for the convective terms of each governing equation (the second order is automatically the most used for viscous terms). For our simulations, the upwind second-order scheme was chosen. The first-order scheme is easy to converge but the results do not sufficiently reflect physical reality. Despite its difficulty in achieving convergence, the second-order scheme gives very good results.

The discretization schemes used in this work are summarized as follows:

Formulation of the simple method Second order

Table.3.2: Formulation of the simple method Second order**.**

Pression	Standard
Quantité de mouvement	Second ordre upwind
Couplage vitesse-pression	Simple
Energie cinétique turbulente	Second ordre upwind

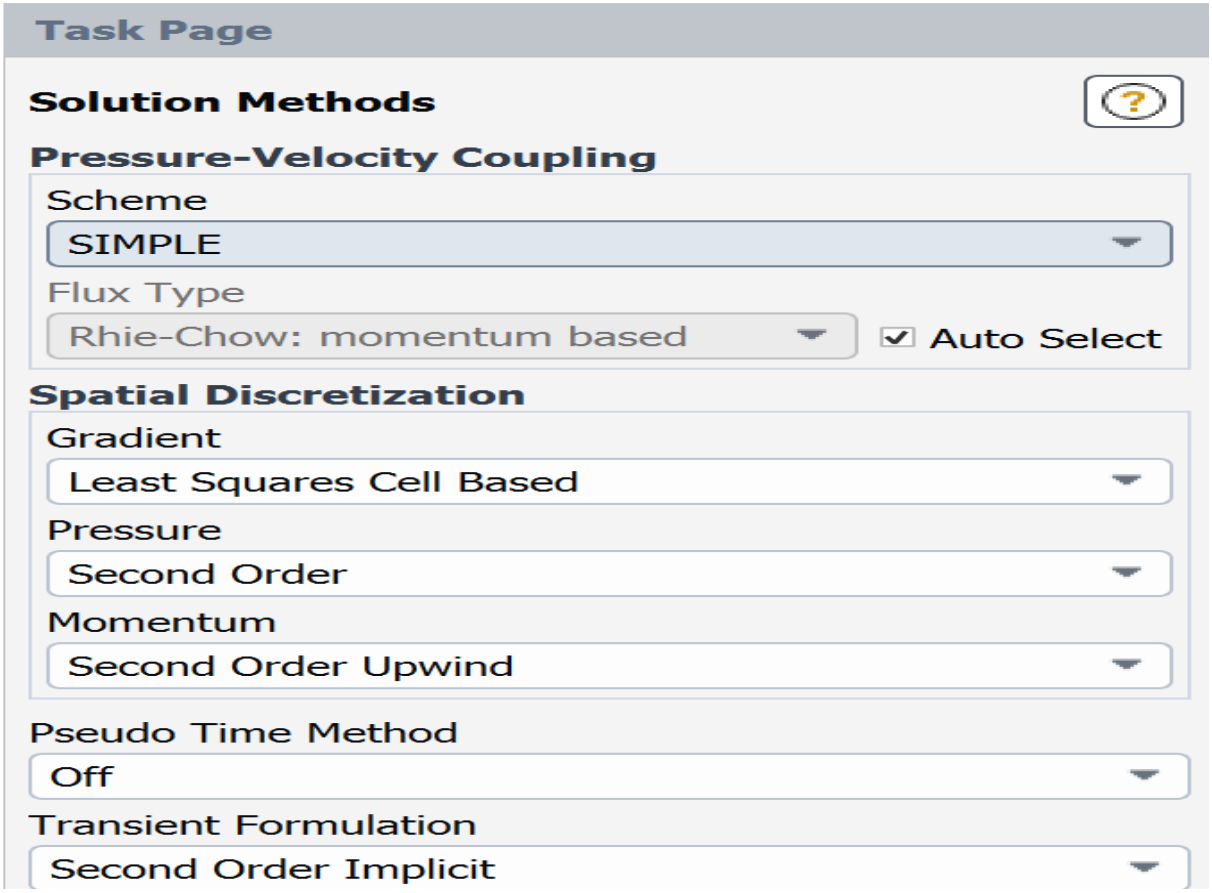

Figure3. 14 : Calculation algorithm choices and discretization schemes.

3.4.12. Report definition

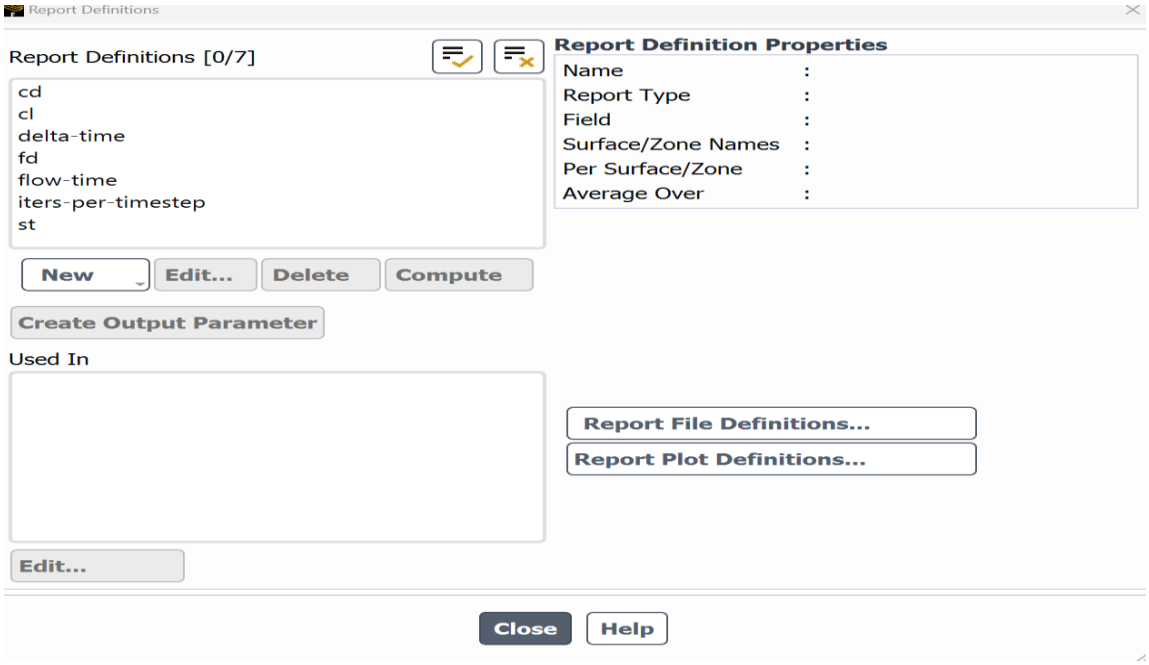

Figure3. 15 : Drag definition

3.4.13 Initialization of Calculations

Before we start the simulations, we need to implement an initial estimate of the flow field solution. The right choice of initial conditions makes it possible to achieve a stable solution and accelerated convergence

3.4.14 Run Calculation

The "Run Calculation" window allows you to initiate iterations of the solution and perform calculations based on the iteration to obtain the results: (500).

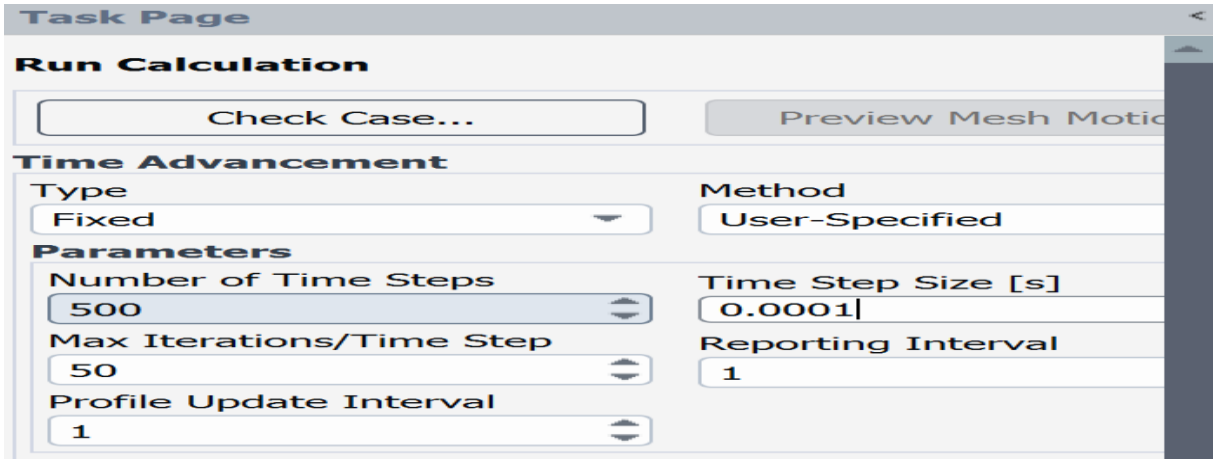

Figure3. 16 : Iteration-based calculations window to get the results.

CHAPTER 3 NUMERICAL SIMULATION

3.5. OPENFOAM software presentation

3.5.1 Introduction:

OpenFOAM is an open source CFD-oriented tool that is interesting in some ways. It is quick to implement, bulky and scalable, and only grows and improves by a community of users and independent programmers around this project; also, in addition to CFDs, meshing and other software. It is also a new tool that allows you to import meshes created in. Post-processing of OpenFOAM calculation results can be performed without conversion using Paraview software, which is already standard in the CFD world.

Each numerical simulation goes through three main steps:

1. Pre-treatment
2. Treatment
3. Post-processing.

OpenFOAM has a solution set for each of these steps. This chapter presents a simple and effective solution for this kind of problem.

3.5.2. Numerical Resolution

Assumptions:

- Incompressible flow.
- Laminar flow.
- Newtonian flow.
- Two-dimensional flow.
- Negligible gravity effects.

4.5.3. Pre-treatment:

In this step the mesh will be generated by "Ansys fluent", then we have saved the mesh file in a folder.

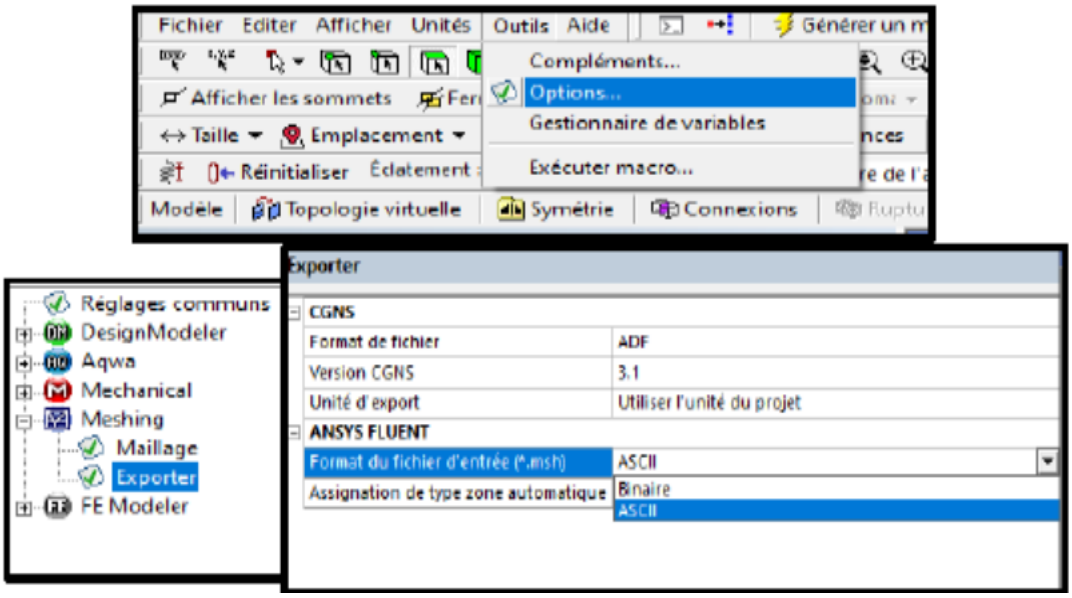

Figure3. 17 : the steps followed to export the mesh in ASCII form.

The following codes contain information to simulate with Re by the Piso Foam solver and with a mesh generated by block Mesh. Its file and subfolder structure are very similar to the one used in the chapter:

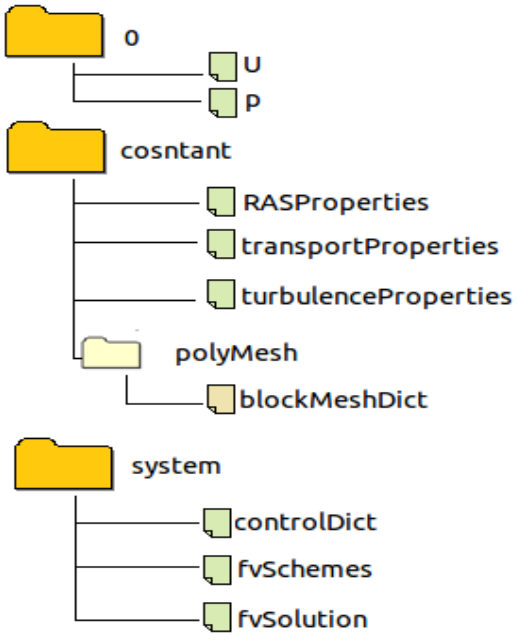

Figure3. 18 : Structure of the OPENFOAM.

The network for this study will not be uniform. Some regions of the domain must contain a higher density of lattices than others (mainly at the circle wall). As a result, it is necessary to divide the domain into different blocks(like our meshes generated by fluent). This arrangement allows us to choose the areas to refine.

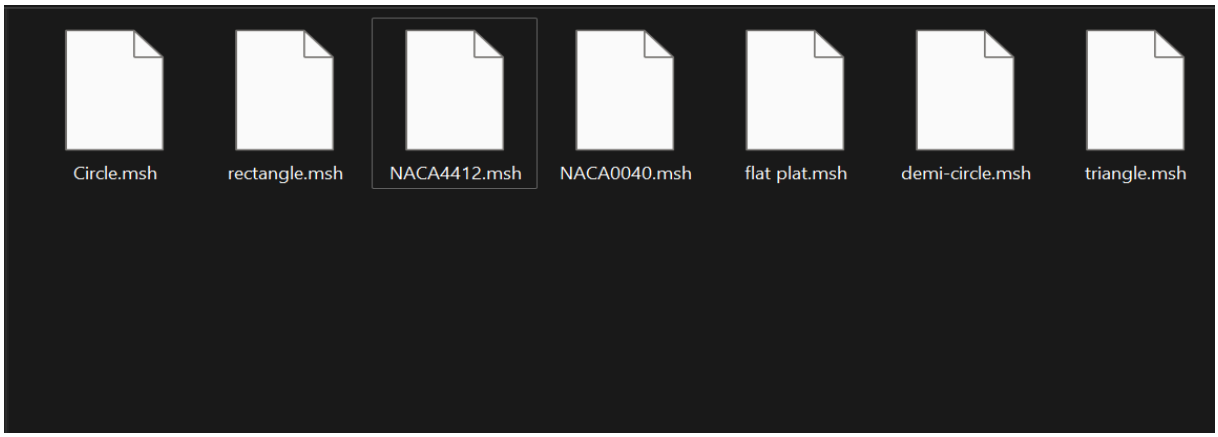

Figure3. 19 : mesh file of different shapes of format. msh

And using the command "fluentMeshToFoam" we converted the Mesh folder to the OpenFOAM, a polyMesh file that will be created.

4.5.4. Structure of the case:

The mesh generated by blockMesh is always structured and the meshes are hexagonal in shape. To run blockMesh, simply navigate to the folder in the Terminal and type the "blockMesh" command.

In this section, we detail Limits and initial conditions for which numerical calculations can be performed grid obtained. Before we get into the case of simulation, there are many OpenFOAM solvers. We choose the case we are interested in and copy it ourselves to Personal Workspace so that you can edit it. This file system initially contains at least three folders: 0, Constants, and System.

4.5.6. Choosing the Piso Foam Solver

The choice of solver depends mainly on the type of problem and these assumptions. Piso Foam is a solver for incompressible, laminar and turbulent flows. It is based on the PISO (Pressure Implicit with Splitting of Operators) algorithm, proposed by ISSA in 1995. It is a pressure-velocity coupling algorithm with a prediction step and two

Corrections. In the prediction step, the momentum equations are solved for an intermediate pressure field. The estimated velocity field at this stage does not meet the

continuity condition. So during the two correction steps, the velocity and pressure fields are corrected in a way that both checked the equations of continuity and momentum.

3.5.7 Mesh of OPENFOAM

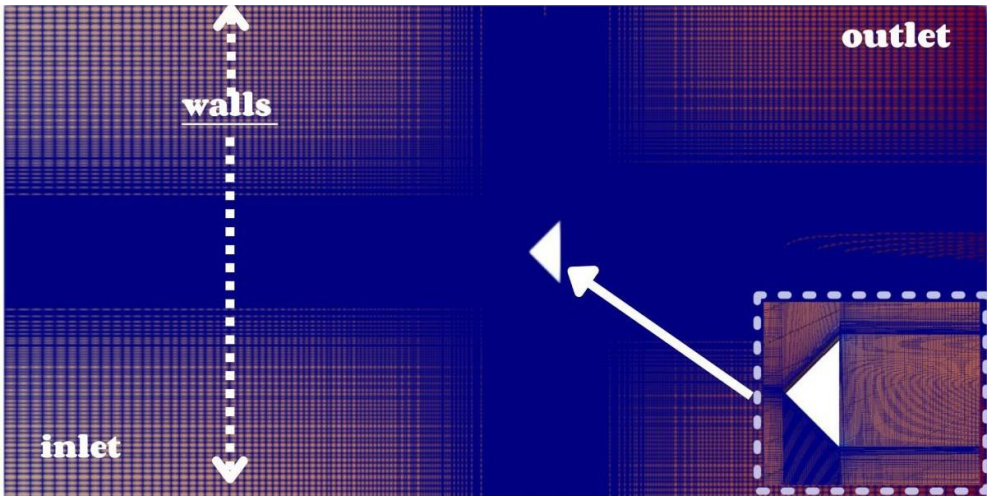

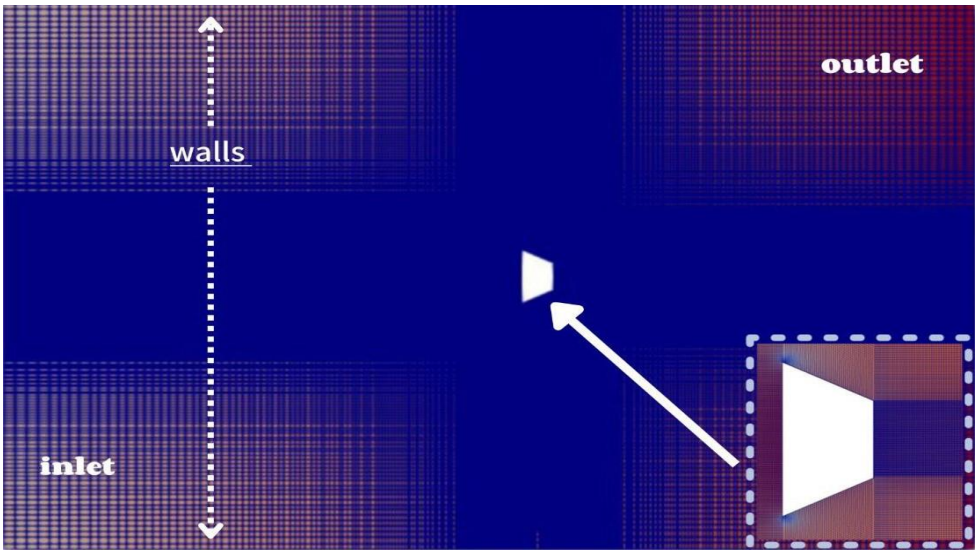

Figure3. 20 : Flat Plat Mesh

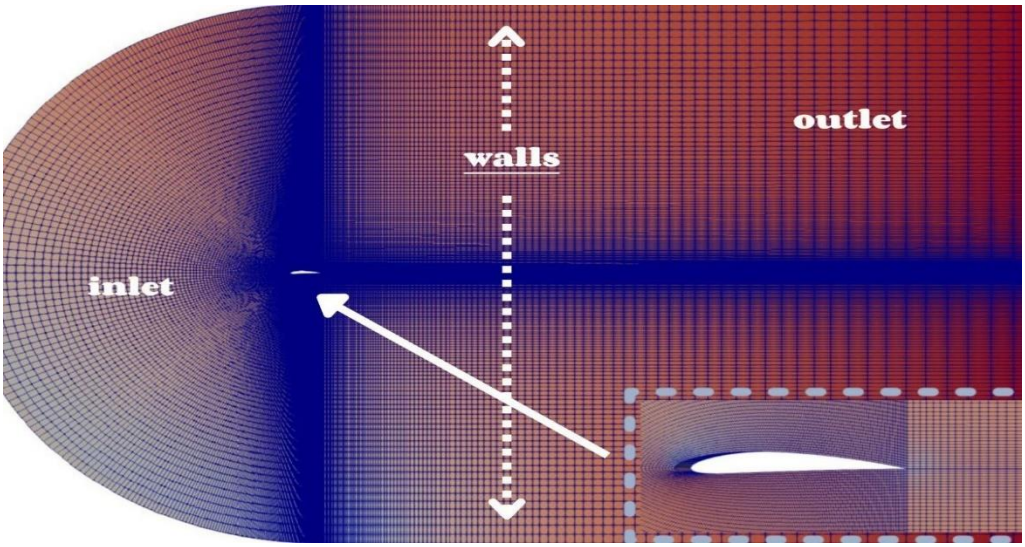

Figure3. 21 : NACA4412 Mesh

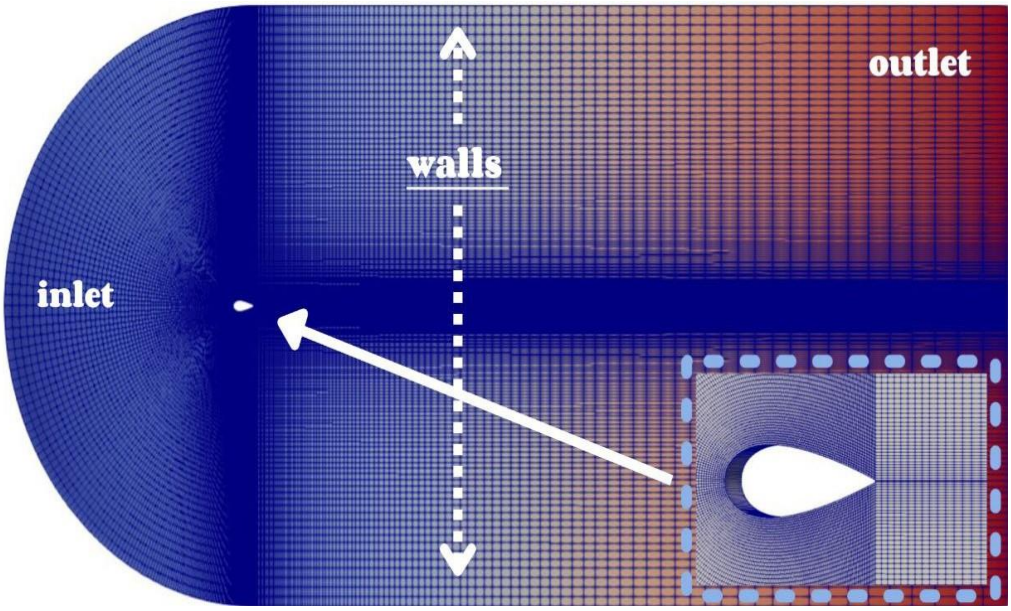

Figure3. 22 : NACA0040 Mesh

3.5.8. Boundary conditions

Folder 0 contains the physical parameters that govern the flow equations. In this case, the velocity U and the pressure p. While the constant/transport Properties file contains the constants that characterize the fluid being studied. Six elementary faces are defined in this problem: inlet, outlet, top, bottom, circle. The upper and lower faces are defined so as to be far enough away from the circle, they are defined as slip walls so as not to affect the flow. Since

this is a 2D case, the side walls are assumed to be empty. The boundary conditions used are summarized in Table 2.1:

Table3. 2 :Boundary conditions.

Parameters	Faces	Conditions aux limits	Description
U	inlet	fixedValue, uniform (1 0 0)	Vitesse uniform 1m/s.
	outlet	zeroGradient	Gradient null dans la direction de la normal.
	circle	fixedValue, uniform (0 0 0)	Vitesse fixe (null).
	top	slip	Condition of sliding of the wall.
	bottom	slip	//
	sides	empty	Faces vides
p	inlet	zeroGradient	Zero gradient in the direction of normal.
	outlet	fixedValue, uniform 0	Fixed pressure (null).
	circle	zeroGradient	Zero gradient in the direction of normal.
	Top	zeroGradient	//
	Bottom	zeroGradient	//
	Sides	empty	Faces vides

4.5.9 post-processing:

In this part, the results obtained are automatically adapted to be viewed under ParaFoam, OpenFoam's standard post-processing software. The calculation of lift and drag coefficients is obtained by entering a function in the "controlDict" file.

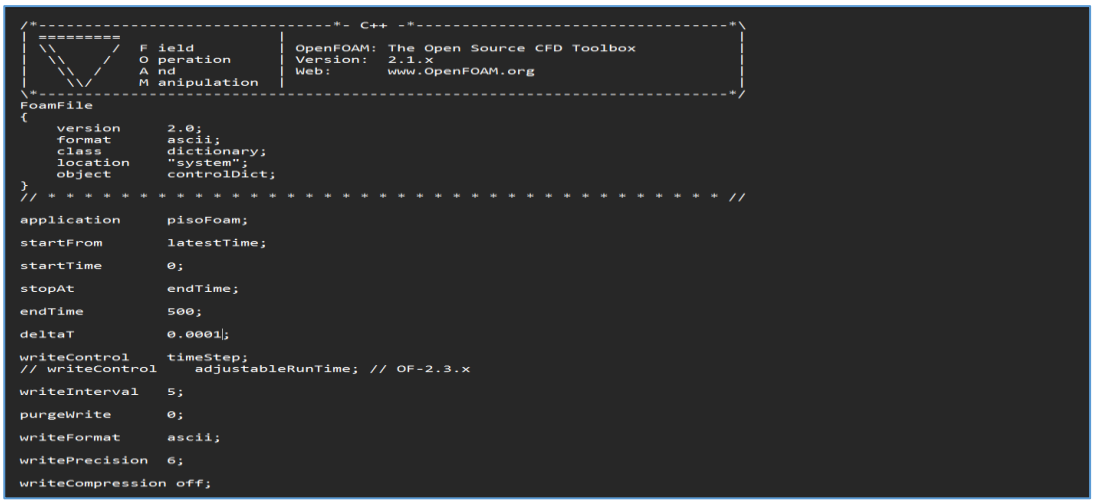

```
/*--------------------------------*- C++ -*----------------------------------*\
| =========                      |                                            |
| \\      /  F ield              | OpenFOAM: The Open Source CFD Toolbox      |
|  \\    /   O peration          | Version:  2.1.x                            |
|   \\  /    A nd                | Web:      www.OpenFOAM.org                 |
|    \\/     M anipulation       |                                            |
\*---------------------------------------------------------------------------*/
FoamFile
{
    version     2.0;
    format      ascii;
    class       dictionary;
    location    "system";
    object      controlDict;
}
// * * * * * * * * * * * * * * * * * * * * * * * * * * * * * * * * * * * * //

application     pisoFoam;

startFrom       latestTime;

startTime       0;

stopAt          endTime;

endTime         500;

deltaT          0.0001;

writeControl    timeStep;
// writeControl    adjustableRunTime; // OF-2.3.x

writeInterval   5;

purgeWrite      0;

writeFormat     ascii;

writePrecision  6;

writeCompression off;
```

Figure3. 23 : File controleDict 1

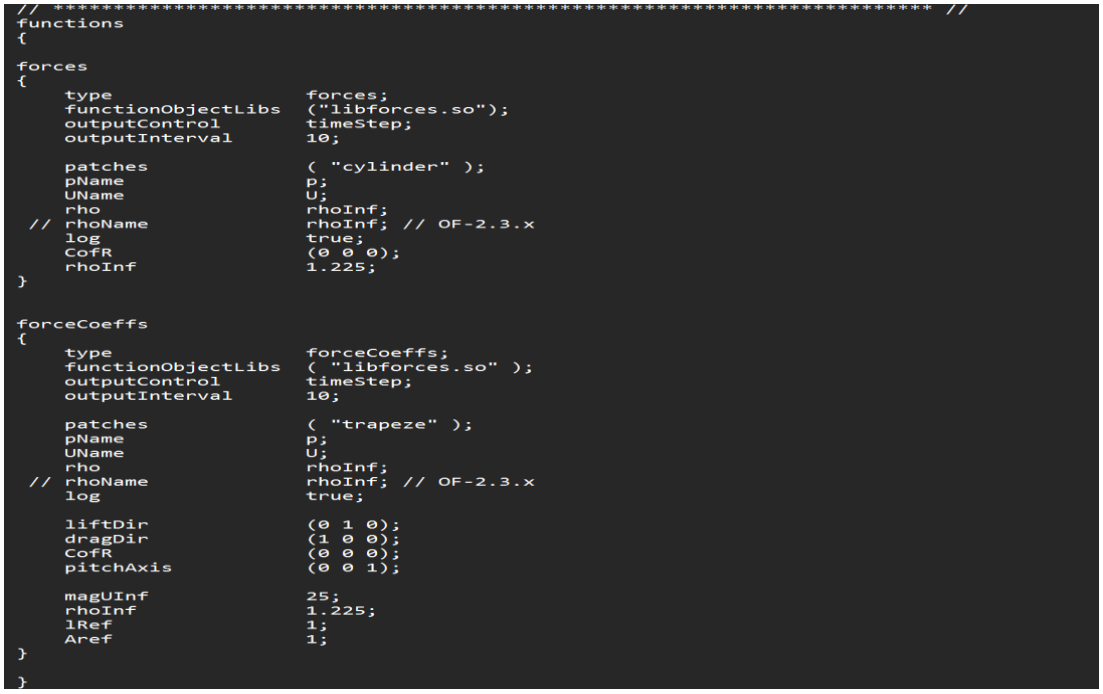

```
// ************************************************************************* //
functions
{

forces
{
    type                forces;
    functionObjectLibs  ("libforces.so");
    outputControl       timeStep;
    outputInterval      10;

    patches             ( "cylinder" );
    pName               p;
    UName               U;
    rho                 rhoInf;
 // rhoName             rhoInf; // OF-2.3.x
    log                 true;
    CofR                (0 0 0);
    rhoInf              1.225;
}


forceCoeffs
{
    type                forceCoeffs;
    functionObjectLibs  ( "libforces.so" );
    outputControl       timeStep;
    outputInterval      10;

    patches             ( "trapeze" );
    pName               p;
    UName               U;
    rho                 rhoInf;
 // rhoName             rhoInf; // OF-2.3.x
    log                 true;

    liftDir             (0 1 0);
    dragDir             (1 0 0);
    CofR                (0 0 0);
    pitchAxis           (0 0 1);

    magUInf             25;
    rhoInf              1.225;
    lRef                1;
    Aref                1;
}

}
```

Figure3. 24 File controleDict 2

4.6 Meshes for the sous-chapter circles with slits

The mesh of 350000 nodes ×270800 elements of circle with horizontal and vertical slit and with slit angle is shown in Fig. 3.24-3.26

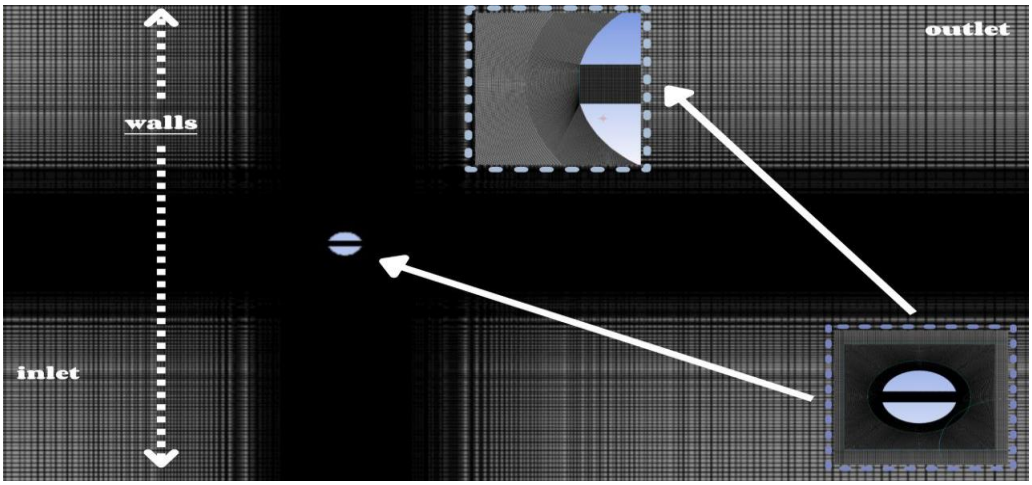

Figure3. 25 Mesh of the circle with vertical slit

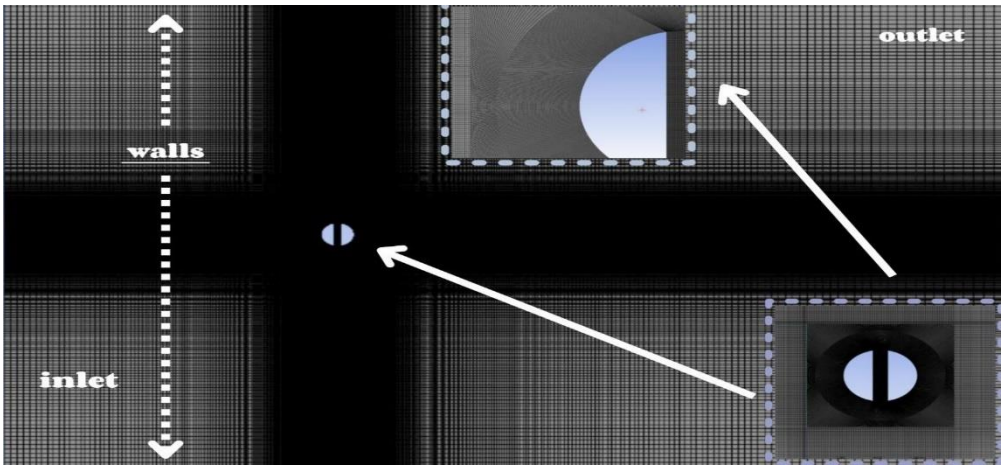

Figure3. 26 mesh of the circle with horizontal slit

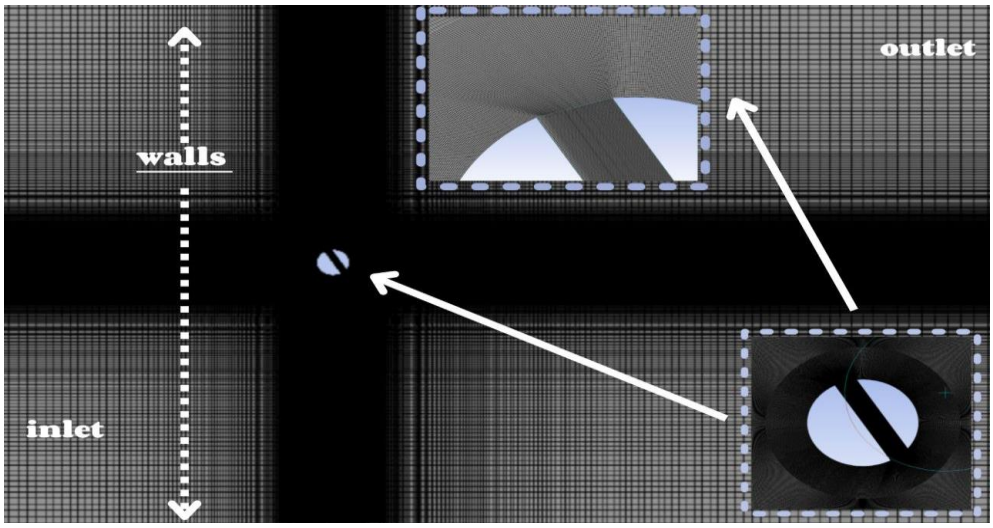

Figure3. 27 mesh of the normal circle

4.7 Conclusion

The present study gives a detailed description of separation flow and its effect under a high and low Reynolds number.

Fluent and OpenFOAM are a computational code that allows to simulate fluid flows with and without heat transfers in complex geometries. It can solve flow problems with structured and unstructured meshes produced through complex geometries with relative ease. The meshes supported in 2D are triangular or quadrilateral.

The simulation of 2D unsteady and transient flow around a geometric pattern of several geometric shapes, using numerical simulation of Computational Fluid Dynamics with the Reynolds number.

4.8. Goals of the simulation

Simulation is therefore used to:

• Understanding the structure and interactions within a system (determining yield, performance, etc.)

• The study of the behavior of the system in relation to its external environment (energy consumption/cost, etc.)

• Prediction of a system's behavior for new or extreme situations.

• The design of new devices/components, system (component) study before the creation of prototypes and implementation of new processes (control strategies and algorithms).

• Optimization of solutions during design.

In the following we will present a study on spherical models. The latter, when subjected to a flow of air, a flow is created around them

of a complex vortex structure. The qualitative and quantitative exploration of these properties are now possible using the ANSYS (Fluent) and OPENFOAM software, which allows you to:

- Draw the different maps of the pressure and velocity fields around seven geometric shapes
- Monitoring the development of longitudinal eddies created by geometry as well as their intensity at different surface states.

CHAPTER 4
Body Design

4.1 Introduction

Simulation The increasing competitiveness of the world is becoming more and more complex. This always leads us to do things faster and with greater added value.

It is not enough to create technical solutions that meet the needs of customers, but it is also necessary that the solutions are delivered with the speed required by the market and that they are as efficient as possible.

Machine tools were not excluded from this request. Indeed, they are required to increase productivity and to be more and more precise. The use of computer tools has made it possible to optimize the structures that meet the client's needs more or less well. However, these needs exceed the capacity to respond to the technical solutions currently in use.

4.2 SOLIDWORKS Software Definition

SOLIDWORKS Parametric Mechanical Design Software is a function-based, parametric, solid-based modeling design tool that takes advantage of the Windows graphical user interface, which is known for its user-friendliness, you can create fully integrated 3D solid models with or without constraints while using automatic or user-defined relationships to capture design intent

4.3 Computer-aided design (CAD):

4.3.1 History:

CAD took off in the years 75-90, when the cost of setting up a workstation was close to the annual cost of a draughtsman. The implementation was a bit painful at the beginning due to a need to rebuild existing plans. It was found that statistically nearly 10% of the quotes on existing plans were inaccurate, that duplicate plan references existed, that a single reference could correspond to several slightly different plans, etc. In the end, the gain in the reliability of the information proved to be an important additional argument for CAD. [18].

4.3.2 Computer science and design support:

Every technical system is a combination of functions. The arrangement of these functions, their interactions, and any incompatibilities are part of the engineer's knowledge. When the system is affected by too many parameters, it becomes difficult to control everything.

CHAPTER 4 BODY DESIGN

CAD makes it possible to design systems whose complexity exceeds the capacity of human beings, such as in micro or nanoelectronics.

Virtual design allows the overall appreciation of the behavior of the object created even before it exists. In CAD, you don't draw, you virtually build an object capable of reacting in its non-real space according to laws governed by software. The result, called a digital model, is then a real evolving prototype.

Each trade can have a CAD tool. In mechanics, you can design a part where each shape meets a functional need as well as a mechanism grouping several parts. In electronics, we can assemble components (resistors, capacitors, logic elements, etc.) that can be simulated: for example, we can "build" a new microprocessor with several million transistors (3.1 for the Pentium). In a way, DTP is part of this set of design tools (document creation). [18]

4.4.1 CAD and mechanics:

Historically, the field of mechanics was one of the first to have CAD software in the 1960s. It allows the designer to express and model a large number of constraints (functionalities, materials, assembly capacity, manufacturing, etc.) during the design phase of a mechanical assembly. The corresponding software is used during one or more phases of development (e.g. product/process specifications, sketches, dimensioning, kinematic analyses, dynamic analyses, manufacturing preparation, etc.).

Modern software allows for a direct three-dimensional design and is especially interesting for the functionalities offered: today a sheet metal part is modeled directly by virtually bending a sheet metal, a hole is placed with a simple click without having to think about the choice of volume shapes - in the mathematical sense - to adopt to model its technological intention. If the first software offered a fixed history (no retouching of already defined shapes possible), the latest versions using parametric design allow all modifications.

These functional and ergonomic advances are due in particular to the evolution of the underlying product/process models, according to the following time progression [Year of pioneering systems - Year of fully popularized systems]:

[1950-1970] 1st generation of 2D CAD: Graphic-based (e.g. AutoCAD graphics system)

[1960-1980] 2nd generation of 2.5D CAD: Depth-based (e.g. MicroStation civil engineering systems, Cadwork),

[1970-1990] 3e génération de CAO 3D : Geometry-based (ex. : système de CSG Euclid),

[1980-2000] 4th generation of 3.5D CAD: Feature-based (e.g. Pro/Engineer parametric system), and recently:

[1990-2010] 5th generation of 4D CAD1,2: Rule-based (e.g. Kadviser deduction-based system)3,

[2000-2020] 6th generation of 5D CAD: Induction-based (e.g., KAD-Office induction-based system) [20].

This software helps not only in the creation of mechanical parts, or in the implementation of their manufacture, but also in the simulation of their behavior, and therefore in the validation of the solutions chosen.

4.4.2 Software Use

SolidWorks: SolidWorks is a proprietary 3D computer-aided design software running on Windows.

Figure 4. 1: Logo SOLIDWORKS

4.4.2.1. Background

Created in 1993 by the eponymous American publisher, SolidWorks was acquired on June 24, 1997 by the company Dassault Systèmes3.

Some of the largest organizations using SolidWorks include Franckie, MMC Packaging Equipment, AREVA, Patek Philippe, Mega Bloks, Axiome, ME2C, SACMO, Le

Boulch, Robert Renaud, Lorenz Baumer 4, the Paris Opera4, Jtekt4, GTT4 and the French Ministry of Education. [20]

4.2.2.2 Operation:

SolidWorks is a 3D modeler using parametric design. It generates 3 types of files relating to three basic concepts: the part, the assembly and the drawing. These files are related. Any changes at any level are reflected in all the files concerned.

A complete file containing all the information relating to the same system constitutes a digital model. Many software programs complement the SolidWorks editor. Business-oriented utilities (sheet metal, wood, construction, etc.), but also mechanical simulation or computer-

generated image applications work from the elements of the virtual model. [20]

4.4.2.3 Software Definition:

SOLIDWORKS Parametric Mechanical Design Software is a function-based, parametric, solid-based modeling design tool that takes advantage of the Windows graphical user interface, which is known for its user-friendliness, you can create fully integrated 3D solid models with or without constraints while using automatic or user-defined relationships to capture design intent

In this part a 3D design of a sphere, a half sphere, a flat plate and a hand-thrown NACA0040 profile was made in SOLIDWORKS at a scale of 1:1 and using the scale function it is only necessary to choose the scale to have the full dimension of the scale model. [21] 5. Geometric formulation of the problem Geometric characteristics:

4.4.2.4 The design stages of the bodies ... under SolidWorks

The 3D drawing of these geometric shapes is obtained from the SolidWorks drawing with the necessary modifications to approximate the actual dimensions with a scale of 1:1; all the parts of the vector are obtained by using the surface features available on SolidWorks.

We designed these shapes in the following steps:

-1-click on the menu <<file >> then <<new>> or directly on the icon
<<new file>>

-2-choose << >> part (to make an assembly you must have already drawn several parts

-3-Choose the face plane and then select<<sketch>>. Figure (3.1)

-4-Select the desired shape.

-5-Choose << smart quote>>

-6-Indicate the correct diameter.

-7- Choose the construction line.

-8-Select the <<base function with revolution>>

-9-Close the sketch.

-10-Shape preview

-11-if the preview is correct you have to validate

-12-final result. Figure (4.2-4.6)

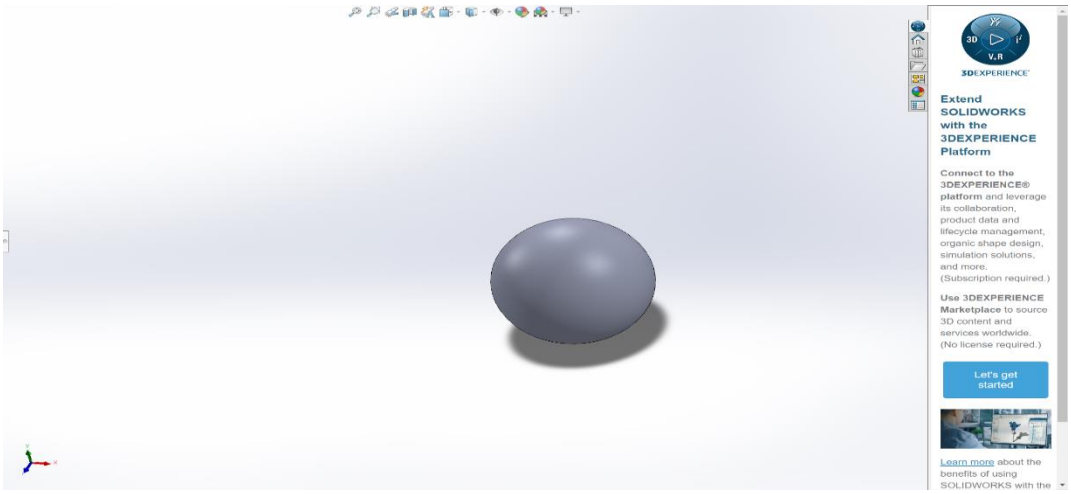

Figure 4. 22 Sphere Smoothing

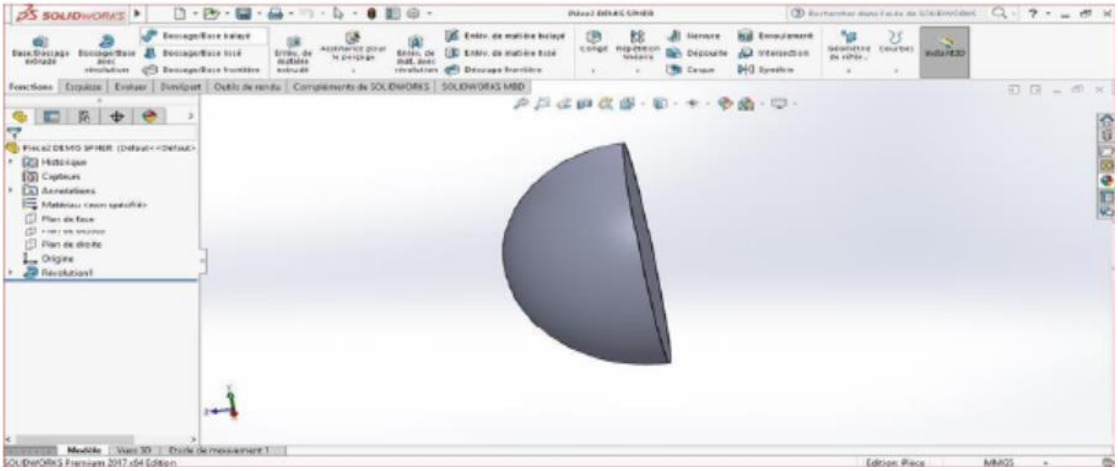

Figure 4. 3 Semi-sphere smoothing

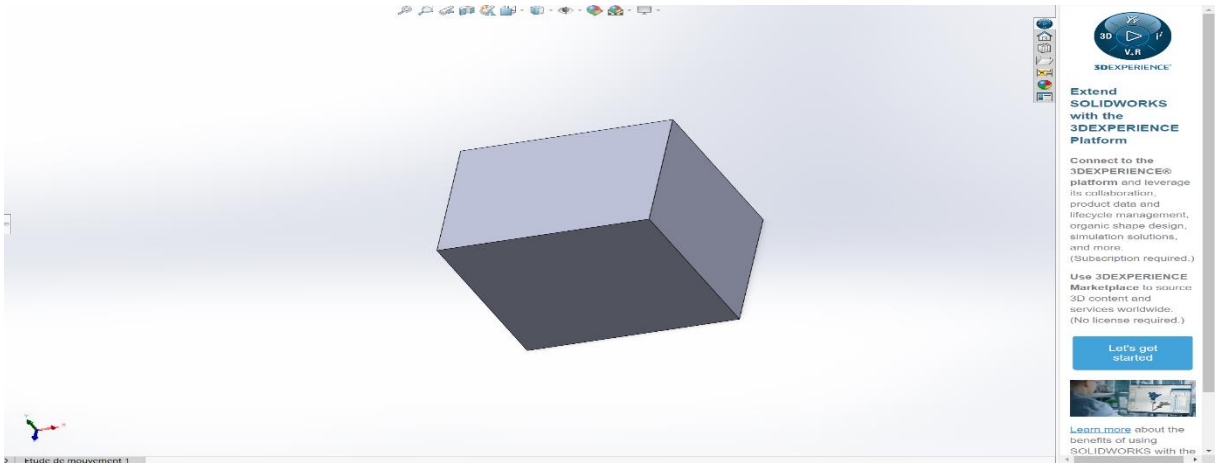

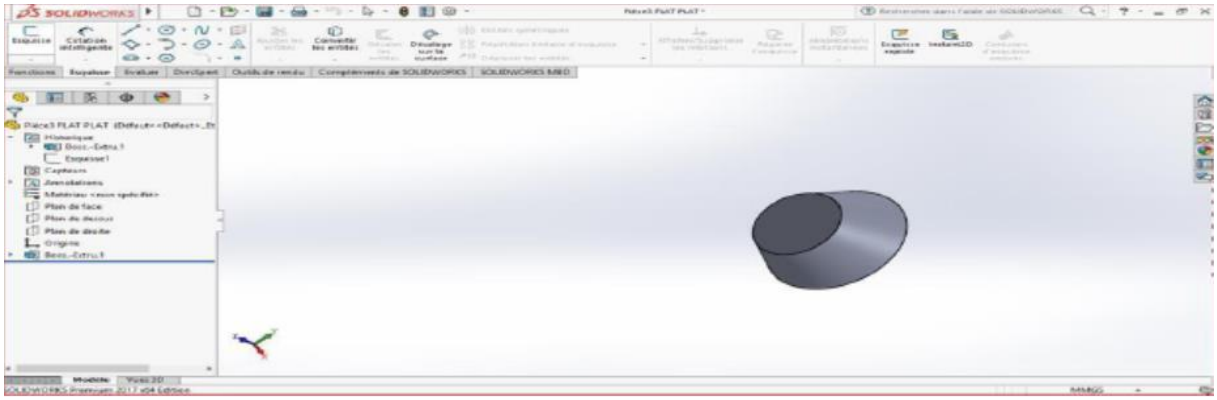

Figure 4. 4 Flat plate smoothing

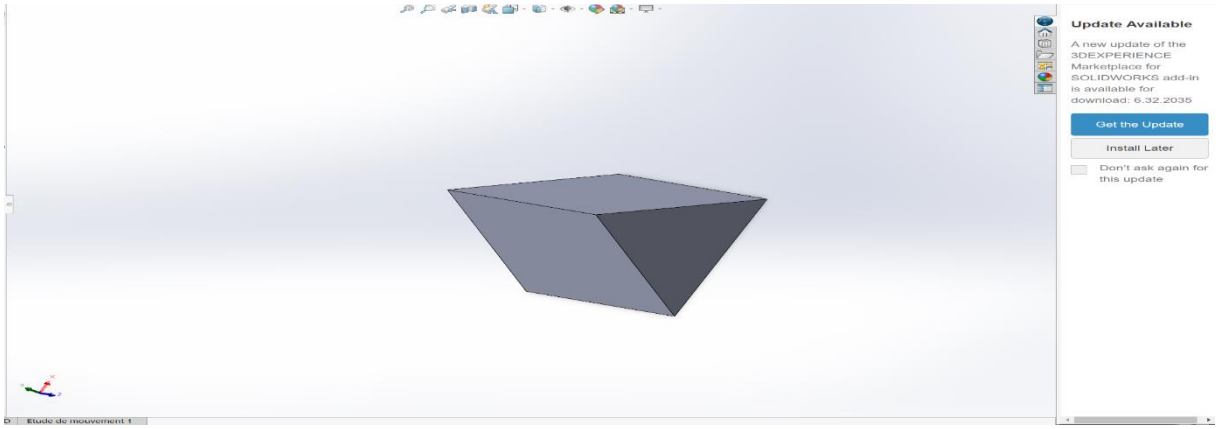

Figure 4. 5 triangle smoothing

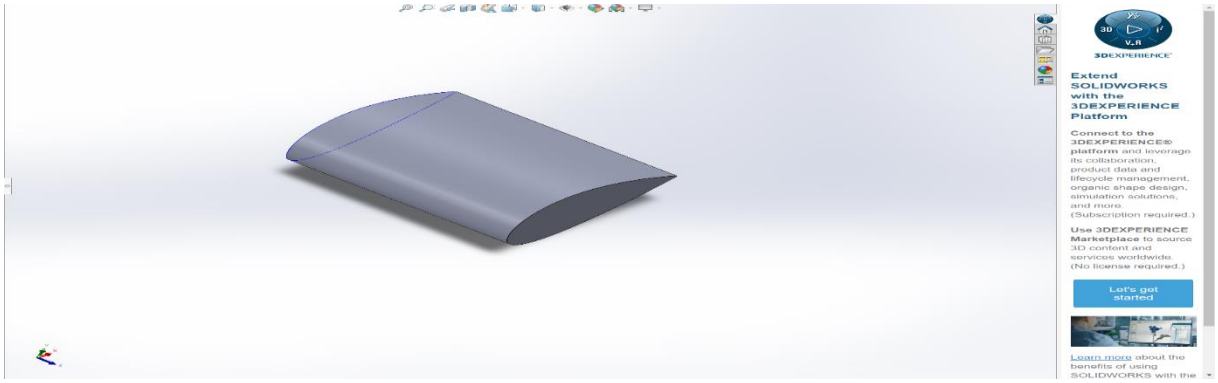

Figure 4. 6 NACA 0040 smoothing

4.5.1 Kil' impression 3d:

After designing these four geometric models with the SolidWorks software on 3D printing the 3D printer is a machine that we hear more and more about on a daily basis and that is about to invade the traditional industry, it represents a global industrial revolution, and the goal of 3D printers is the flexibility of production and the speed of the transformation of new ideas, in this chapter we will see the definition, history and field of application of the 3D printer. [22]

4.5.2 Definition of 3D printing:

3D printing or additive manufacturing, is a new rapid prototyping technology and it is easy to manufacture a part or model with precision, for example the production of a spare part in the space field, or the manufacture of organs in the Biomedical field, etc., it is the creation of a three-dimensional object from a digital model. We use materials such as: plastic, metal, concrete, etc. [22]

4.5.3 Additive Manufacturing (AM or 3D Printing)

3D printers manufacture their final products using an additive process.

In concrete terms, the 3D printer builds the object layer by layer: first, it cuts it into thousands of "slices" and superimposes them to create the final object. Our type of 3D printing is based on the FDM (Fused Deposition Modeling) technique. The advantages of technology

– Manufacture of very complex parts that are impossible to achieve in conventional processes, with identical mechanical characteristics

– Relocation of design and production sites

– Shortening of lead times from design to production

– No material loss, unlike machining

– Significant mass gain

– Mainly used for prototypes and small series

4.5.4 FDM

This technique involves melting a resin (usually plastic) through a heated nozzle. A small plastic thread, about a tenth of a millimeter, comes out of it. This thread is deposited online and is glued to what has been deposited beforehand.

- Advantages: Strength of materials, color patterns can be created.
- Cons: Rough surface finish.

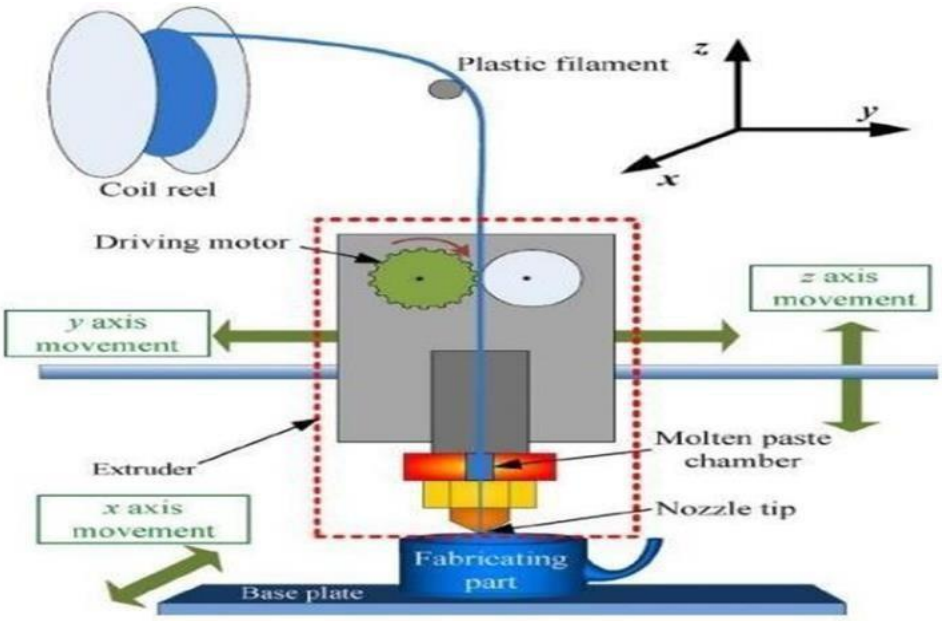

Figure 4. 7: Representation of the FDM

4.6 The stages of the experiment

An experimental study is carried out in this part in order to determine the aerodynamic performance, namely the coefficient of lift, drag, and Drag force.

4.6.1 AF1600 Introduction

Figure 4. 8The AF1600 with Instruments on the Instrument Frame

In studies of aerodynamics, few engineers have access to full scale wind tunnels or actual airborne laboratories. Most rely on what is probably the most common tool for aerodynamic study; the laboratory-based wind tunnel. This tool saves both money and time. It gives very accurate results, as long as the scale effect and reduced Reynolds numbers are taken into account.

The Wind Tunnel shown in Figure 1 is of the closed working section, open return suction type. It is supported on a tubular steel framework with castors and adjustable feet. This makes the apparatus mobile.

Air passes into the AF1600 through a honeycomb flow straightener and a grille. It then passes into an aerodynamically designed effuse (cone) that accelerates the air in a linear manner before it moves through the working section. Finally, it passes through a diffuser, then into the variable speed axial fan. The grille protects the fan from damage by loose objects. The air leaves the fan, passes through a silencer unit and then back out to atmosphere.

The speed of the axial fan (and therefore the air velocity in the working section) is controlled by an electronic drive control in the separate on/off unit mounted on the tunnel's associated instrument frame along with other ancillaries.

4.6.2 Working Section

The working section is of a square section with tapered chamfered corners and an acrylic roof and floor. The sides are full length acrylic panels, one side is hinged at the top and the other is removable. The whole unit is supported in an aluminum framework. Each side panel has a holder to support wind tunnel models. On the top of the working section are two Pitot devices and a wall tapping to measure the static pressure upstream and downstream of the working section.

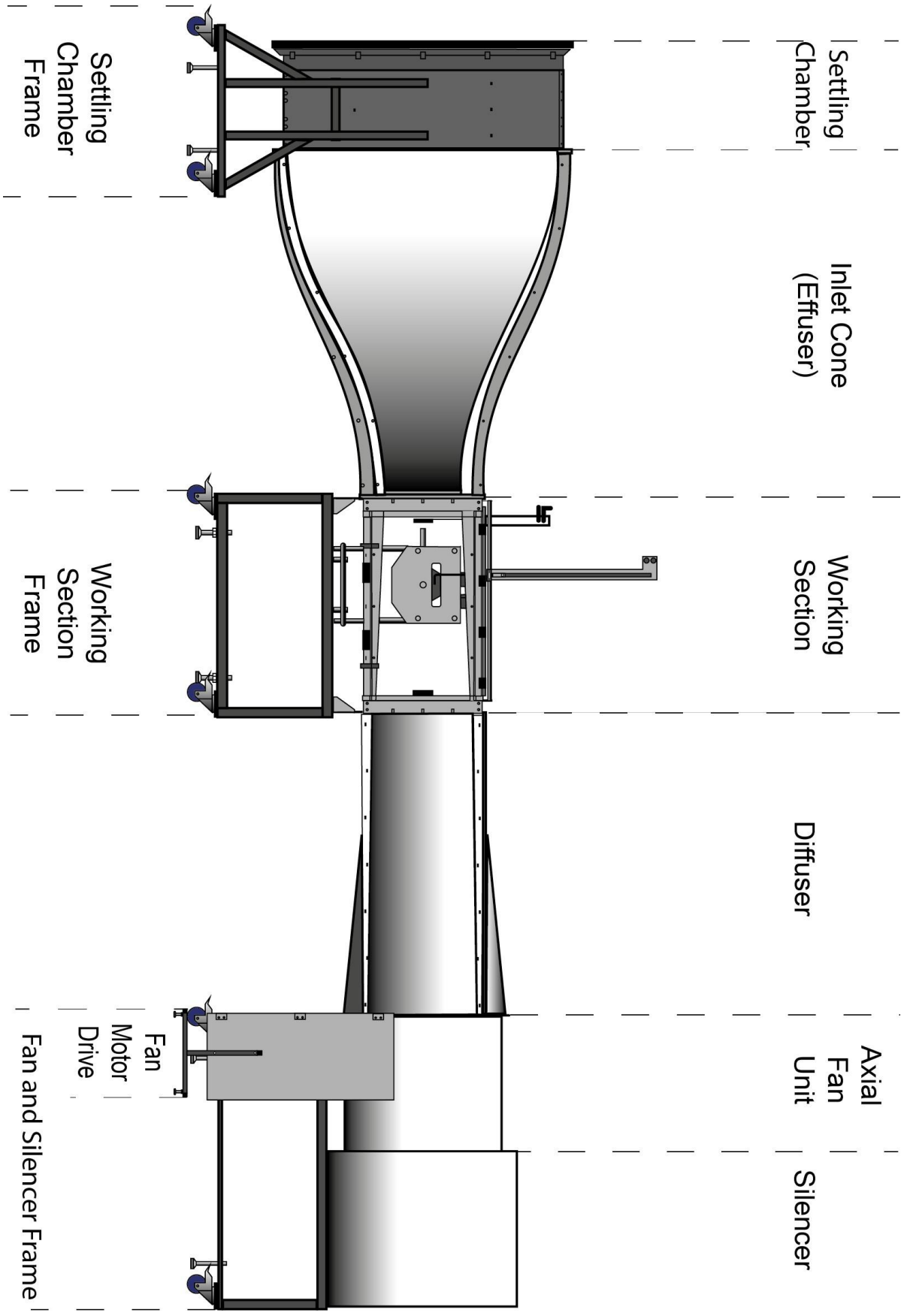

Figure 4. 9AF1600 General Layout.

CHAPTER 4 BODY DESIGN

This experience includes the use of the three-component aerodynamic scale:

-In order to determine the coefficient of friction for the geometric shapes we have created, we first make sure that the area around the wind tunnel is clean, to avoid any practical accidents when sucking in air from the outside.

-Then we connect the device with a three-component scale to read the results obtained through the experiment

To confirm that the scale is working properly, we need to make sure that it is balanced, so we put it on a stand installed on height-adjustable feet to test the aerodynamic models.

- ❖ To Fit the Models to the Three Component Balance (AF1600t)

These instructions assume that the Three Component Balance is fitted to the working section and is setup correctly. Refer to the Three Component Balance User Guide.

1) Switch off the electrical isolator of the Wind Tunnel.
2) Remove the side window opposite the Three Component Balance.
3) Tighten the Centering Clamps of the Three Component Balance. From outside the
4) Wind Tunnel,insert one of the models into the collet of the Three Component Balance, so that its support shaftpasses into the Wind Tunnel Working Section (see Figure 4.6).

Figure 4. 10 Insert the Model from Outside the Working Section

5) Inside the working section, measure the distance from the center of the model shaft to the bottomsurface of the working section (see Figure 5). This is nominally 300 mm.
6) Remove the model from the balance.
7) From inside the Working Section, insert the model into the model clamp of the balance. Set the angle of the Three Component Balance scale to zero degrees. Do not tighten the model clamp yet.
8) Looking into the wind tunnel from its inlet, make sure the model is in the center of the working section(see Figure 6).
9) Hold the model so that it faces into the airflow and adjust its center line to the same height as thatmeasured in step 4 and tighten the model clamp of the balance (see Figure 7). The model is nowperfectly straight (zero incidence angle) and at right angles to the airflow.
10) Recheck the adjustments and release the centering clamps of the Three Component Balance.

Figure 4. 11Model in Middle of tunnel

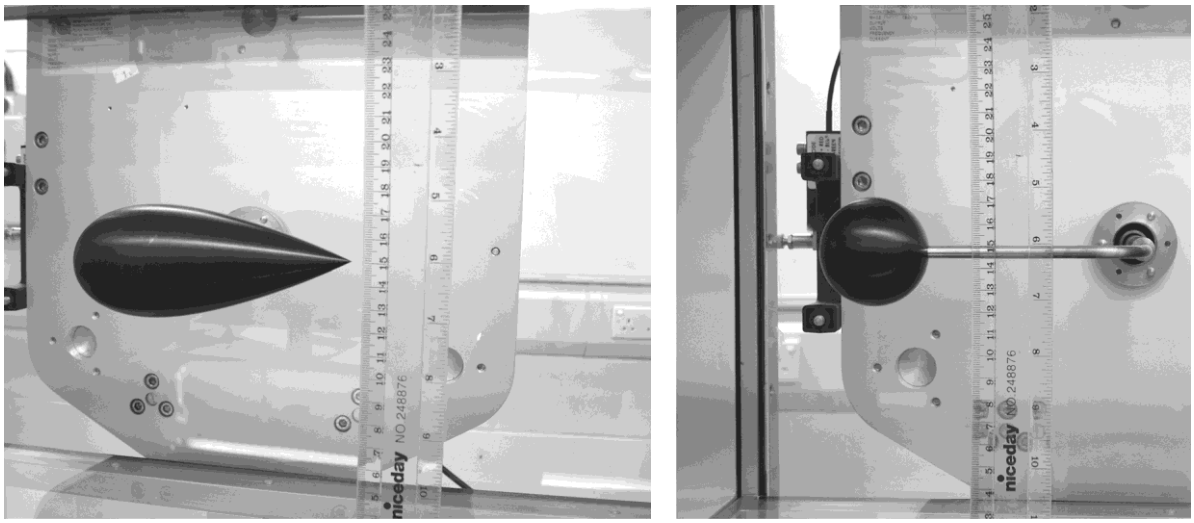

Figure 4. 12: Sitting the model center line

11) Refit the side window and fix the collar to the outside of the circular mounting in the window usingthe three thumbscrews provided (Figure 8).
12) Slide the Dummy Stem through the collar so that it almost touches the model or its arm (leaving justover 1mm gap) (Figure 9). Tighten the collar so that the Dummy Stem is firmly gripped in place.

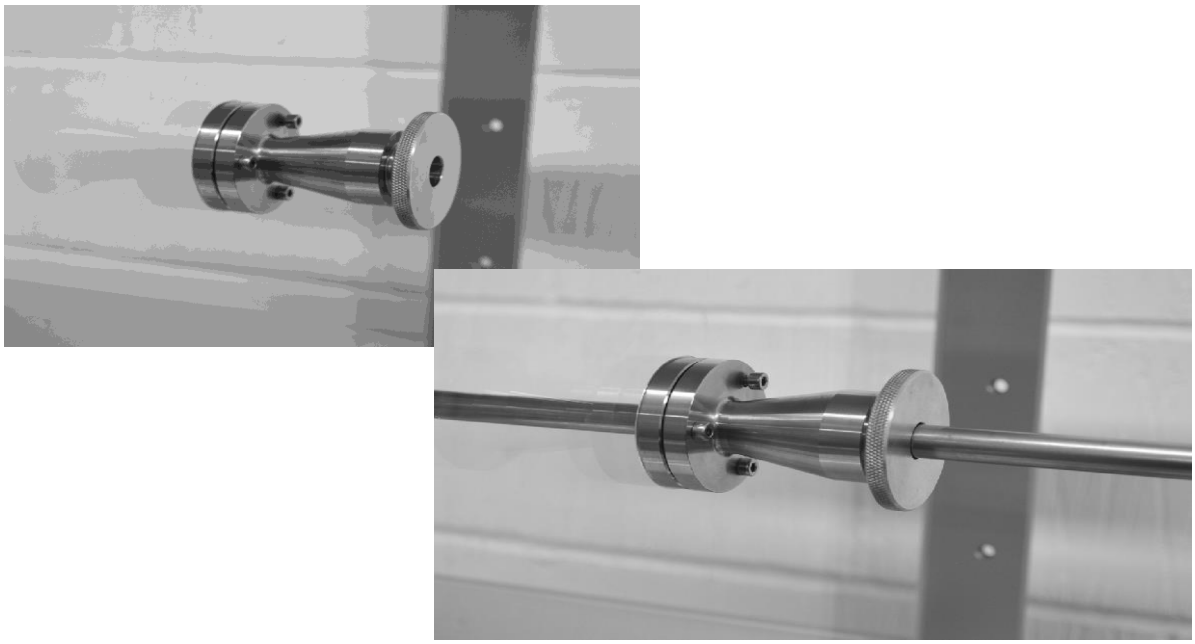

Figure 4. 13Fit the dummy Stem

13) Create a blank table of results similar to Table 1. If using the optional VDAS® software, it will automatically create a results table. Record the ambient temperature and pressure (in absoluteunits).
14) Start the Wind Tunnel, set the RPD to give a velocity (V) of about 15 $m.s^{-1}$. If using the optionalVDAS®, it will calculate this automatically, but remember to enter the correct values of ambientpressure and temperature.
15) Record the Drag value from the Three Component Balance display unit
16) Repeat the test for all models.

CHAPTER 5
COMMENTS AND RESULTS

5.1. Introduction

As we saw in the previous simulations the geometer shape is strongly influences the wake behind a shape on the hydrodynamic forces. Several articles and scientific research papers based on the study of this physical phenomenon and the importance of the problem have been found [32-36].

A deep understanding of a phenomenon determines the successful of a design. Like any phenomenon such as vortex shedding, more research needs to be done carefully to avoid damage or failure is inevitable. Although vortex meter has been known and many research done over the years, the nature of this vortex meter is still not fully recognized yet. It should be noted that many factors affect the phenomenon is defined worse (Pankanin, 2007).

Based on principle working of vortex flow meter, the speed of incoming flow affects to the measurement of the vortex shedding frequency and an unsteady phenomenon flow over a bluff body. Therefore, the bluff body shape plays an important role in determining the performance of a flow meter. Predicated on research conducted by Gandhi et al. (2004), the size and shape of bluff body strongly influence the performance of the flow meter and Lavish Ordia et al. (2013) also supported the statement by adding the least dependence Strouhal number on the Reynold number and minimum power will provide the stability of vortex.

According to Błazik-Borowa et al. (2011), although many methods have been proposed over the years to control dynamics of wake vortex, unfortunately the turbulence models still do not properly describe the turbulent vortex shedding phenomenon. The calculations results are not properly for all cases. Sometimes errors occur in a small part of calculation domain only, but sometimes the calculation results are completely incorrect. Thus, the computer calculation shall be checked by comparison with measurements results which should include the components of velocity and their fluctuations apart from averaged pressure distribution. The researches about geometrical shape of bluff body have been conducted by many researchers. However, the flow around circular, rectangular and triangular have been choose to get better understand fluid dynamics and related accuracy of numerical modeling strategies. The research was carried out with various bluff body shapes to identify an appropriate shape which can be used for optimize the configuration of the bluff body on the performance of flow meter.

We present in this chapter the results of the numerical simulations obtained by the calculation codes. Our problem concerns the study of aerodynamic behavior and numerical

simulation on different bodies to determine our drag coefficient Cd and lift coefficient Cl.

For this reason, seven simulations were carried out concerning respectively seven geometric shapes which are as follows: circle, semi -circle, flat plate (Trapezoidal Shape), rectangle, triangle and two airfoils (symmetrical airfoil NACA0040 and non-symmetrical airfoil NACA4412).

- For the first simulation we will calculate and trace the Cd and Cl curves by OriginPro 64b with the comparison between the results of the two calculation codes OPENFOAM 8 and ANSYS (fluent) at different Reynolds numbers (20,100 and 1000) and see the geometer effect on the drag and lift coefficients.
- For the second simulation we will trace the curves of Cd and Cl and calculate the Strouhal number in the Reynolds number equal to 200 By the calculation code OPENFOAM with the solver Piso Foam and we will compare the curves of the aerodynamic coefficients and the Strouhal number
- The third simulation is the numerical simulation of the flow around circular circle with slits be the flow around a circle with slits has been investigated numerically. The main purpose of this study is to show the effect of the slits on the vortex detachment behind a circle smooth, and stationary using the finite element approach to solve the fluid governing equations system at Re = 200.

  The variation of the angle of the slit is strongly influenced both the various physical parameters and the vortex detachment behind a circle. We found that the drag coefficient varies when I changed the angle of slits, we also found that the values of the Strouhal number vary when I use the slits
- For the fourth simulation we will measure the drag force and drag coefficients of each geometer using the ANSYS Fluent and compare between the two results and see the VIV phenomenon and the bodies effect on frequency generation.

5.2 Validation of Numerical Model

First, we validated our result of the flow around our shapes at Re = 100 and 200 with experimental results from Norberg [21] and Roshko [9] and other numerical simulations from Thompson et al. [8] Arnab Kumar[37] , C. Norberg[38] and arpnjournals[40] . After a series of simulations, it was found that the error between this present work and the experimental results do not exceed 15% and are shown in Tab 1. We studied the independence of the flow around seven shapes at Re = 10,100,200 and 1000 and after five (5) series of simulation, we found that the mesh of at 120000 elements gave sufficiently precise results compared with the articles and

studies experimental precedents.

Table5. 1 : Values of, CDav and St of different cases at Re =200

The case	circle	Semi-circle	rectangle	triangle	Flat plat	NACA4412	NACA0040
Elements	120000	-	160000	116500	-	125000	-
CDav	1.39	-	1.44	1.7607	-	0.12	-
St	0.198	-	0.165	0.1916	-		-

Table5. 2 : Values of, CDav and St of circle at Re =200

Studies	The Circle Case				
References	My study	Marouane Salhi	Williamson [22]	Braza et al. [23]	Experiment (St) Roshko [9]
CDav	1.35	1.45	-	1.35	-
St	0.198	0.208	0.196	0.200	0.16-0.17

Seven shapes so seven geometers and after this search bibliographic we can say that the circle case is the most common case in bibliographic search and we compare with the other numerical and experiments studies and get close results of our aerodynamics coefficients.

So, after this short search about von Karman phenomenon, we can apply this experience in our other shapes. So, we have almost a small and limited idea that shape type and the contact surface play an important role in determining the aerodynamics parameters and the Strouhal number (St).

5.3 Solution Method (Residual Interface)

Permanent flow problems are often solved by a pseudo-temporal process or an equivalent iterative scheme since the equations are non-linear.

These methods use successive linearization of the equations and the resulting linear systems are usually solved by iterative techniques. The method followed to reach the solution must have certain properties which are briefly summarized in the following:

After convergence, the results are retrieved and saved.

5.3.1 Study of the convergence and independence of the mesh

It doesn't take much for a finite element analysis to produce results. But, for the results to be

accurate, we need to demonstrate that the results converge to a solution and are independent of the mesh size. To get started, let's define some key terms:

- ✓ Convergence: Mesh convergence determines how many elements are needed in a model so that the results of an analysis are not affected by a change in the mesh size. The response of the system (stress, deformation)

will converge to a repeatable solution with decreasing element size.

- ✓ Mesh independence: After convergence, further refinement of the mesh does not affect the results. At this stage, the model and its results are independent of the mesh.

We can then plot the maximum vertical deviation based on the number of elements in the model. At some point, the system's response converges into a solution. Mesh refinement (the addition of additional elements) has little or no effect on the solution.

5.3.2 Visualization of results

We present below the results of the different simulation cases. Figure VI.4 shows the velocity and pressure contours around the structure for a Reynolds number. We find the well-known results of the flow around four geometric shapes.

Note that these results are not perfectly symmetrical, which is clearly visible on the pressure contours, and this is perfectly logical given the slight shift of the structure with respect to the computational domain.

5.4 The First simulation

- ➢ Vorticity contours at Re =100

From Figure 5.1, it was found that the all shapes are in laminar regime because the Reynolds number “20’’ is small so the velocity is very small so we can say we are in pair of vortices in the wake.

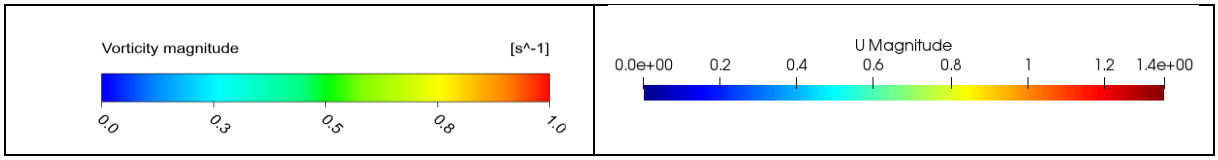

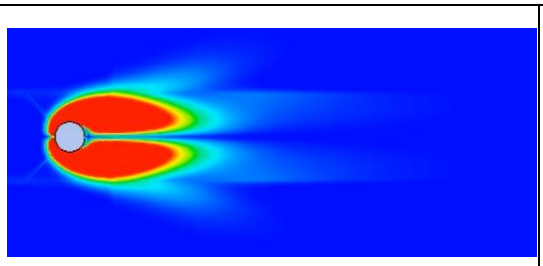
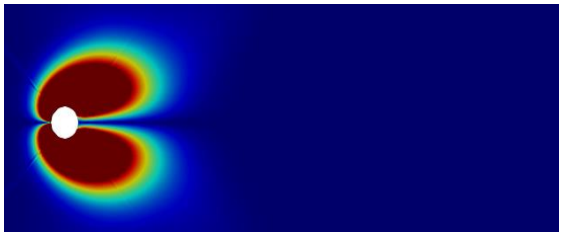
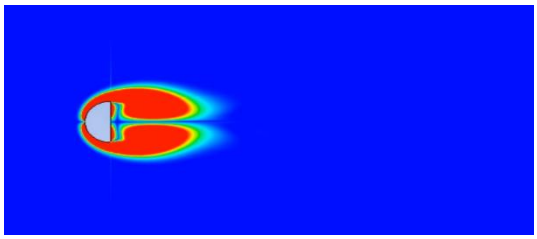
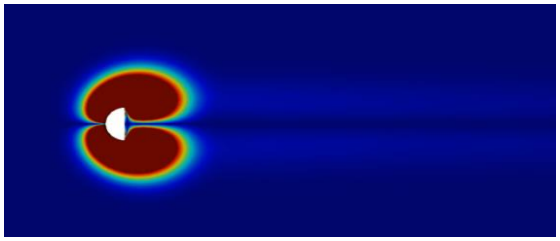
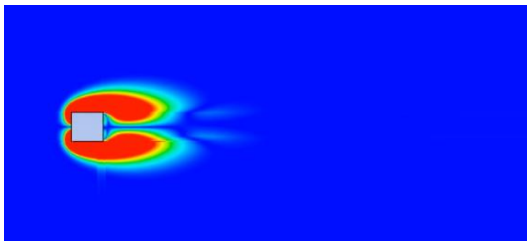
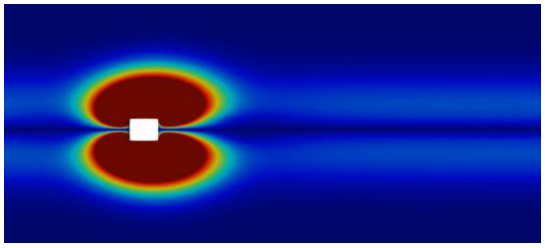
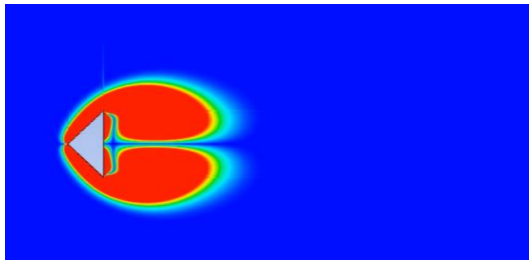
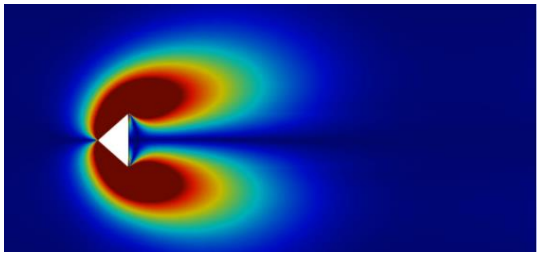
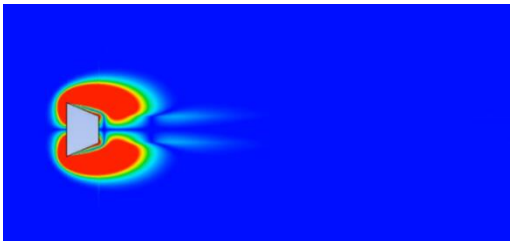
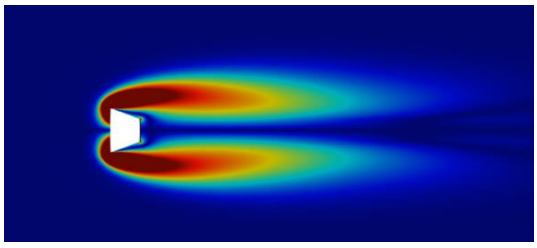
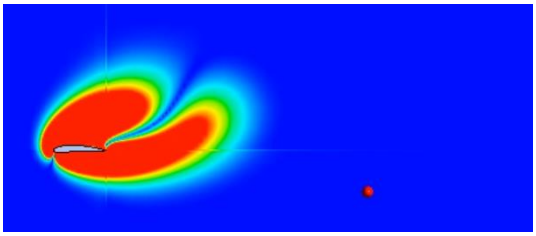
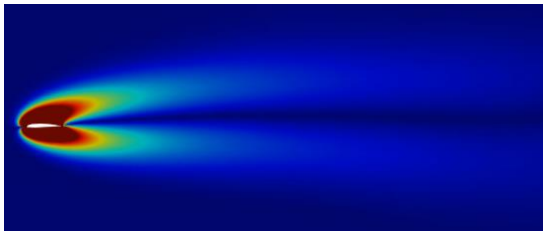

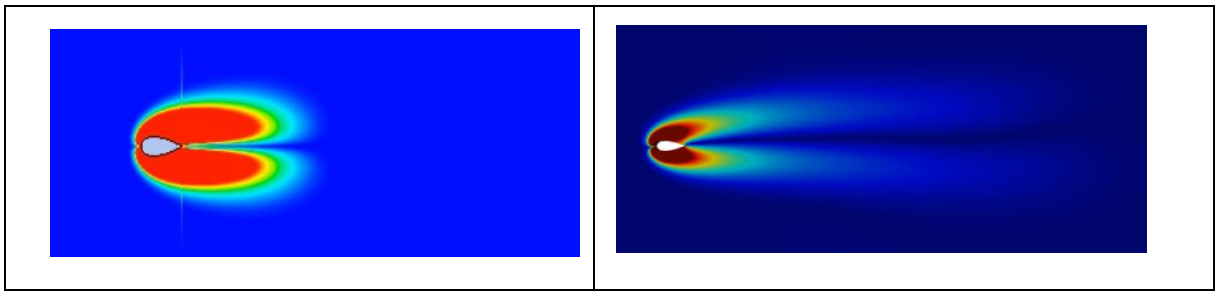

Figure 5. 1: Vorticity contours of all shapes at Re =20

After the first case of Re =20 we can say that the evolution of the vortices is very small because of the velocity magnitude is so weak, and We can also see a similarity in the display of the vorticity contour for both calculation codes, and we can see and say the OpenFoam display (in PARAVIEW) is better than fluent

- Vorticity contours at Re =100

From Figure 5.2, it was found that we have like two kinds of shapes because in the same Reynolds we have change of regime in many shapes and we have a shape is still in laminar regime and we have in Tab I.1 from the chapter one in the range of Reynolds number we can say this range is the start of von Karman vortex.

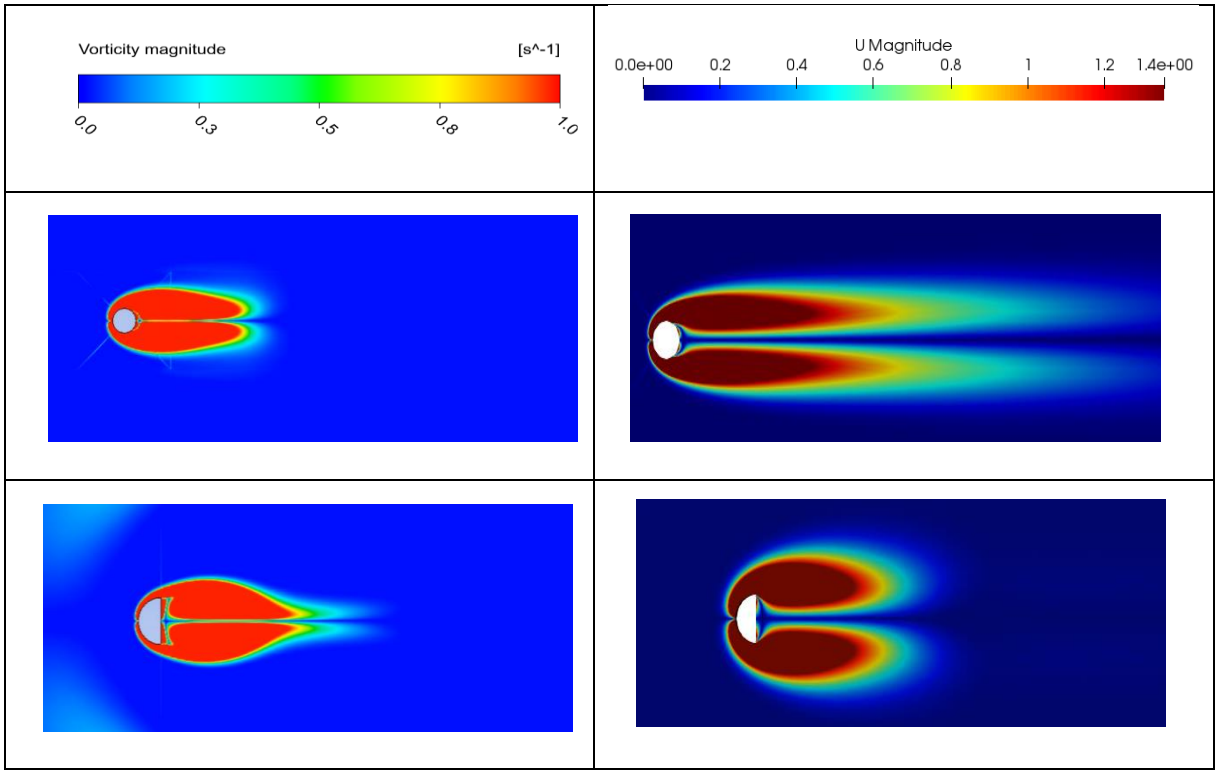

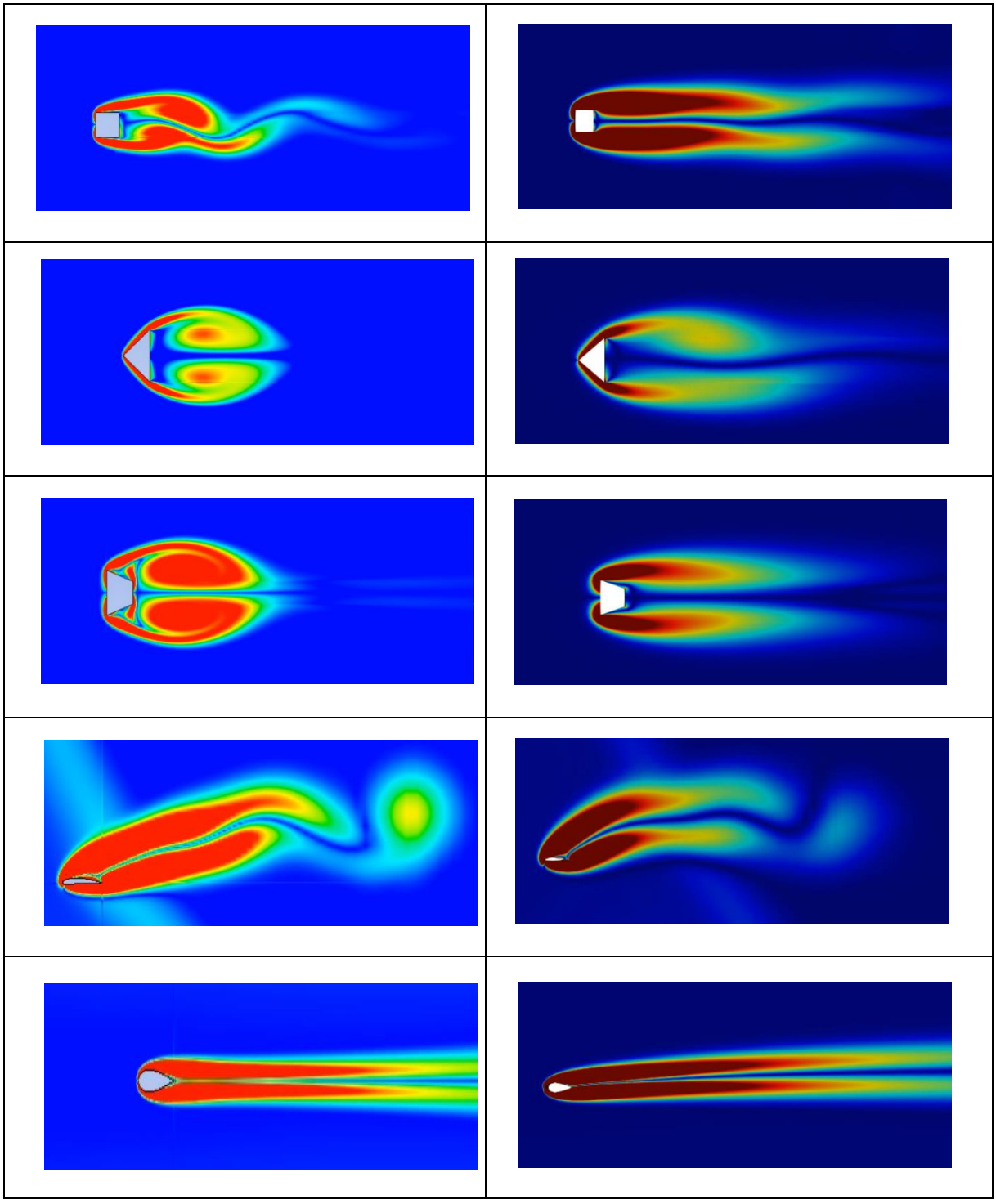

Figure 5. 2: Vorticity contours of all shapes at Re =100

The first case of Re =20 we can see that the evolution of the vortices is big compared with the previous case because of the velocity magnitude is bigger than the previous one, We can observes that the less aerodynamics cases like rectangle, flat plat and triangle is changed the regime, and We can also see a similarity in the display of the vorticity contour for both calculation codes, and we can also see the OpenFoam display (in PARAVIEW) is better than

fluent .

- Vorticity contours at Re =1000

In this range of Reynolds number, we can say we are pure vortex of Von Karman because we can see the vortex over our shapes but each form and how it produces these vortices is due to the type and dimension of each shape.

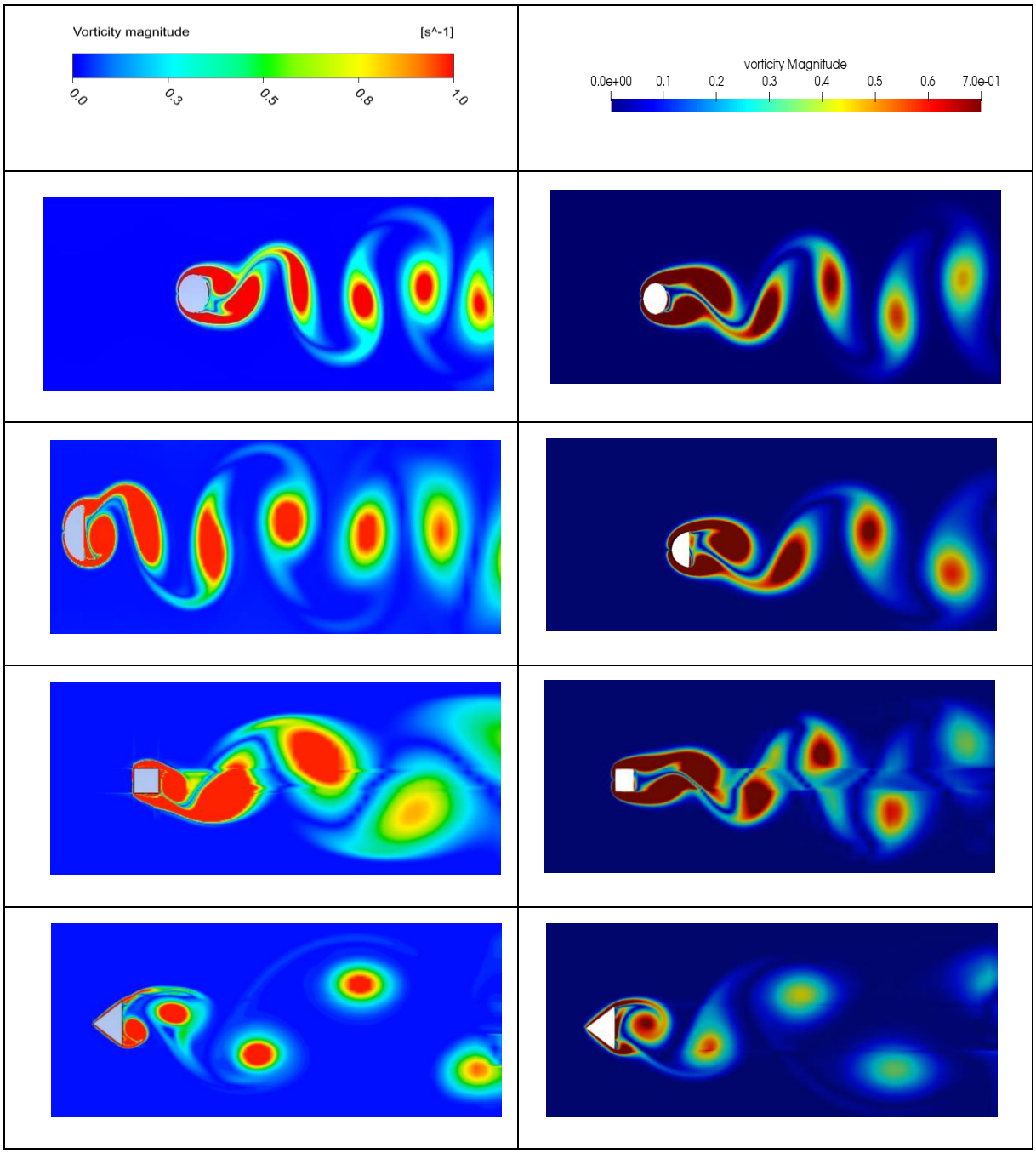

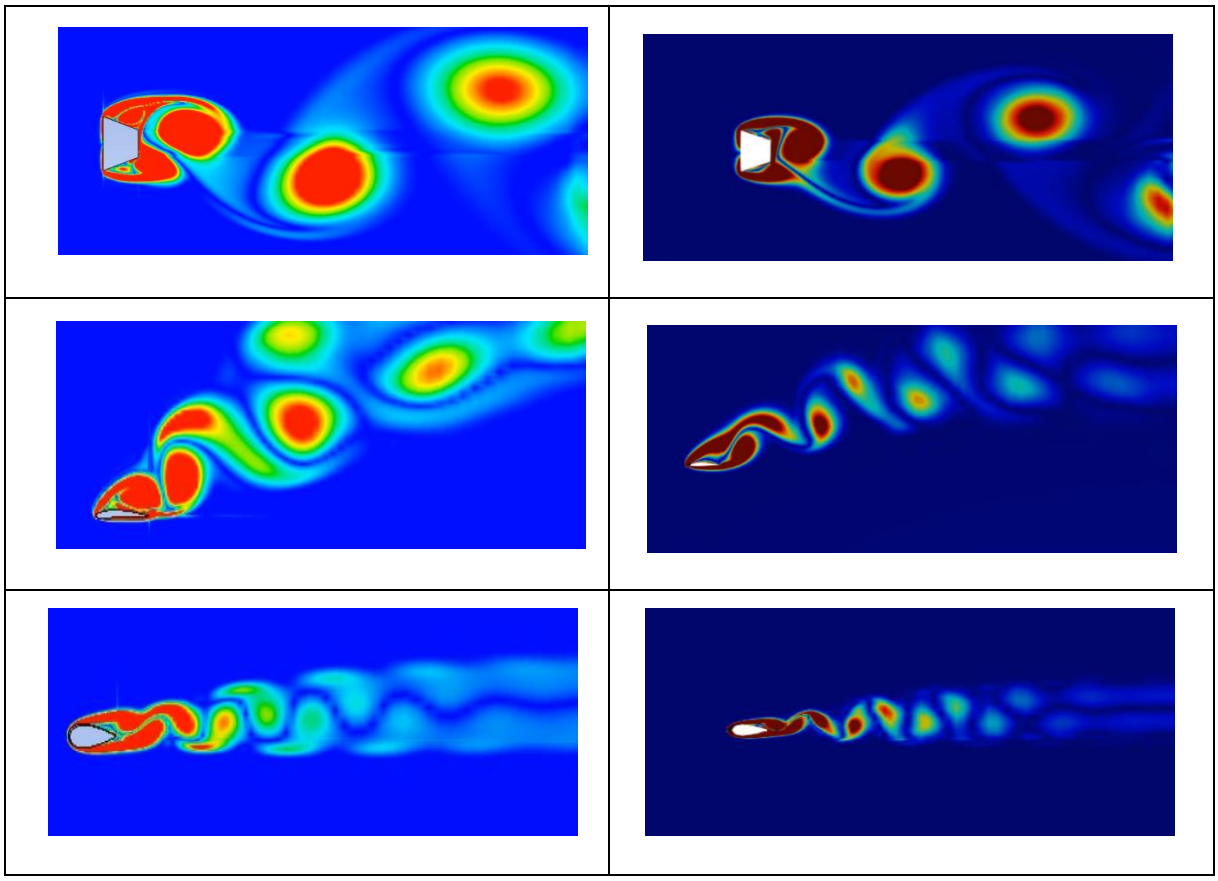

Figure 5. 3: Vorticity contours of all shapes at Re =1000

In the last case we can see that all shapes produced the vortex behind them so we can talk about the turbulent regime so we can say that the Reynolds critique of all shapes is less than 1000

5.4.1 Plotting Drag and Lift Coefficient Curves by OpenFoam and Fluent

After the simulation (seven shapes with 3 different Reynolds number) by the two-calculation code OpenFoam and fluent and the big similarity between the vorticity contours (using OpenFOAM and fluent) we will plot the curves of CDav and CLav using OriginPro 64b

- **Circle**

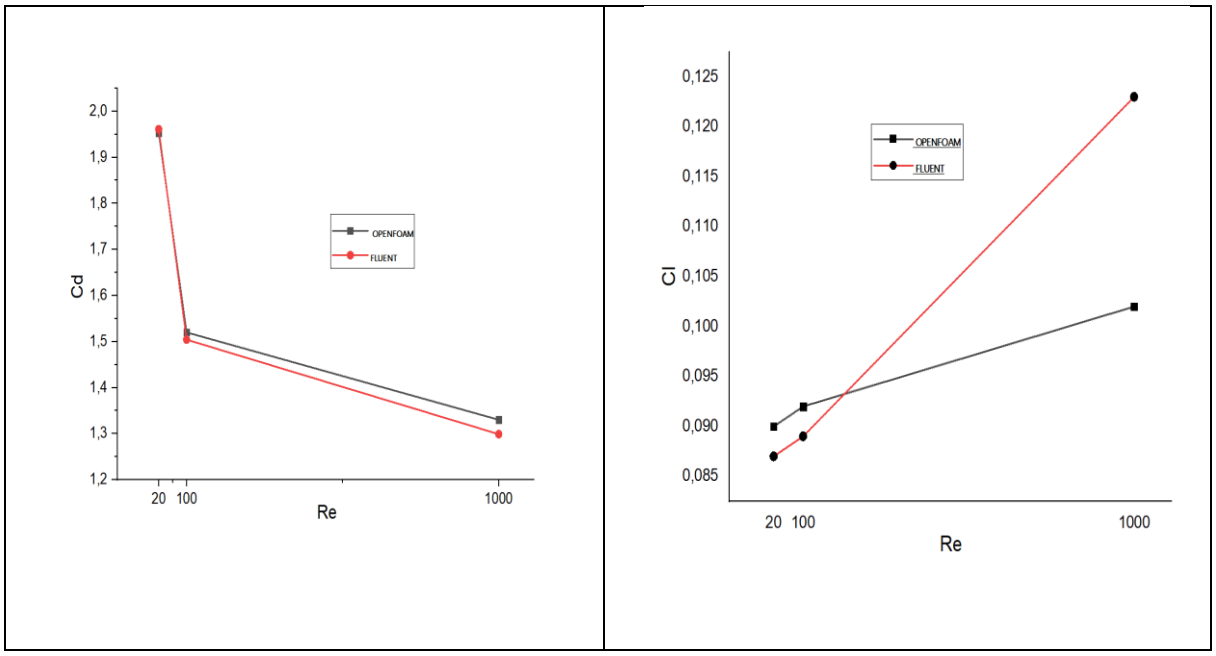

Figure 5. 4: Behavior of CDav and CLav of circle at Re =10,100 and 1000.

- **Semi -Circle**

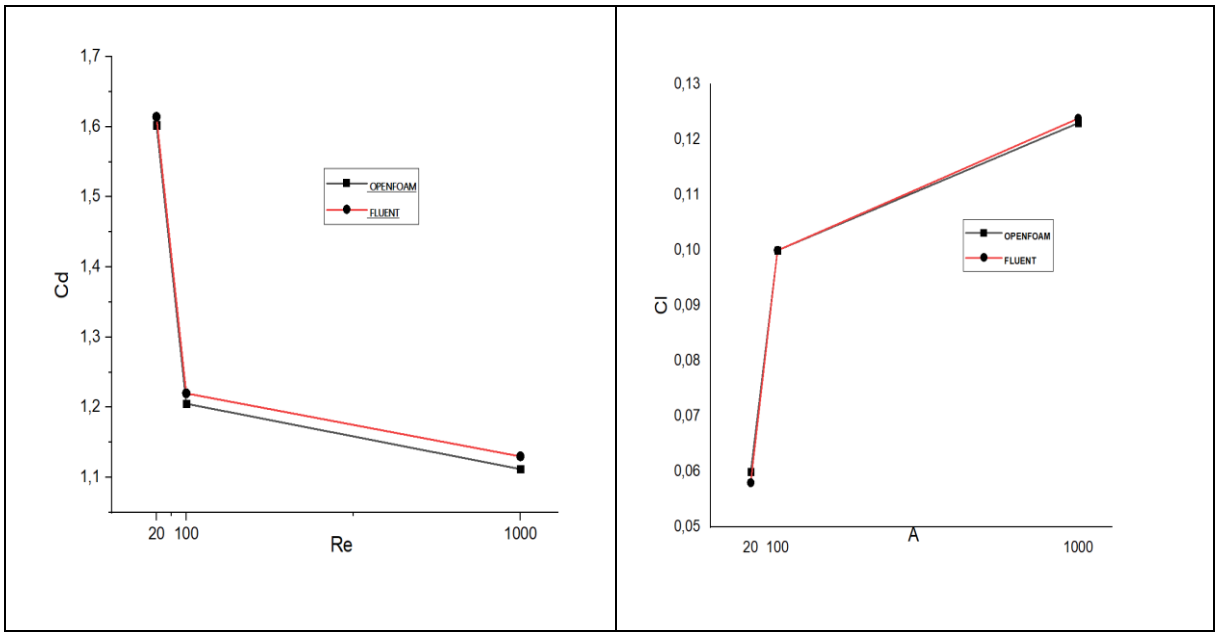

Figure 5. 5: Behavior of CDav and CLav of semi-circle at Re =10,100 and 1000.

- **Rectangle**

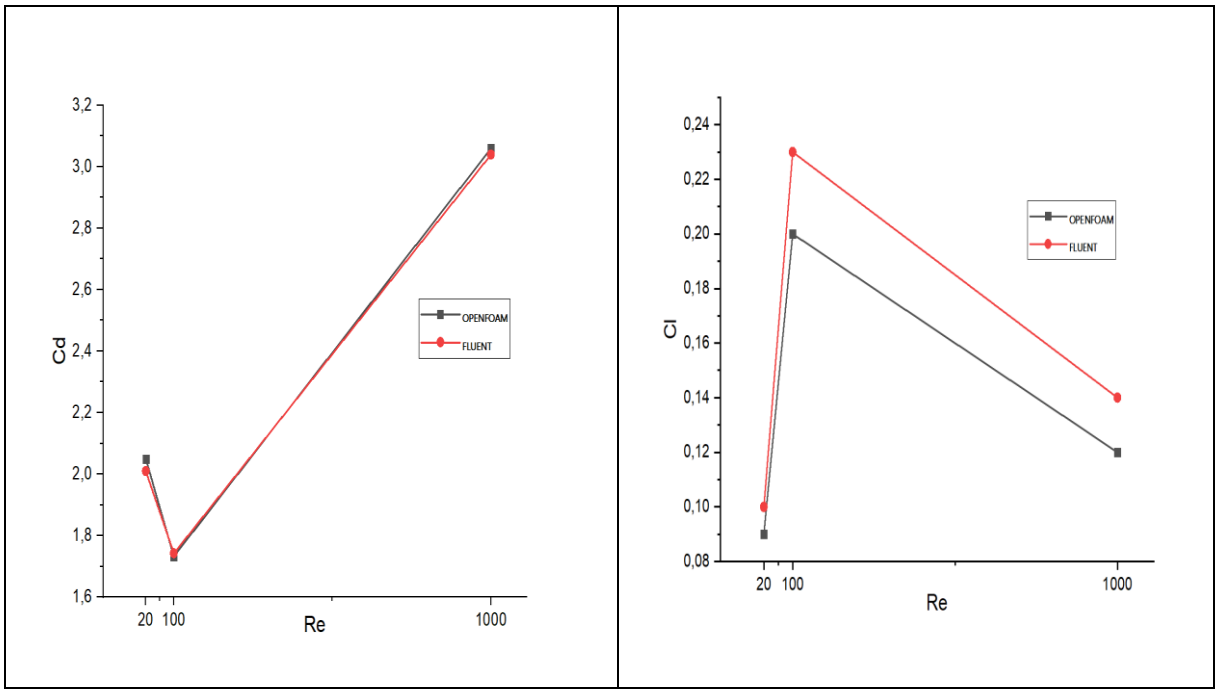

Figure 5. 6: Behavior of CDav and CLav of rectangle at Re =10,100 and 1000.

- **Triangle**

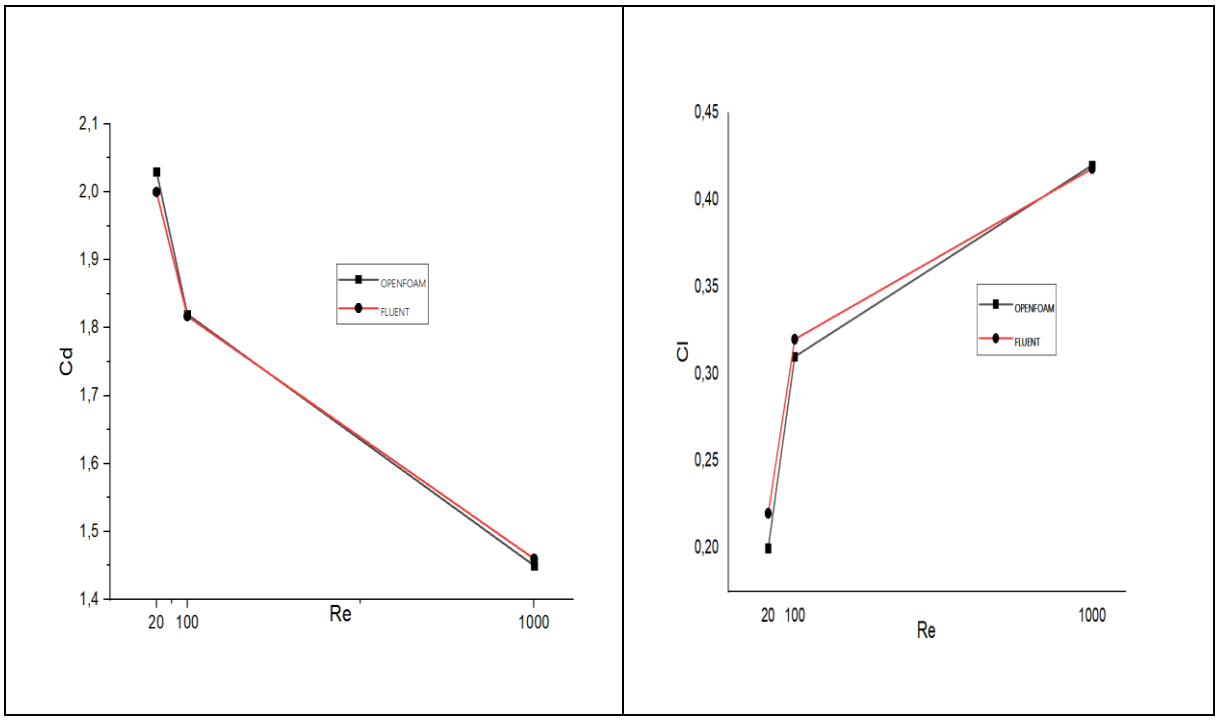

Figure 5. 7 : Behavior of CDav and CLav of triangle at Re =10,100 and 1000.

- **Flat Plate**

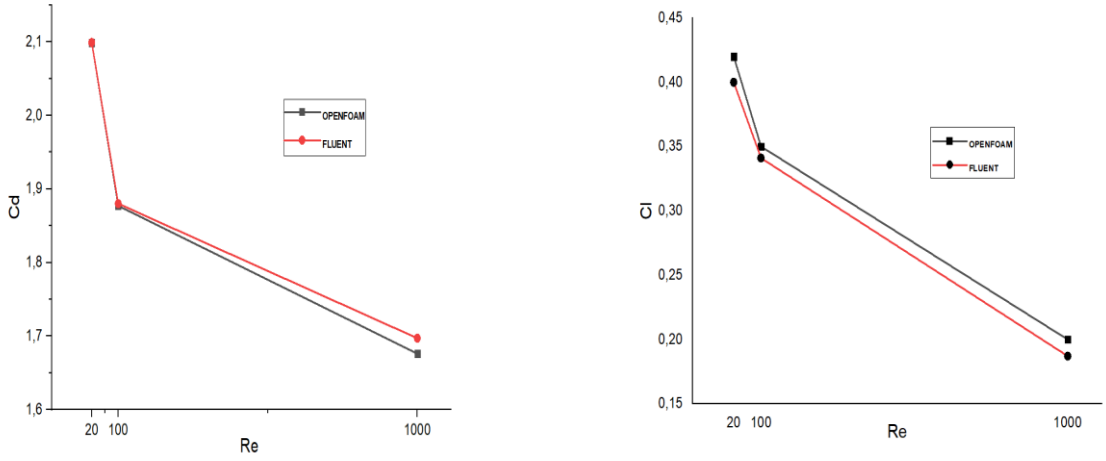

Figure 5. 8 Behavior of CDav and CLav of Flat Plate at Re =10,100 and 1000.

- **NACA4412**

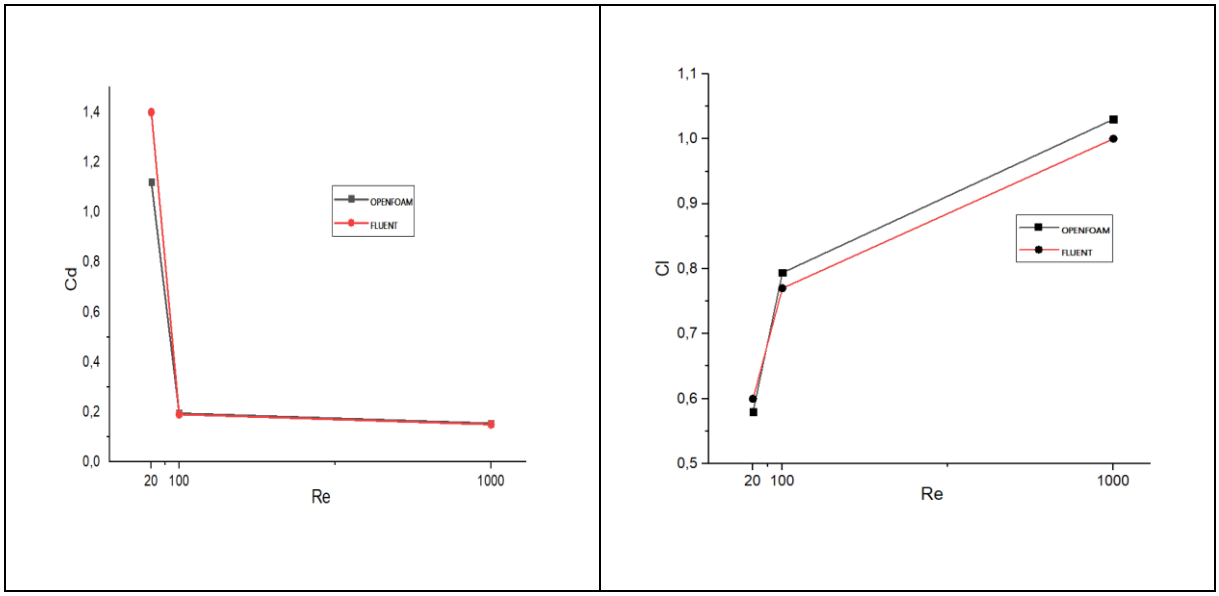

Figure 5. 9 Behavior of CDav and CLav of NACA4412 at Re =10,100 and 1000.

- **NACA0040**

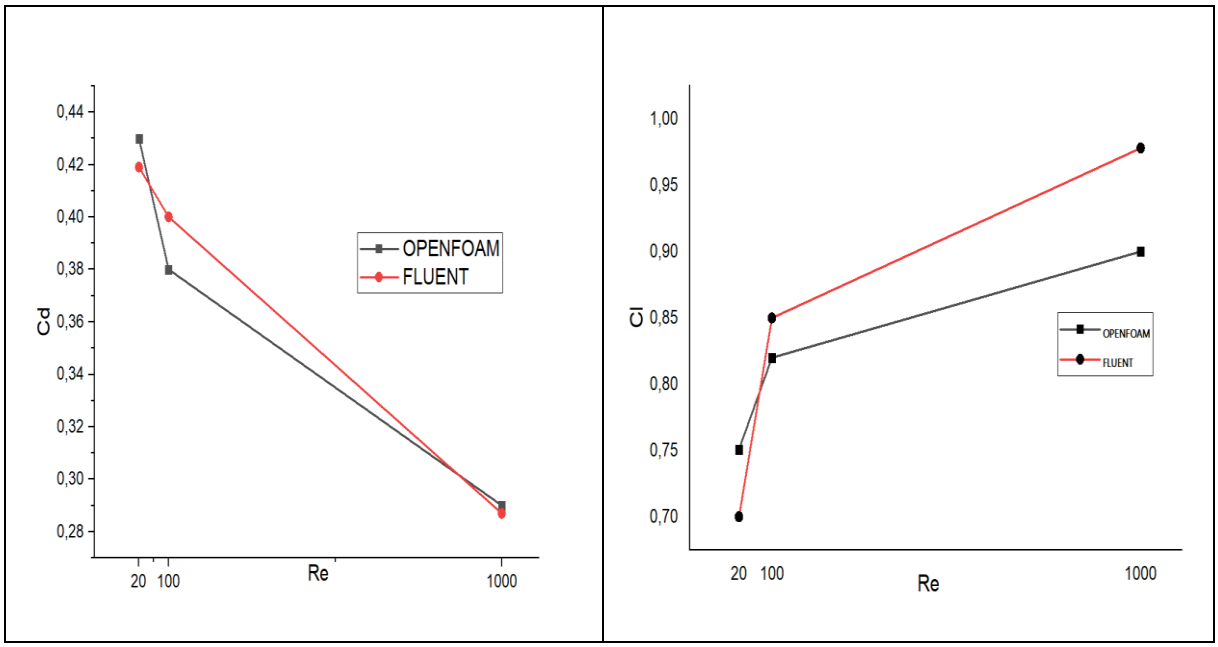

Figure 5. 10 : Behavior of CDav and CLav of NACA0040 at Re =10,100 and 1000.

From the previous curves designed by ANSYS and OPENFOAM of the aerodynamics coefficients we can see that the results of the two calculation codes are so close and we can see that when we see the figures of the vorticities

5.5 The second simulation

In this part we simulate our seven shapes at Re =200 by OpenFOAM and compare our aerodynamics coefficients and the St.

5.5.1 Visualization of Streamlines

For 200 < Re < 2.1056, the wake is turbulent and the regime is called subcritical in this regime, the flow is turbulent in the wake but the boundary layer upstream of the detachment point remains laminar. At low Reynolds numbers, small secondary eddies develop on either side of the vortex alley following the amplification of the local Kelvin Helmholtz instability in the shear zones around the sphere. As the Reynolds number increases (Re - 2600), this instability is more pronounced and covers a significant region of the mixing zone, Figure 1.9. Regime under criticism. So, we going to represent the results of

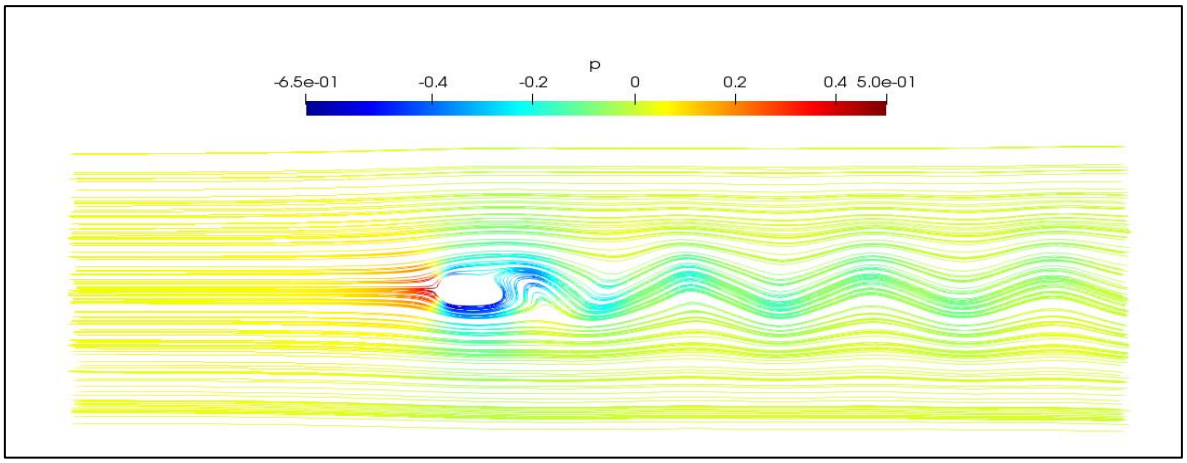

Figure 5. 11: streamlines of circle at Re =200

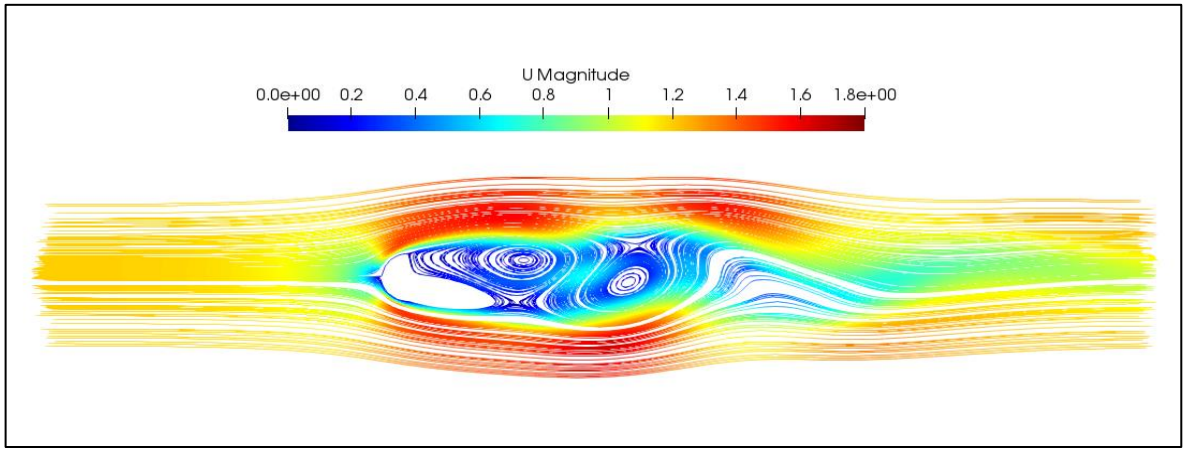

Figure 5. 12 : streamlines of semi-circle at Re =200

.

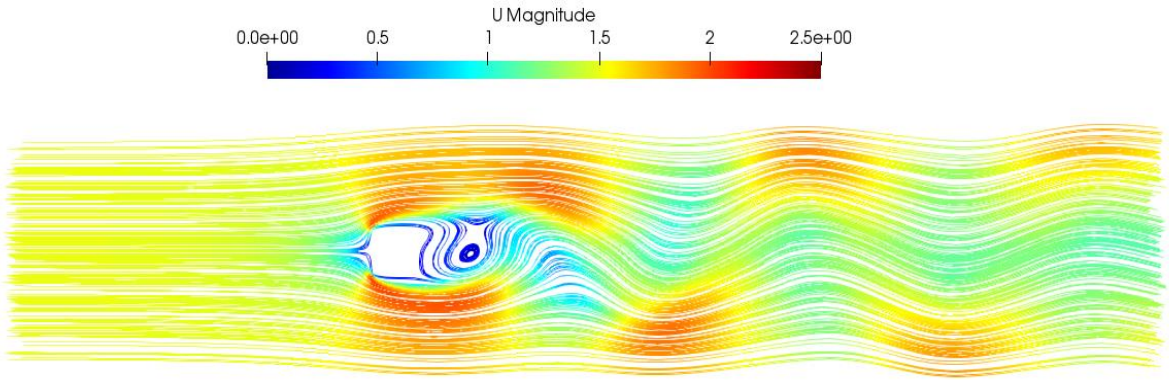

Figure 5. 13: streamlines of rectangle at Re =200

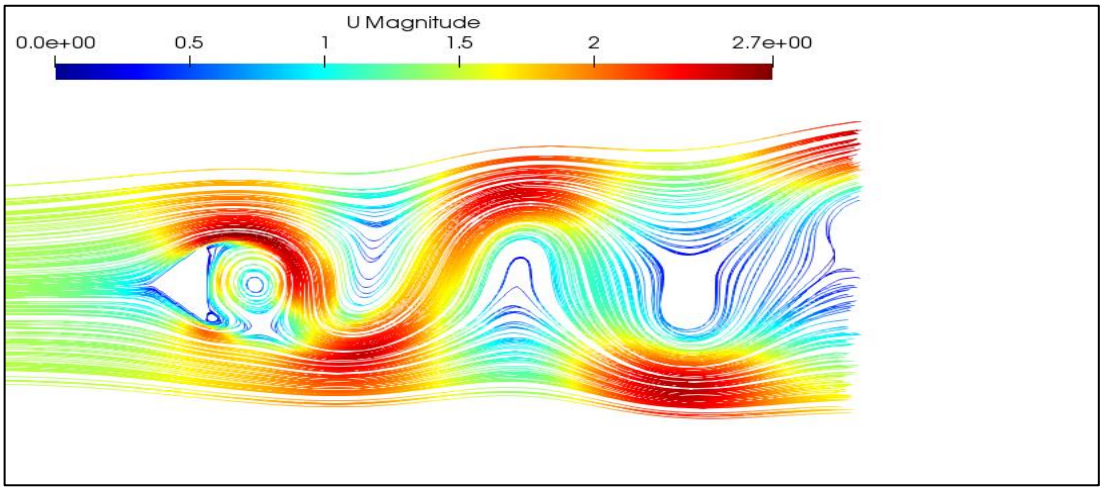

Figure 5. 14 streamlines of triangle at Re =20

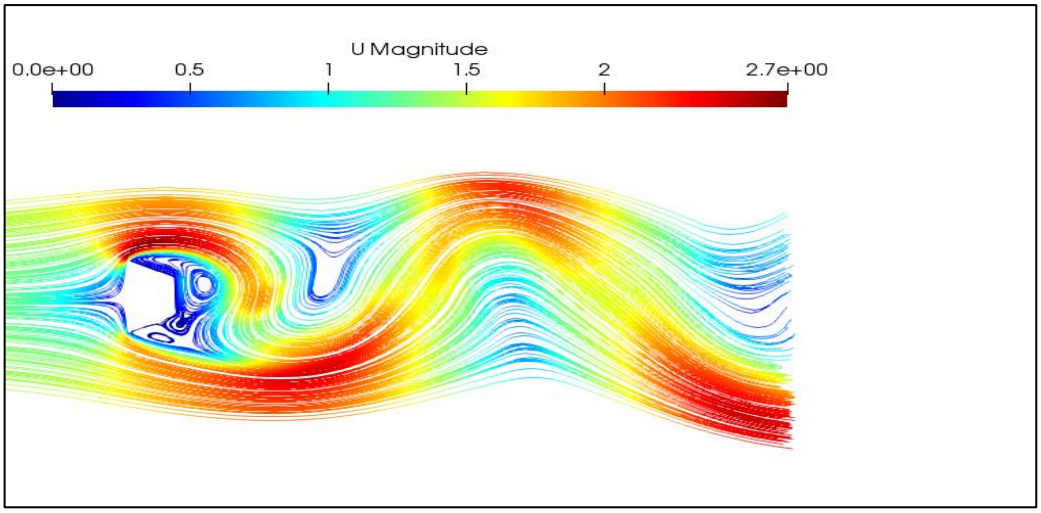

Figure 5. 15: streamlines of flat Plate at Re =200

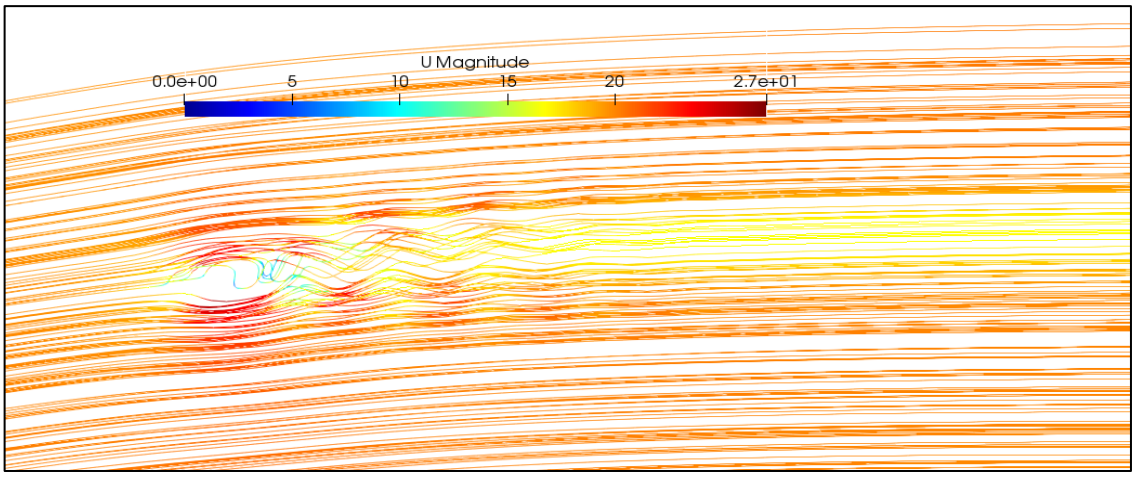

Figure 5. 16: streamlines of NACA0040 at Re =200

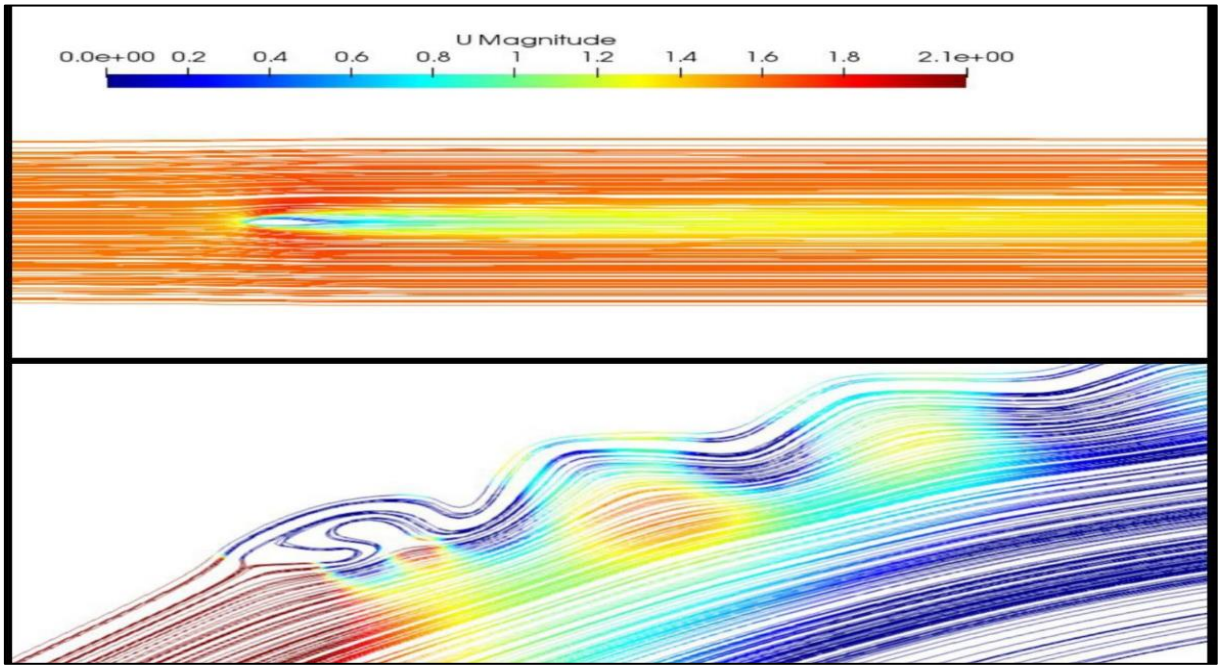

Figure 5. 17: streamlines of NACA4412 with AOA=à=0° and AOA=36°recpectively at Re =200

The vortices associated with this higher frequency phenomenon than the vortex escapement due to von Kármán instability, periodically detach and interact with the primary vortices. The frequency f of this instability in relation to the Strouhal frequency has been the subject of numerous studies.

5.4.3 Contour of the resulting pressure

This regime is reached when the transition point that rises upstream during the critical regime reaches the point of detachment.

The value of this critical Reynolds number varies significantly according to the different experimental studies (between 10 and 30000) because of the high sensitivity of the flow to the boundary conditions of the flow (turbulent intensity of the incident flow, elongation ratio and roughness of the flat plate and semi-sphere, etc.).

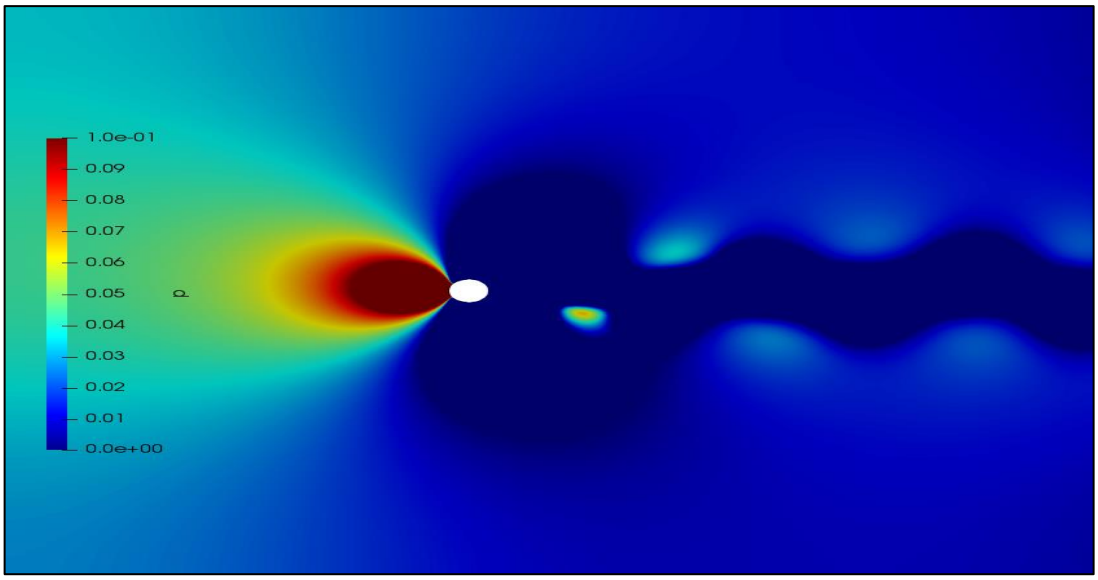

Figure 5. 18 : pressure contour of circle at Re =200

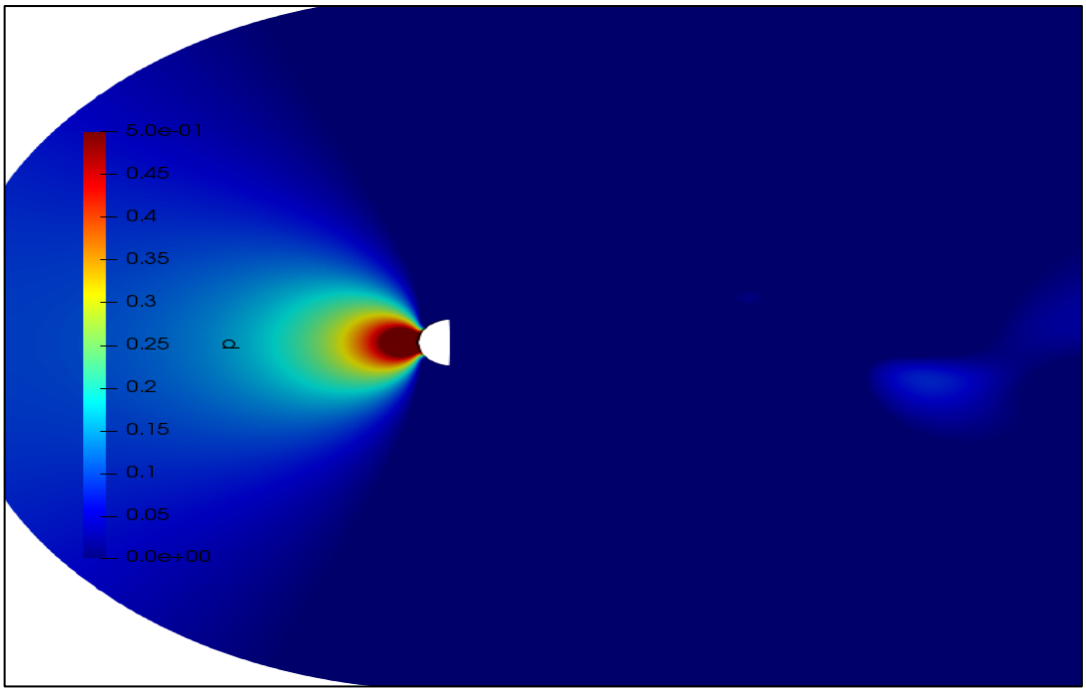

Figure 5. 19 : pressure contour of Semi circle at Re =200

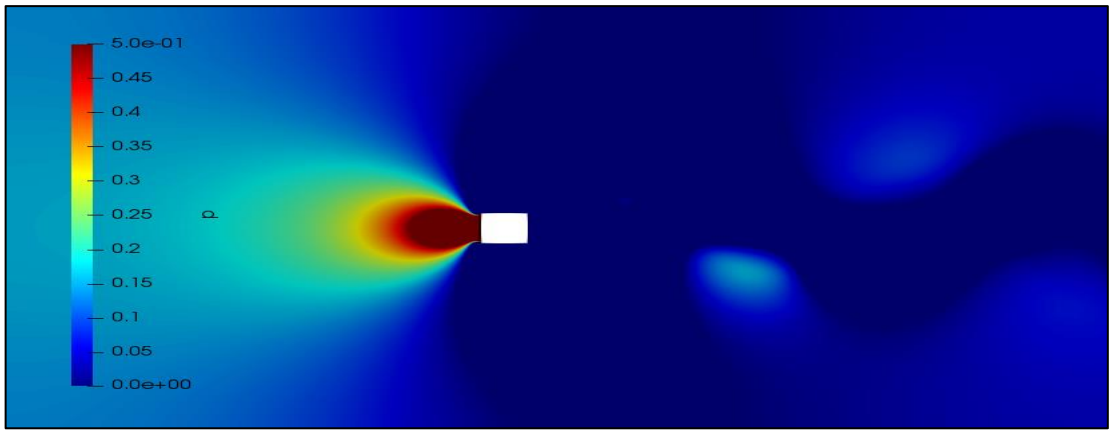

Figure 5.20: pressure contour of rectangle at Re =200

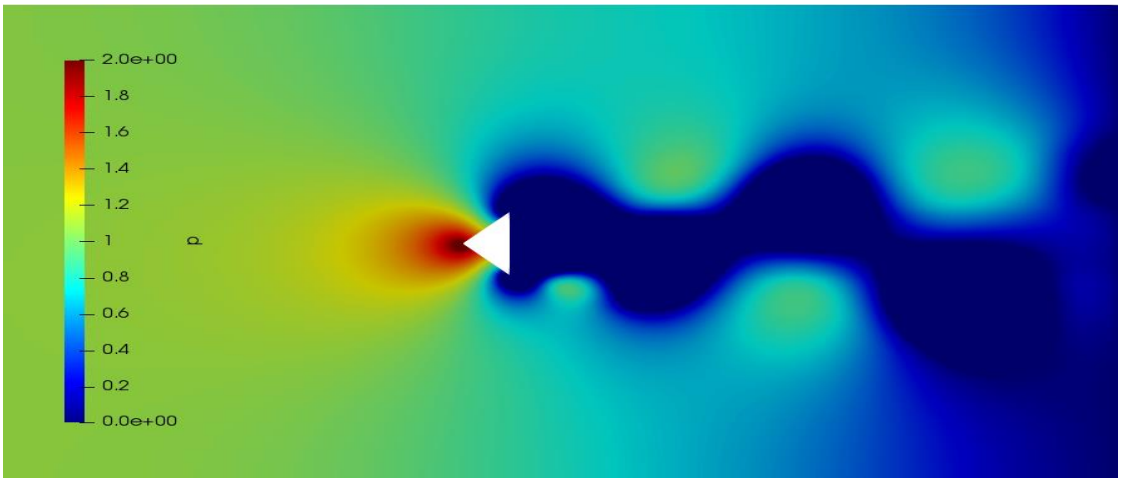

Figure 5. 20: pressure contour of triangle at Re =200

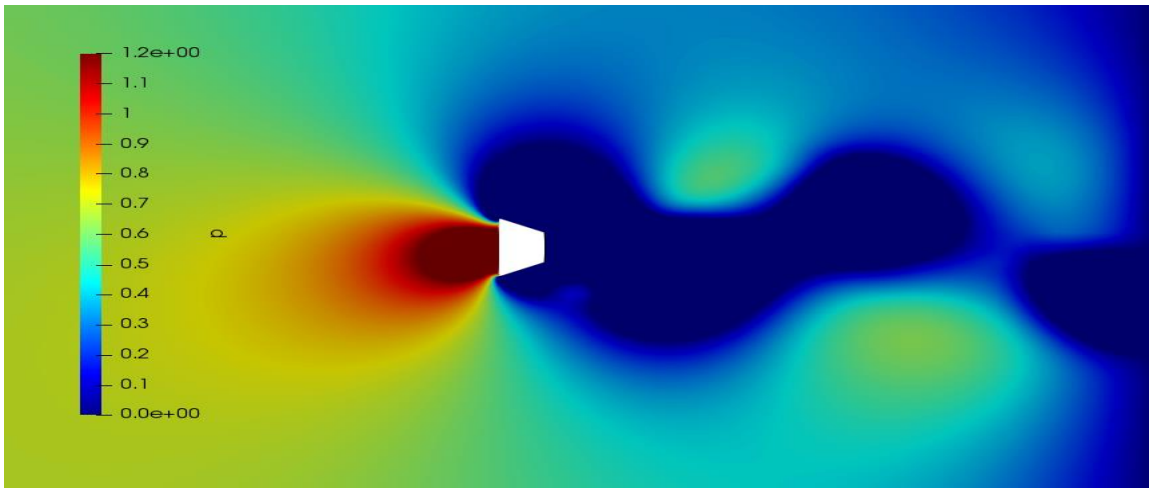

Figure 5. 21: pressure contour of Flat plate at Re =200

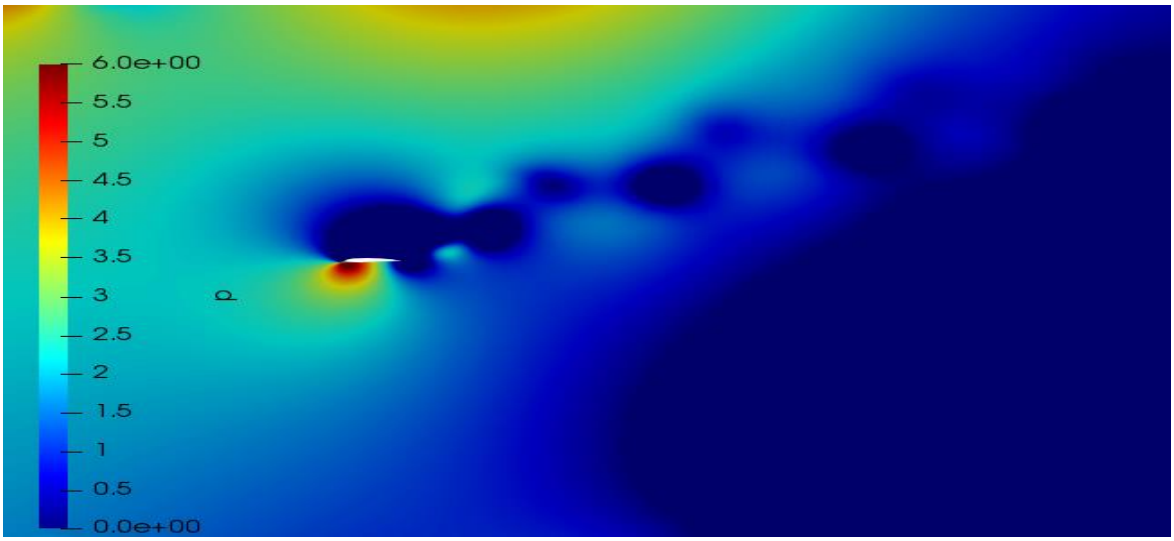

Figure 5. 22: pressure contour of NACA4412 at Re =200

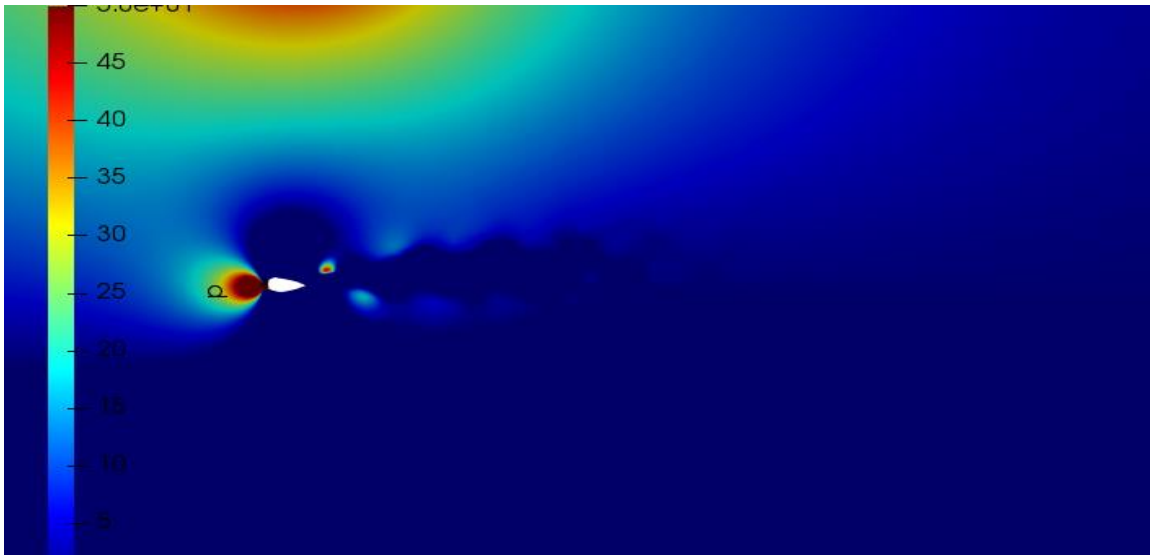

Figure 5. 23 : pressure contour of NACA0040 at Re =200.

5.5.2 Vorticity Contours

Less aerodynamic shapes and shapes with a large surface area give higher coefficient of friction values. The coefficient of friction depends on how the air passes around the object and leaves.

This means that the wake (flow pattern behind the object) also affects the drag. A wide wake creates more drag than a narrow wake behind an object. Therefore, even the shape of the object behind the frontal area affects friction.

- **Circle**

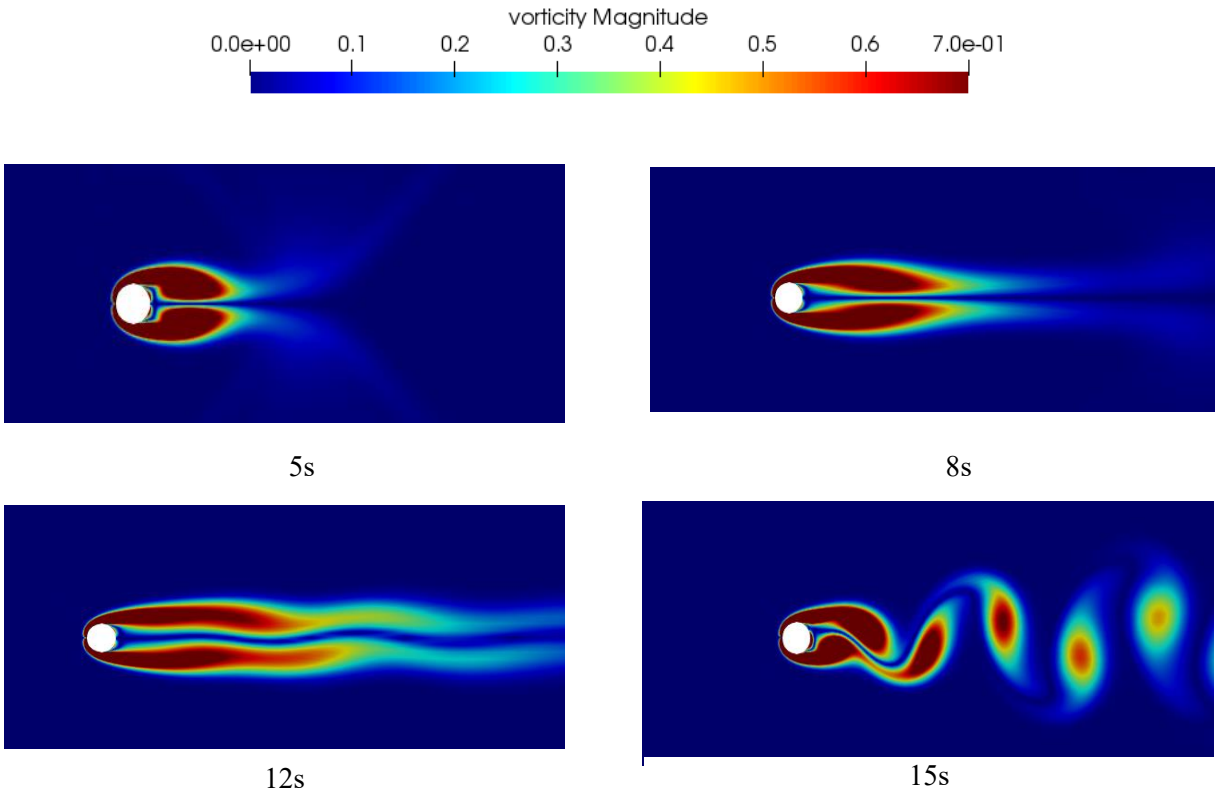

Figure 5. 24 : Evolution of vortex field of circle at Re=200.

- Semi circle

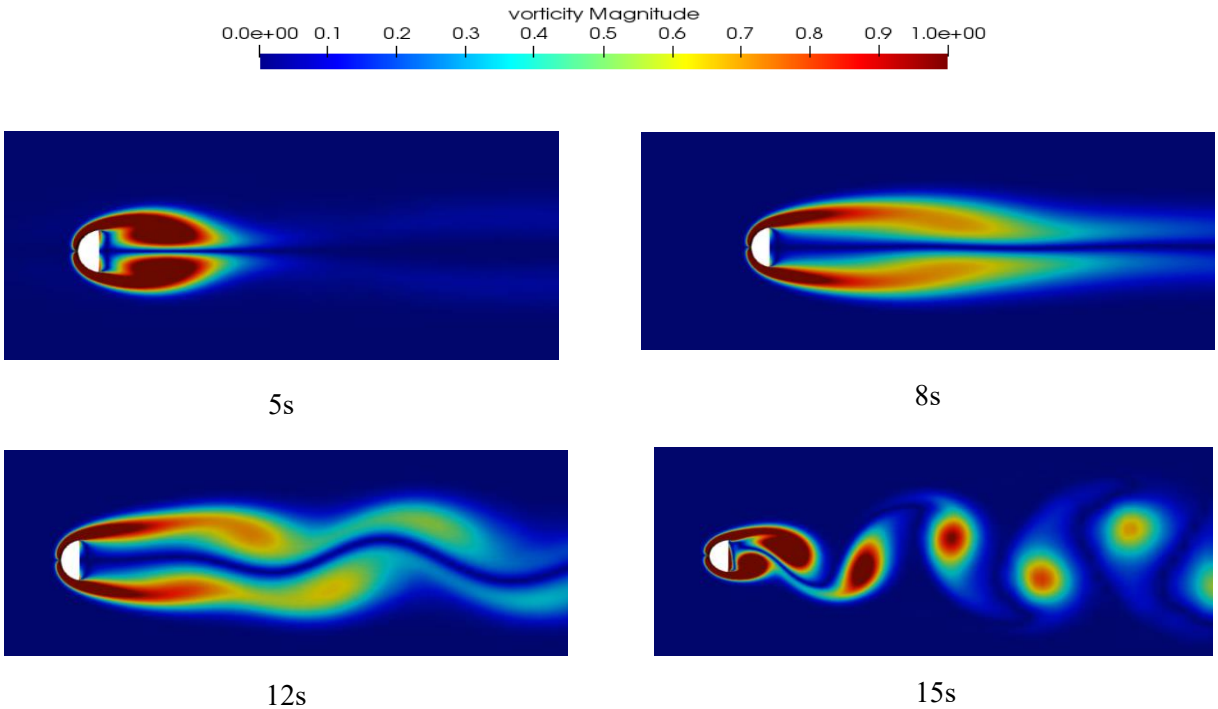

Figure 5. 25 : Evolution of vortex field of semi-circle at Re=200.

- Rectangle

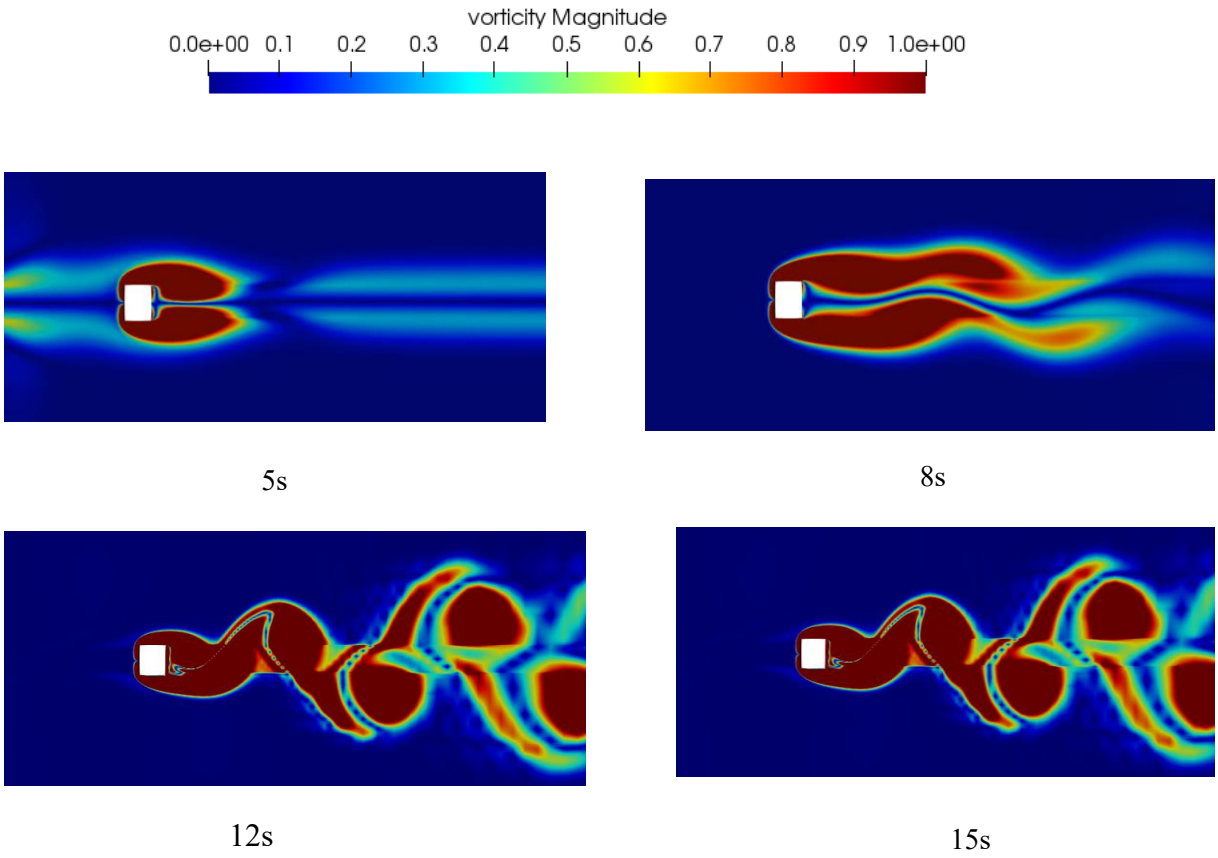

Figure 5. 26 : Evolution of vortex field of rectangle at Re=200.

- Triangle

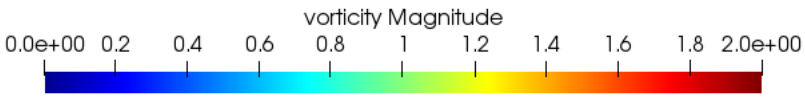

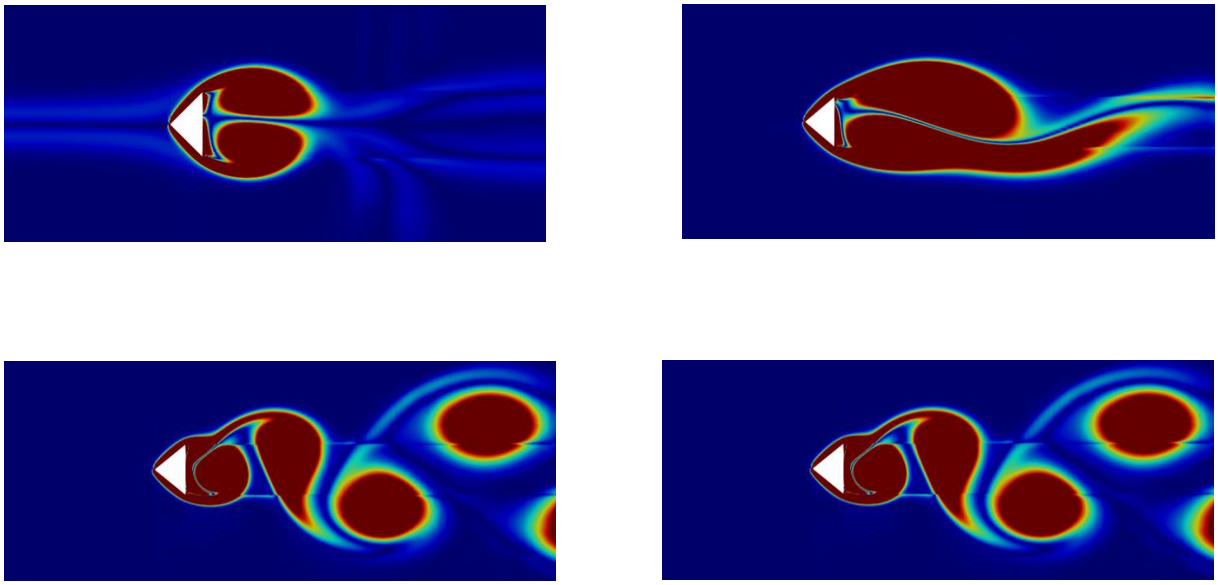

Figure 5. 27 Evolution of vortex field of triangle at Re=200

Flat plate

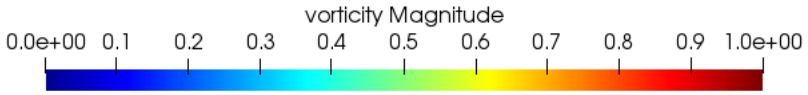

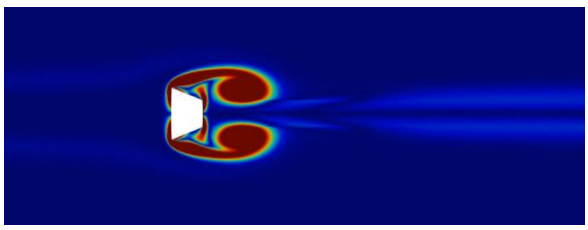

5s

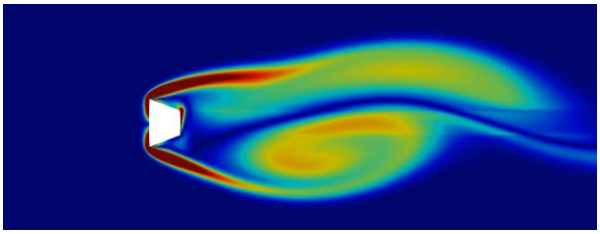

8s

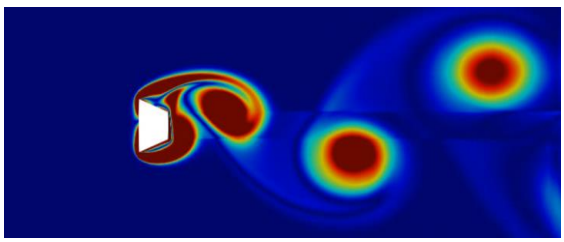

12s

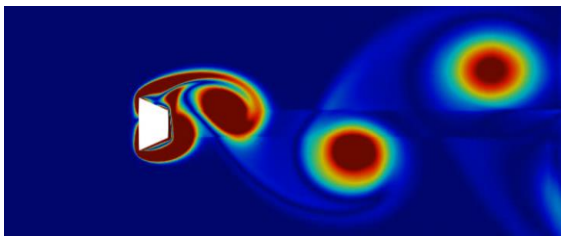

15s

Figure 5. 28 Evolution of vortex field of NACA4412 at Re=200

- NACA4412

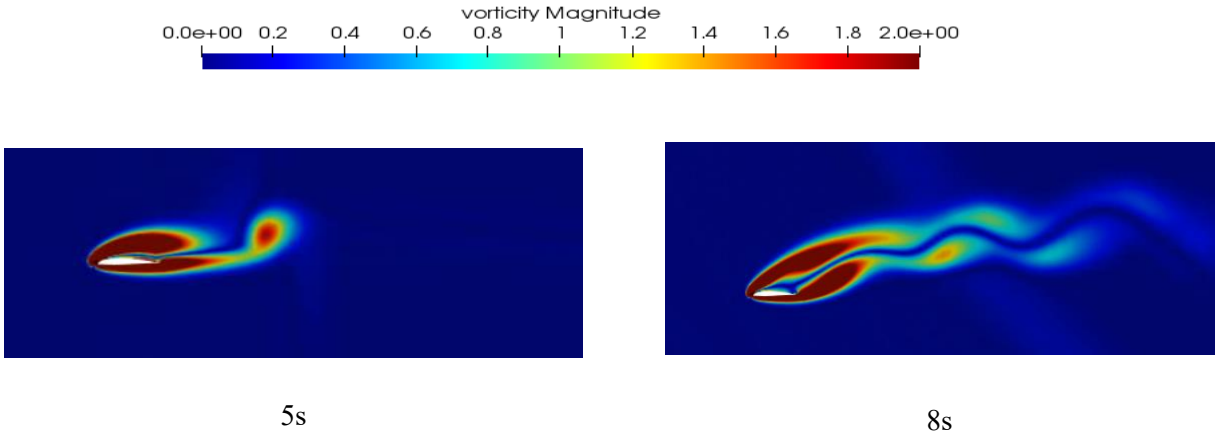

5s

8s

15s

Figure 5. 29 : Evolution of vortex field of NACA4412 at Re=200.

- NACA0040

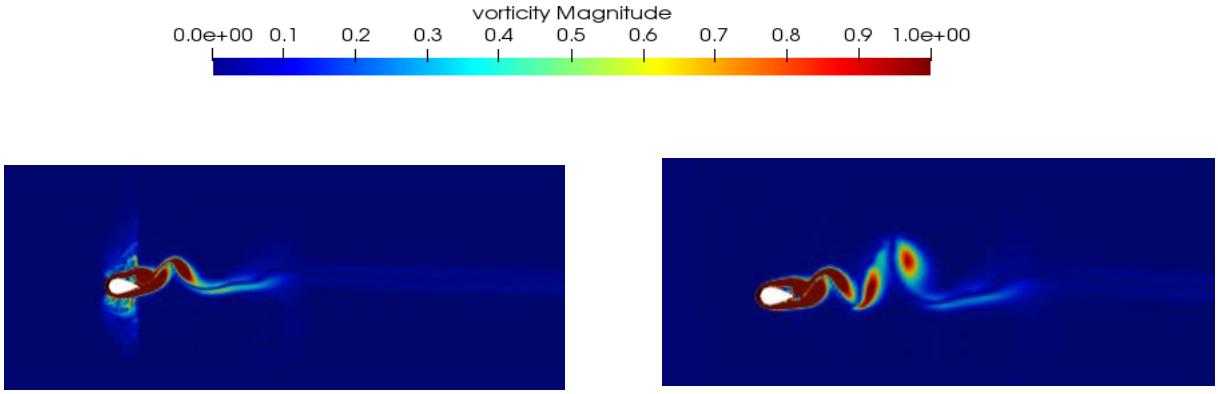

5s

8s

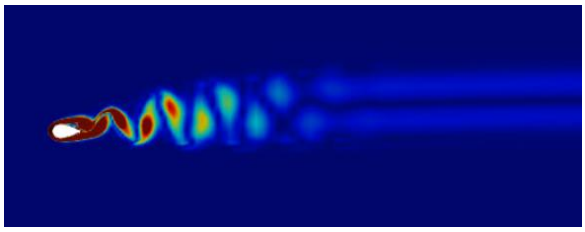

15 s

Figure 5. 30 : Evolution of vortex field of NACA0040 at Re=200.

5.5.3 Behavior of drag coefficient

The variation of the average drag coefficient as a function of the shapes is shown in Fig5.31. The drag coefficient curves are periodic and varied, so the amplitude and period depend on the geometer. When the going more be more of the shape be non-aerodynamically, the period is increased but the amplitude is decreased. This is especially true in the case of rectangle and flap plat compared with the case of airfoils. Therefore, the geometer strongly weakens the appearance of vortex detachment and influences the wake structure.

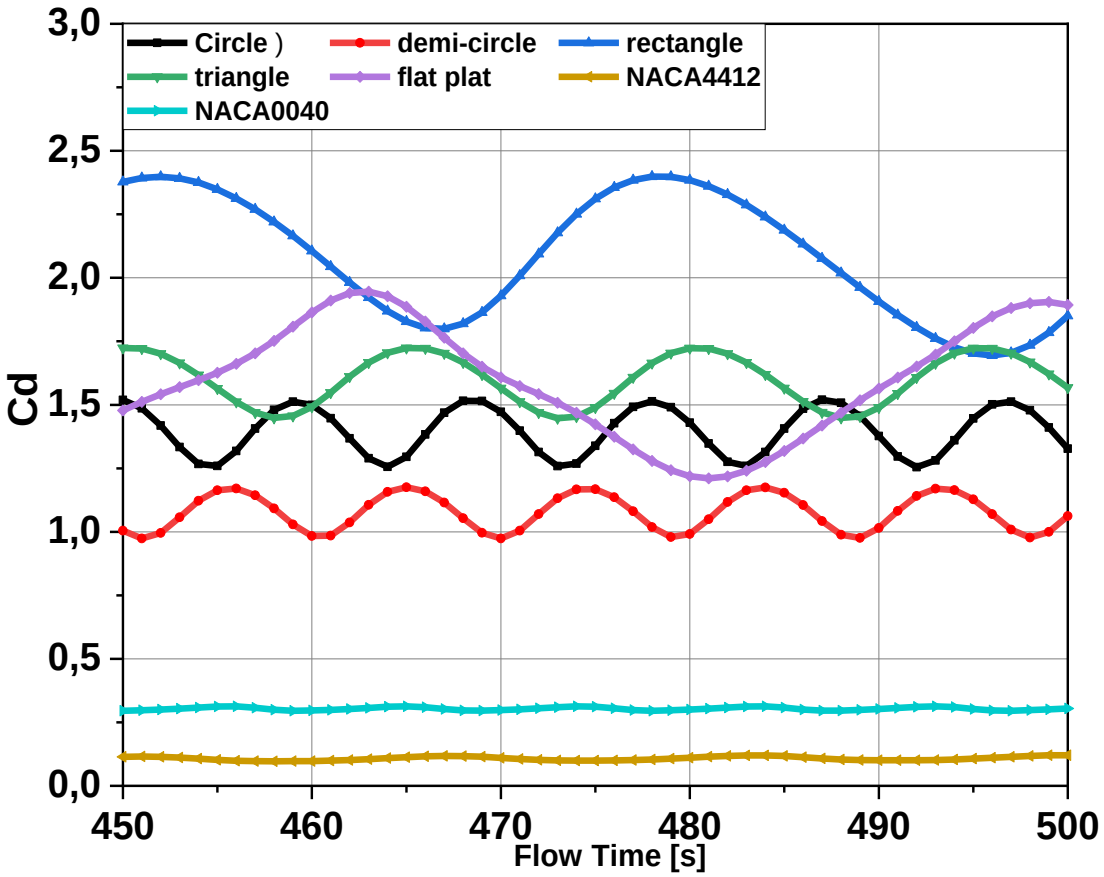

Figure 5. 31 : Behavior of CDav with shapes at Re =200.

5.5.4 Behavior of lift coefficient

The variation of the average lift coefficient as a function of the shapes is shown in Fig5.32**.** The drag coefficient curves are periodic and varied, so the amplitude and period depend on the geometer. When the going more be more of the shape be non-aerodynamically, the period is increased but the amplitude is decreased. This is especially true in the case of the airfoil NACA4412 compared with the case of semi. Therefore, the geometer strongly weakens the appearance of vortex detachment and influences the wake structure.

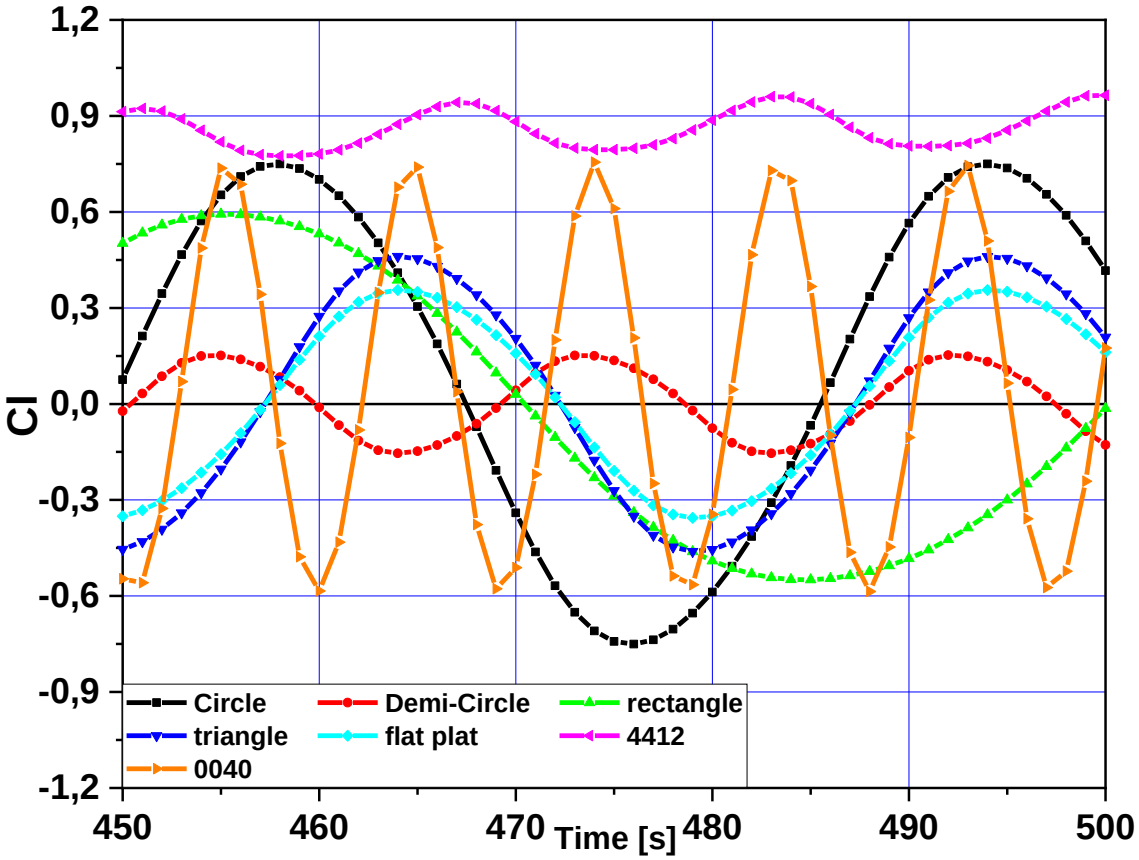

Figure 5. 32 : Behavior of CLav with shapes at Re =200.

5.5.5 Strouhal number

Tab.5.4 shows the variation of Strouhal number (St) as a function of our case. This parameter represents the intensity of vortex detachment behind a circle. And we know from [3] and for $200 \leq Re \leq 300000$ the Strouhal numbers remain approximately constant and St = 0.2 (the case of circle is the perfect case in the Strouhal number) is good and perfect results for it.

According to FigV.29**,** the Strouhal number varies with the shape (the geometer). It shows a increase in the case of the of semi- circle and NACA0040 and decrease in the case of triangle and rectangle and gave us results close in the cases of NACA 4412 and triangle with the circle's results

Table5. 3 : Values of, CDav and St of circle at Re =200

	Circle	Semi-circle	Rectangle	Triangle	Flat Plat	NACA4412	NACA0040
St	0.213	0.18	0.18	0.197	0.14	0.154	0.16

5.6 Conclusion

Figures (5.1,5.2,5.3) represent the vorticity contours behind the shapes by the two calculation codes OPENFOAM and FLUENT respectively.

As we see in this figure the gradual rise of the vortex behind each of the previous shapes, The vortex behind the shapes rise gradually with the Reynolds number, so it increases with V∞

We know that the Von Karman vortex is determined by periodic detachment of alternating pairs of vortices that bluff a body immersed in a flow of fluid, this phenomenon appear at low Reynolds Number (10-2500) when the Vitesse is very low so it can be so clear when the flow passed our shapes.

From the of the vorticities, we can say that each of the previous shapes has a Reynolds number through which it changes its regime, and this is dependent the effect of the type and the geometer.

We have two types of the geometer non-aerodynamically and aerodynamically shapes, as we can see in this previous figure's shapes like Rectangle, flat plat, triangle and semi-circle reach the regime turbulent before the other shapes and reaching this regime means the emergence of the phenomenon of the von Karman.

The circle is not a aerodynamically shape but it gave low turbulent and drag compared with the other non-aerodynamically shape.

The aerodynamically shapes are the airfoils (NACA0040 and NACA 4412) specifically to make all following settings suitable in CFD simulation and to give the results in very acceptable especially in vortex behind the airfoils and lift, drag coefficients, for example if we talk about the vortex over each of the two airfoils in our simulation, they will be non-existent in angle of attack equal 0

The case of symmetry airfoil it will start to appear at angle of attack equal 13°

The non symmetry airfoil it will start to appear at angle of attack equal 36°

The curves (5.6-5.10) and Tab5.3 represent the average drag and lift coefficient as a function of Reynolds number by OPENFOAM and FLUENT designed by ORIGIN 2019b

CHAPTER 5 COMMENTS AND RESULTS

We can see that the Drag coefficient in rectangle, trapezoidal, triangle; semi -circle and circle are high compared by the remaining shapes (airfoils)

On the contrary, we found a significant decrease in the lift coefficient in all shapes, except for the airfoils, this is due to the non-aerodynamic shape, which causes an increase in the drag coefficient and a decrease in the lift coefficient (the lift coefficient is always perpendicular to the drag coefficient).

The airfoils gave us with very excellent rates of drag and lift coefficient at the small Reynolds coefficient (the effect of viscosity).

The non aerodynamically non symmetric airfoil the NACA4412 gives a low drag coefficient with a higher lift coefficient than the rest, and this confirms its use in the field of aerodynamics and aviation.

At Re =200, It was found that the shape strongly influenced the wake structure and the vortices generated behind the shapes were due to the interference of the fluid. Despite the difference in the previous shapes, we were able to produce a simulation of this very important phenomenon in aerodynamic (Von Karman), which is represented by the vortices generated Which you can see when you see the curves of the drag and lift coefficients, which are periodic and varies according to each shape and how it deals with the flow Figures 5.31,5.32.

5.7. The third simulation

5.7.1 Validation of Numerical Model

First, we validated our result of the flow around a circle without a slit and circle with horizontal and vertical slit at Re = 200 with numerical results from Marouane Salhi article and other numerical articles. and after series of simulations, it was found that the error is less than 10 %, And what helped me the most was the quality of the Mesh which was large and reasonably good, around 350,000 elements which gave sufficiently precise results. we therefore chose this mesh and number of elements.

5.7.2 Effect of slits

From Marouane Salhi's article about the slits and their effect on the lift and drag coefficient and the Strouhal Number. we learned that the value of (D/S), which is represented by the ratio of the length of the slit over area of the circle, effects on the aerodynamic coefficients.

And for the horizontal and vertical slits the value of (D/S) equal 8.0 is strongly

influenced the wake structure so the flow passing through the slit is so big so the Van Karman vortex generated behind a circle depends on the ration (D/S) value so the horizontals and verticals slits weaken the vortex detachment behind the circle

Knowing that the ratio affects the vortex behind the circle, the study that I will appear on this chapter is to study the effect of the slit with the ratio of an (D/S) =8.0 through studying the Van Karman effect, the aerodynamic coefficients and the number of Strouhal, starting from the horizontal slit to the vertical slit, passing through angles represented 30°, 45° and 60°.

Our goal is to minimize the effect of the van Karman vertex over our circle so we tried to do simulations in circle with those angles and compared them with the horizontal and vertical slits, after that we can optimizing or improve our circle very good shape which gave a small drag coefficient versus acceptable lift coefficient.

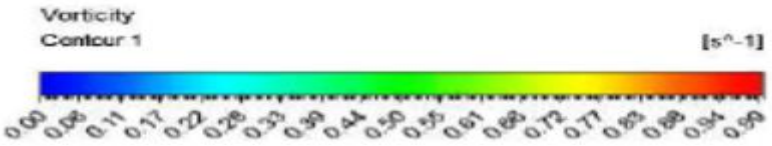

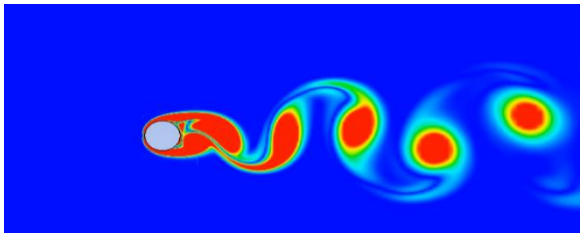

Normal circle

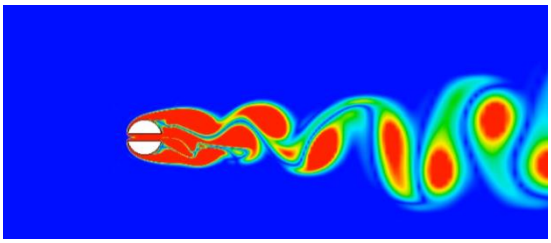

horizontal slit

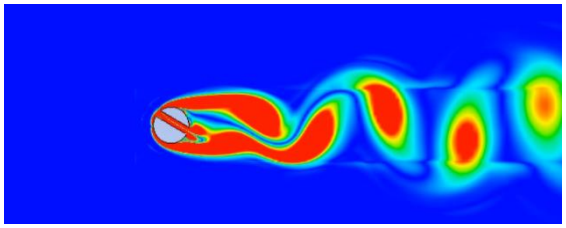

Circle with slit in 30°

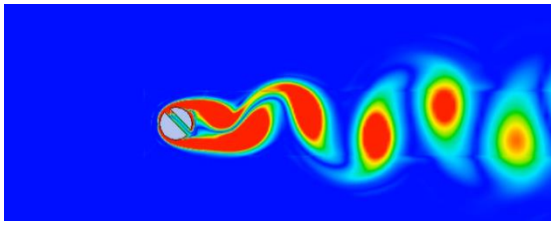

circle with slit in 45°

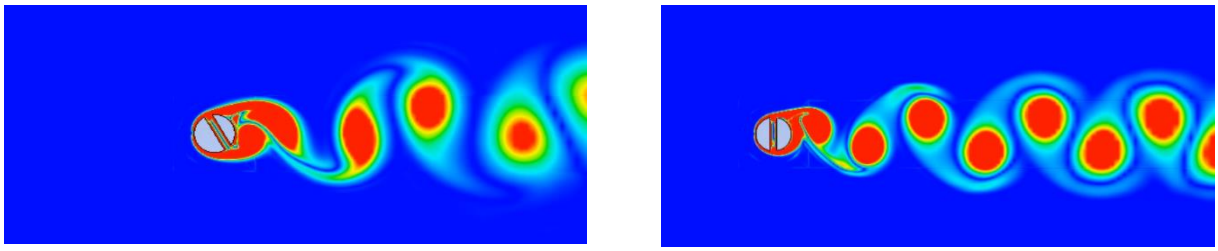

Figure 5. 33 : Vorticity contours of different spacing ratios from horizontal to vertical slits at Re=200.

5.7.3 Behavior of drag with horizontal slit

The variation of the average drag coefficient as a function of the spacing ratio (D/S) from horizontal to vertical slit is shown in Figure.5.34 The drag coefficient curves are periodic and varied, so the amplitude and period depend on the spacing ratio (D/S) of the slit and we choose the ratio D/S equal 8. so, we know all that the case of (D/S) = 8.0 generated number of vortices so enormous behind our circle Therefore, this phenomenon negatively affects for the aerodynamic coefficients, and therefore the solution to the slit that has an angle can be the solution to reducing the vortices behind the circle.

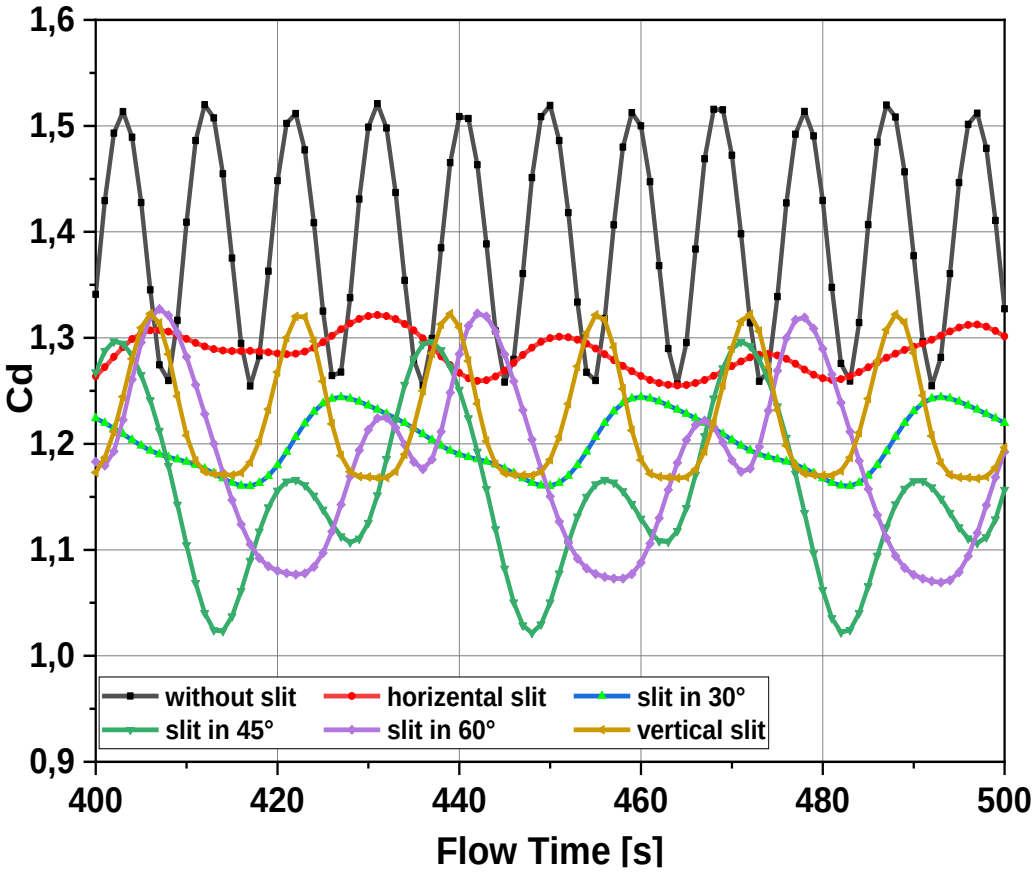

Figure 5. 34 Behavior of CDav from horizontal to vertical slits at Re =200

5.7.4 Behavior of lift with different slit Horizontal

The average lift coefficient of a circle with a horizontal slit is shown in Figure.5.35 the lift coefficient curves are periodic and varied, so the amplitude and period depend on the spacing ratio (D/S) of the slit and we choose the ratio D/S equal 8. so, the lift force tends to zero and there is a great repulsive pressure force among all cases. However, in our case, the attractive force is dominant, and therefore there is a great interference in the wake. The intensity of this force depends on the spacing ratio (D/S) and our other cases (the angle cases) gave us very good lift coefficient compared with the case of horizontal slit.

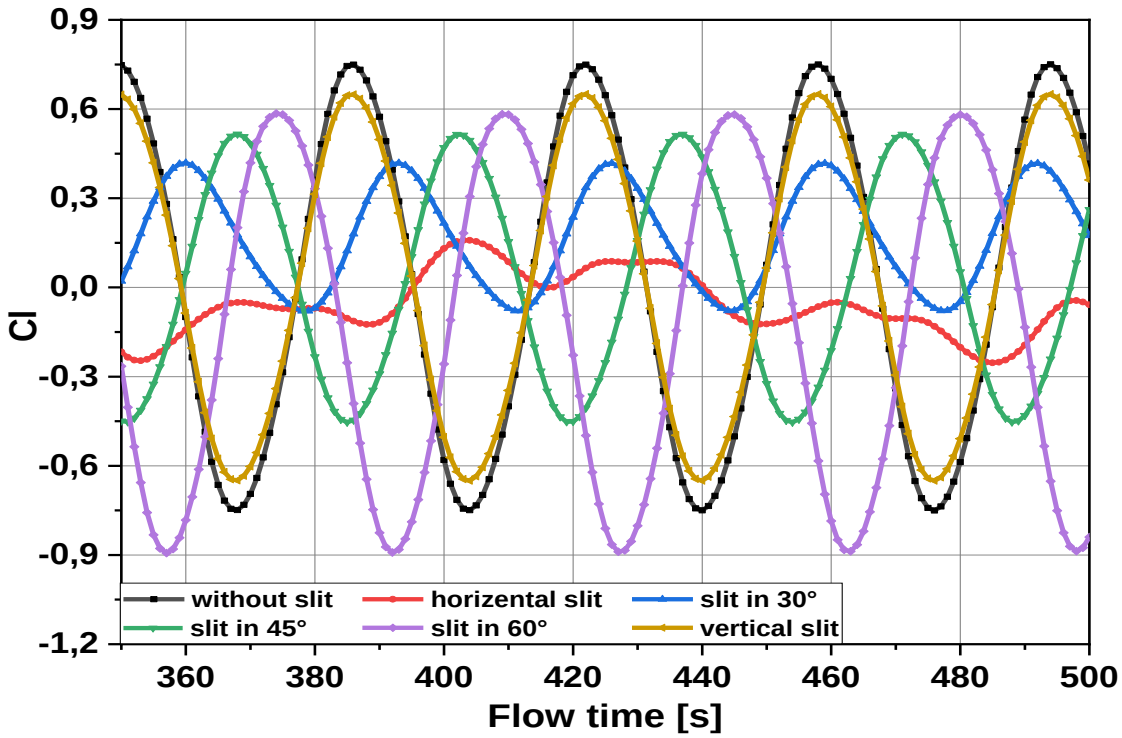

Figure 5. 35 Behavior of CLav from horizontal to vertical slits at Re =200

5.7.5 Strouhal number

Table.5.5 shows the values of Strouhal number (St) as a function of our case the spacing ratio (D/S) equal 8.0 with our other cases without slit and horizontal and vertical cases. This parameter represents the intensity of vortex detachment behind a circle. According to Marouane Salhi's article, the Strouhal number varies with the variation of the spacing ratio(D/S). It shows an increase in the case of the horizontal slit of (D/S) = 8.0, And a decrease and an alternative variation of this parameter in the case of the vertical slit. The Strouhal number in the angle cases is so close with the perfect number in range of Reynolds number known

On the other hand, in the case of the horizontal slit and the vertical, this parameter increases

slightly at the beginning then increases enormously. So, the spacing ratio (D/S) =8.0 of the slit strongly influences this parameter, but if we use this slit and applicated this with an angle we may got nice results.

Table5. 4 Strouhal number as a function of the ratio (D/S) at Re=200.

The case	Without slit	Horizontal slit	Slit in 30°	Slit in 45°	Slit in 60	Vertical slit
St	0.21	0.23	0.24	0.19	0.2	0.26

Fig.15 shows the evolution of the vorticity contours around a circle with one horizontal slit and the other vertical for (D/S) = 8.0 and (D/S) = 12.5 at Re = 200. It shows a great variation in the wake structure behind the circle, especially in the case of (D/S) = 8.0. This depends on the variation of the (D/S) spacing ratio. As the (D/S) spacing ratio of the slit widens, the fluid flow passed through the slit increases, and creates repulsive forces. The latter influence the forces applied around the circle, as well as the vortex detachment and the wake structure.

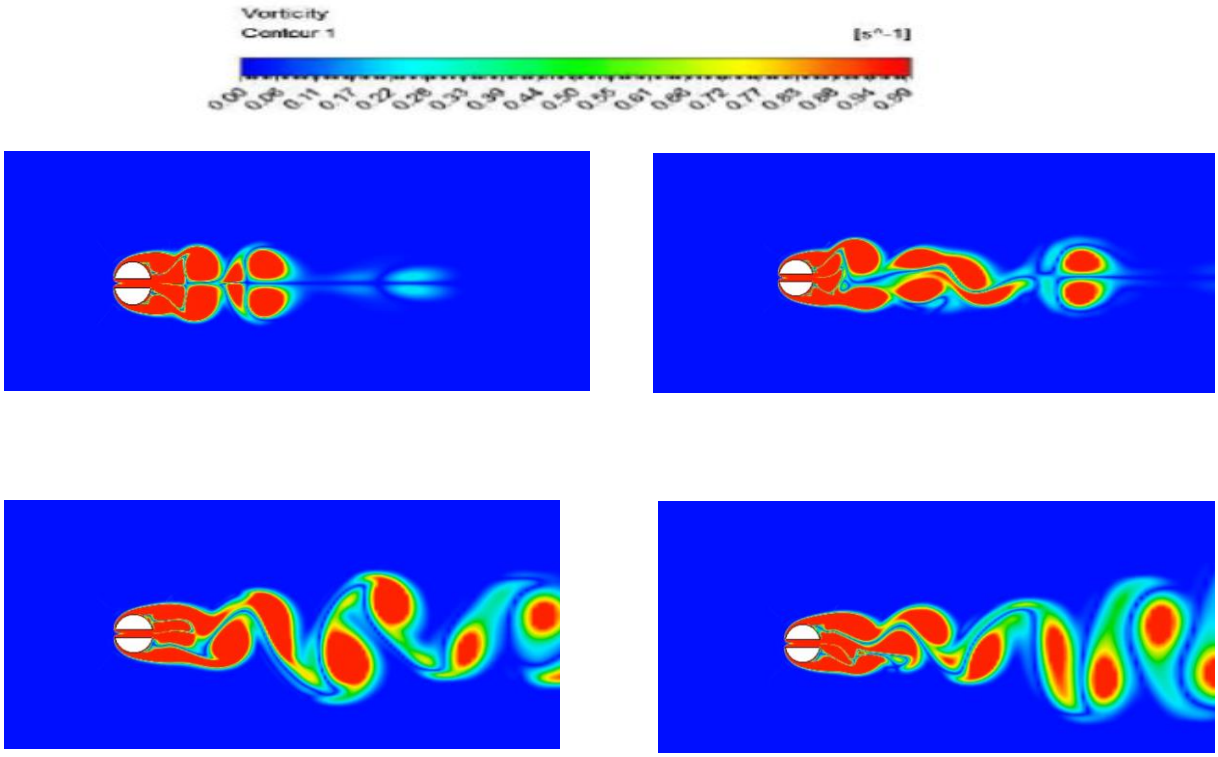

Figure 5. 36 Evolution of vortex field of horizontal slit at Re=200

:

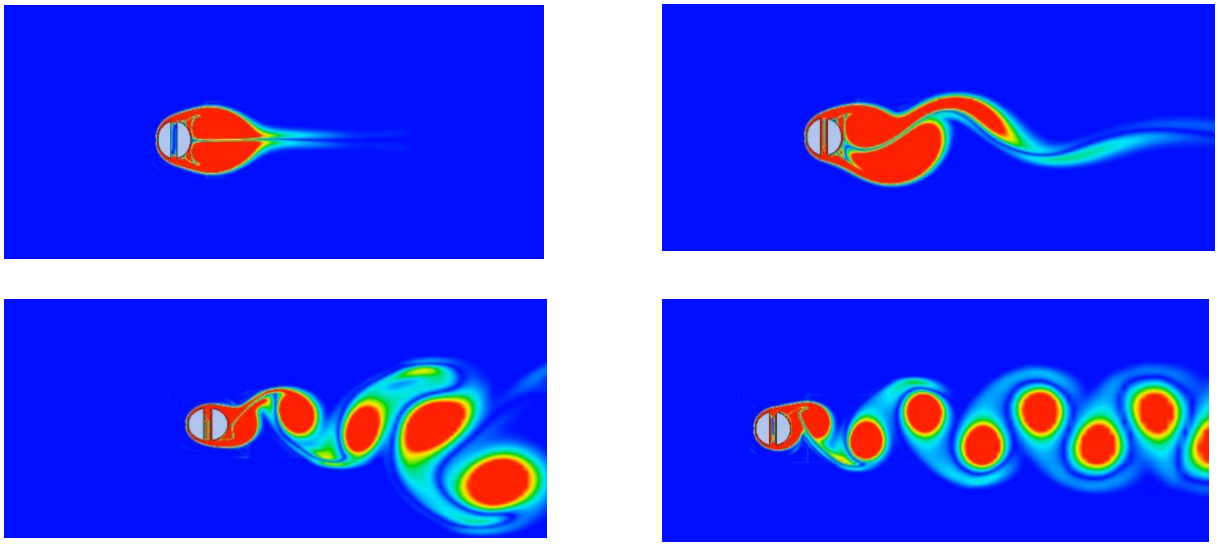

Figure 5. 37 : Evolution of vortex field of vertical slit at Re=200.

5.7.6 Visualization of Streamlines

For 200 < Re < 2.1056, the wake is turbulent and the regime is called subcritical in this regime, the flow is turbulent in the wake but the boundary layer upstream of the detachment point remains laminar. At low Reynolds numbers, small secondary eddies develop on either side of the vortex alley following the amplification of the local Kelvin Helmholtz instability in the shear zones around the sphere. As the Reynolds number increases (Re - 2600), this instability is more pronounced and covers a significant region of the mixing zone, Figure 1.9. Regime under criticism.

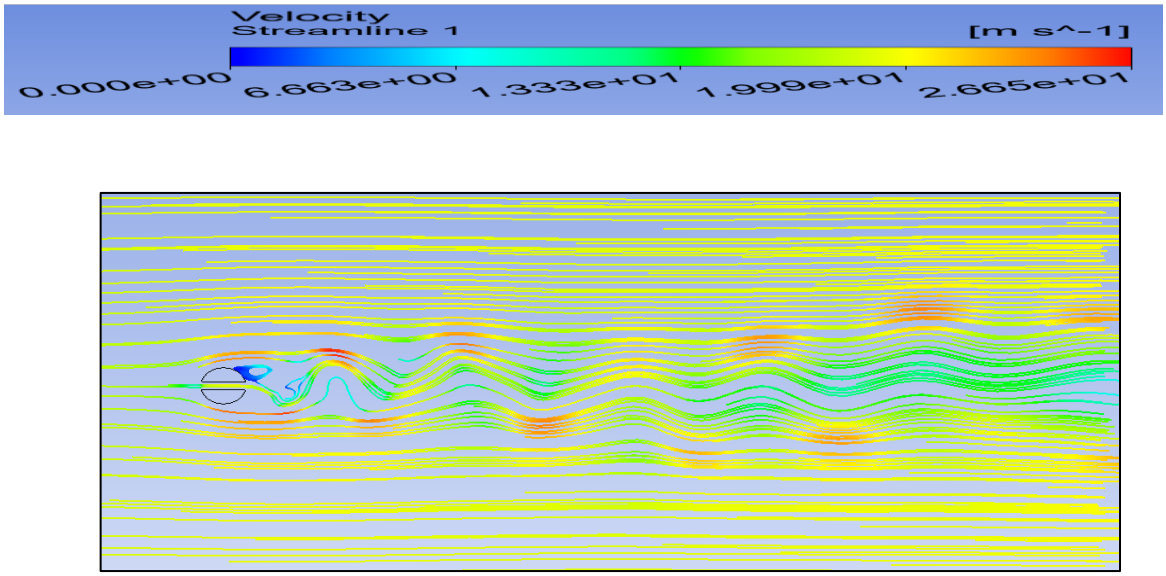

Figure 5. 38 : streamline of horizontal slit at Re=200

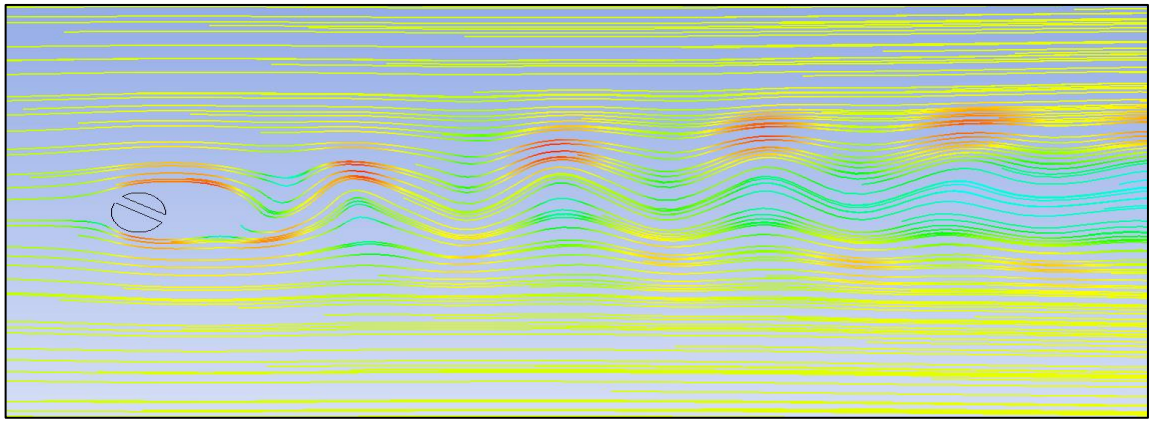

Figure 5. 39 : streamline of slit in 30° at Re=200

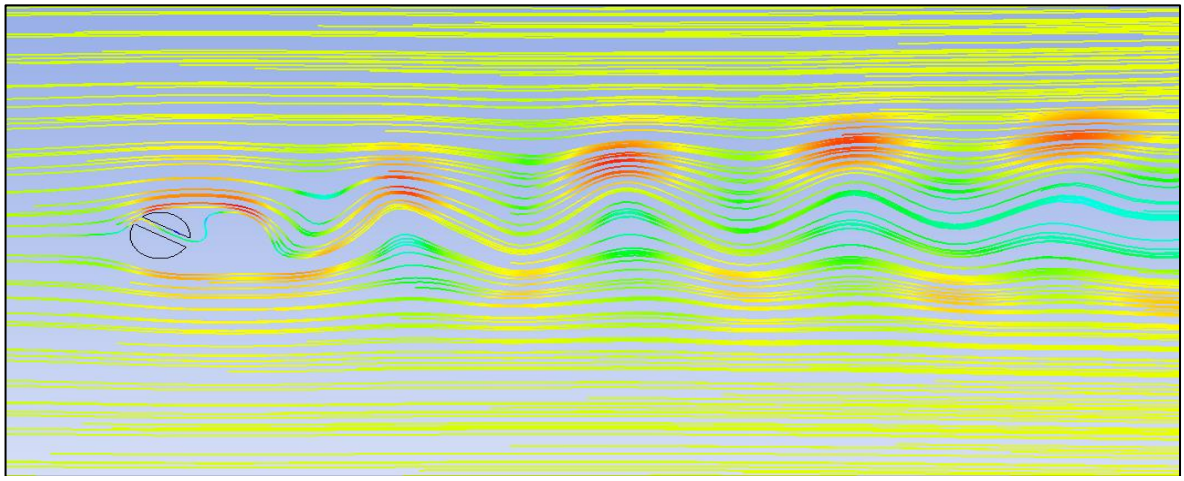

Figure 5. 40 : streamline of slit in 45° at Re=200

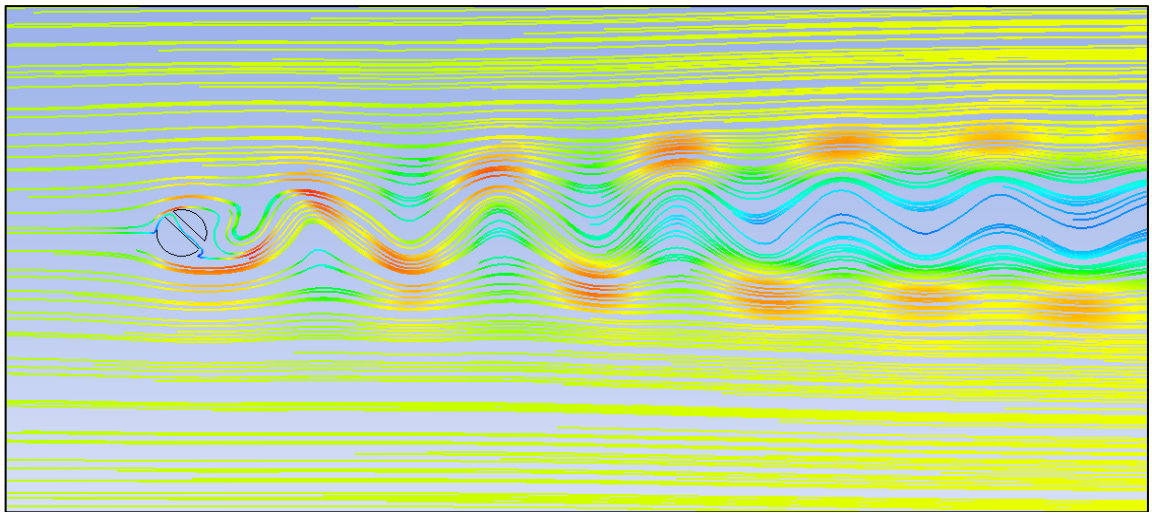

Figure 5. 41 : streamline of slit in 60° at Re=200

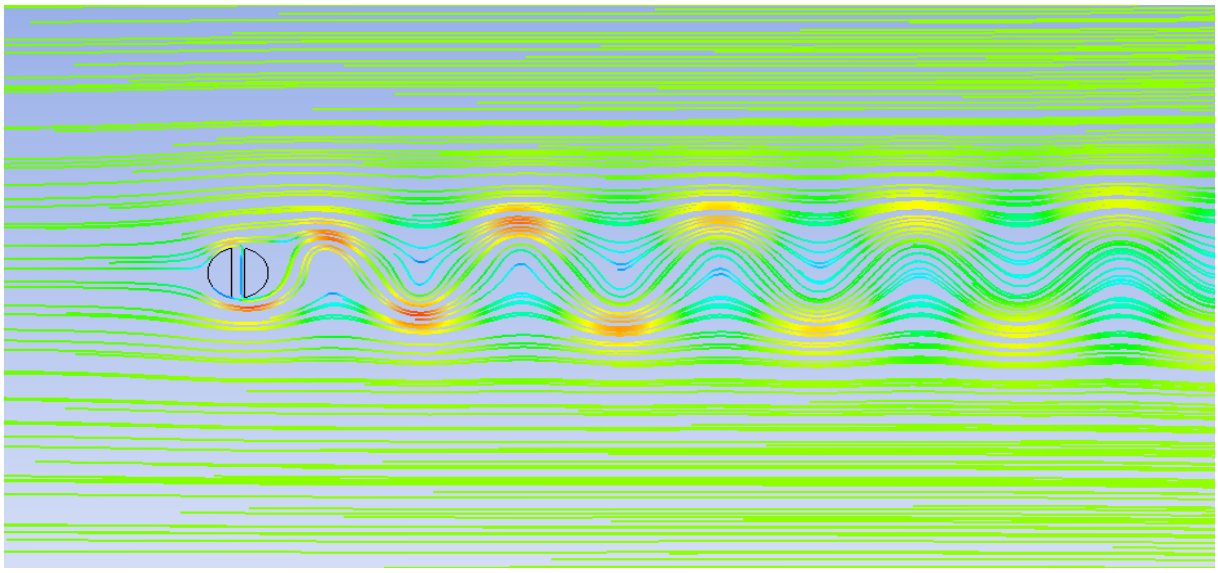

Figure 5. 42 : streamline of vertical slit at Re=200

5.7.7 Contour of the resulting pressure

This regime is reached when the transition point that rises upstream during the critical regime reaches the point of detachment.

The value of this critical Reynolds number varies significantly according to the different experimental studies (between 10 and 30000) because of the high sensitivity of the flow to the boundary conditions of the flow (turbulent intensity of the incident flow, elongation ratio and roughness of the flat plate and semi-sphere, etc.).

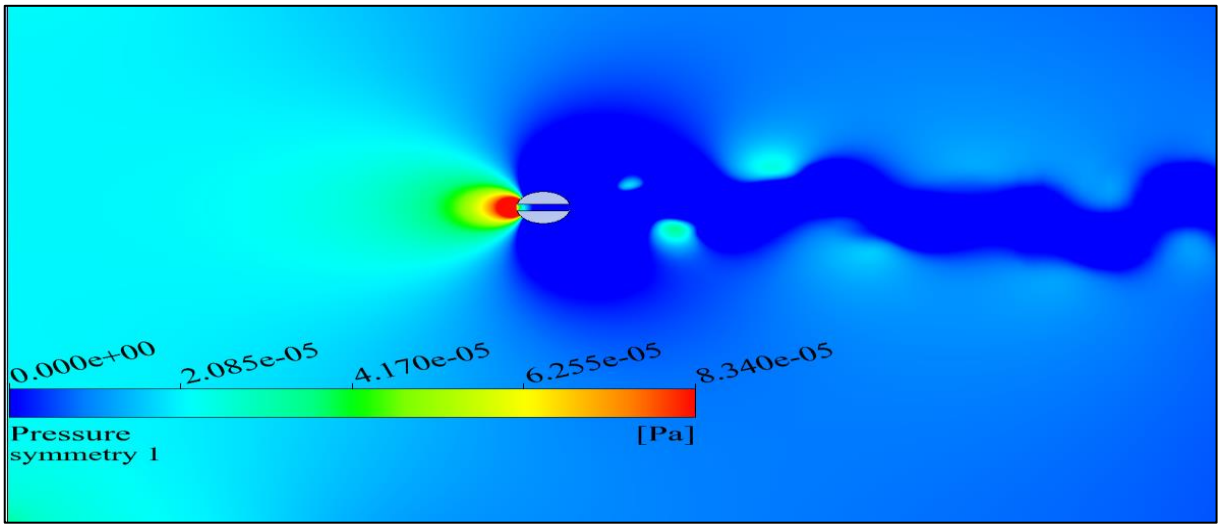

Figure 5. 43 : pressure contour of circle with horizontal slit at Re =200

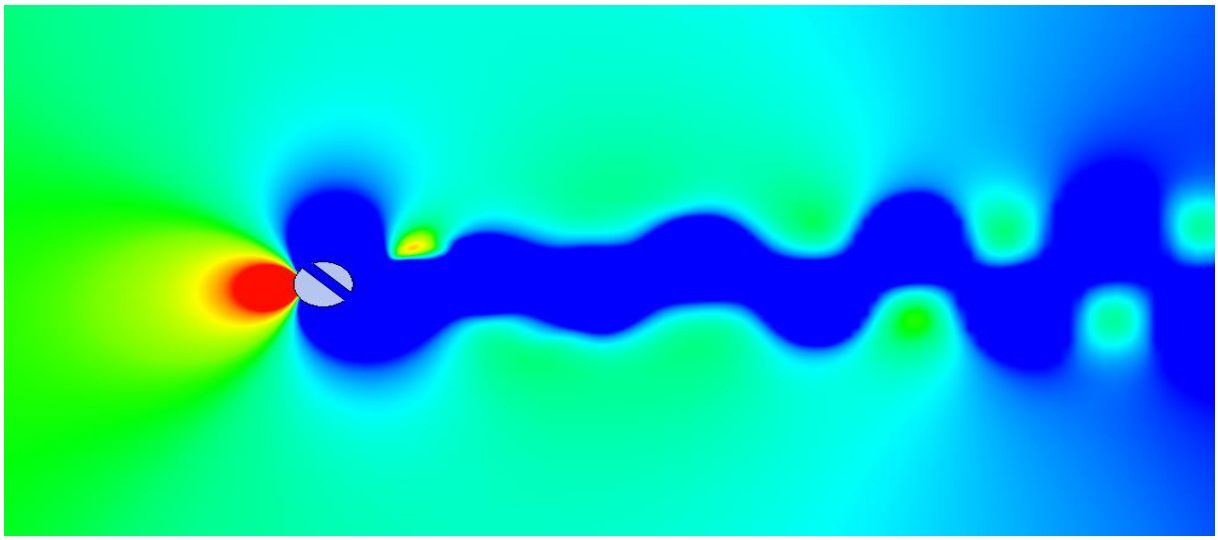

Figure 5. 44 : pressure contour of circle with slit in 30° at Re =200

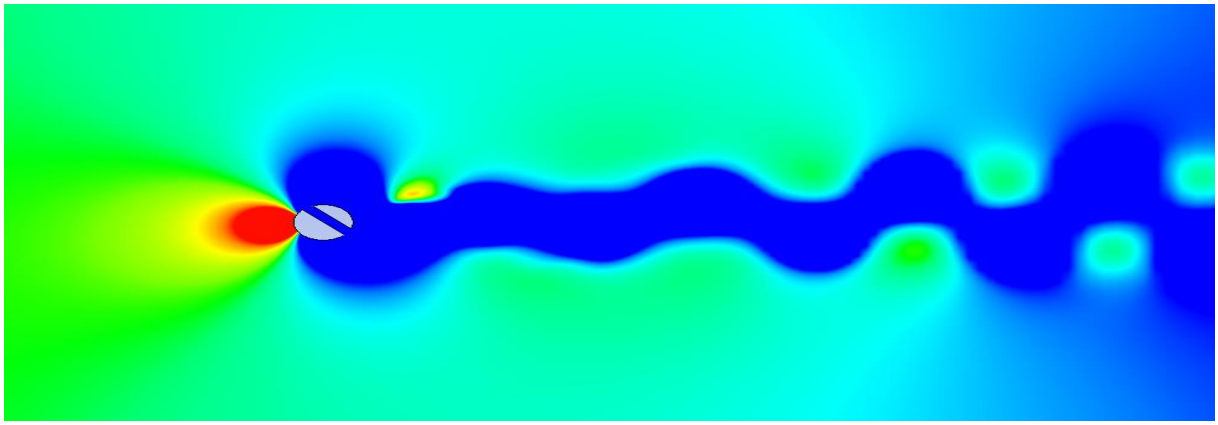

Figure 5. 45 : pressure contour of circle with slit in 45° at Re =200

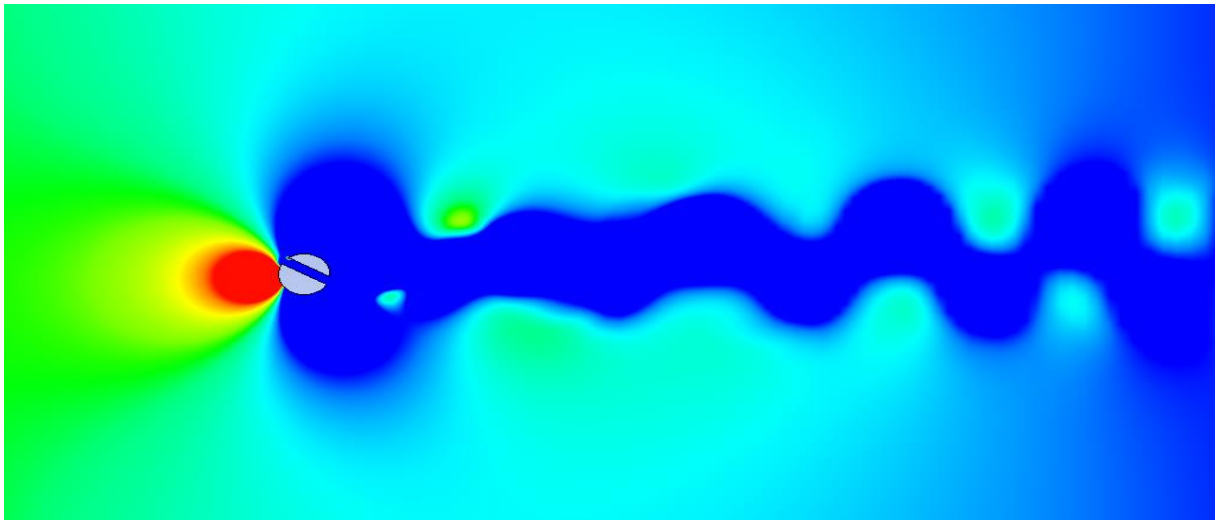

Figure 5. 46 : pressure contour of circle with slit in 60° at Re =200

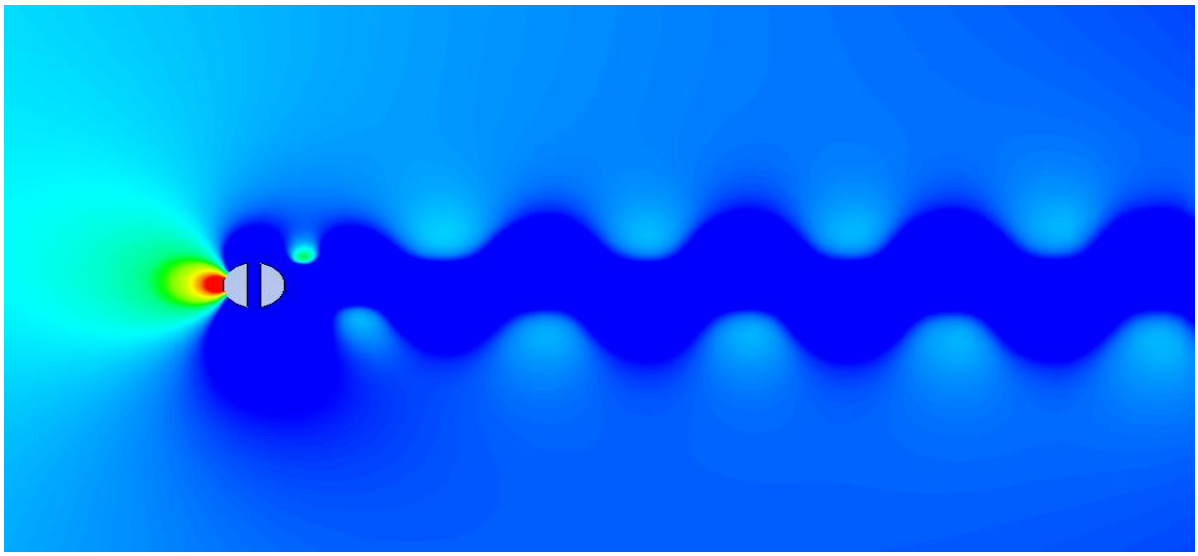

Figure 5. 47 : pressure contour of circle with vertical slit at Re =200

5.7.7 Conclusion

In this sous chapter and from the results of the work of Marouane Salhi on the flow behind circles with slits and he chooses some spacing rations and after simulation he finds that decrease the drag coefficients compared with the normal case but also, he was found that the slits strongly influenced the wake structure and the vortices generated behind the circle were due to the interference of the fluid in some spacing ratio.

And finally got the circle with spacing ratio = 8.0 is reduced the lift coefficient in two cases the horizontal and vertical case and for optimizing this case.

To improve the results of this case, we resorted to the method of slits, but at different angles, and as we obtained in the curves **Fig.5.30** and **Fig.5.31,** the idea of slits at an angle was a good idea by improving the lift coefficient and drag coefficient at the very least, the number of Strouhal has an important relation with the vortex detachment. This parameter was influenced by the position and the nature of the slit, especially where the spacing ratio (D/S) = 8.0.

5.8 the fourth simulation

In this part, we will perform simulations of four shapes (Circle, Semi-Circle, Flat Plate and NACA0040), at several different speeds (15,20and 25), and we will compare them with the experimental results by making comparisons between both results, and we will see the improvement of the important coefficients drag and the drag force in the eyes of aerodynamic specialists. Also, let us not forget the coefficient that is very important in several fields, the most important of which are the aerodynamic fields and the field of Generating renewable energies, which is the Strouhal number that we talked about previously. In the midst of this comparison, we calculate the frequencies with the help of the Strouhal number and see which gives us a greater frequency among the bodies that we have.

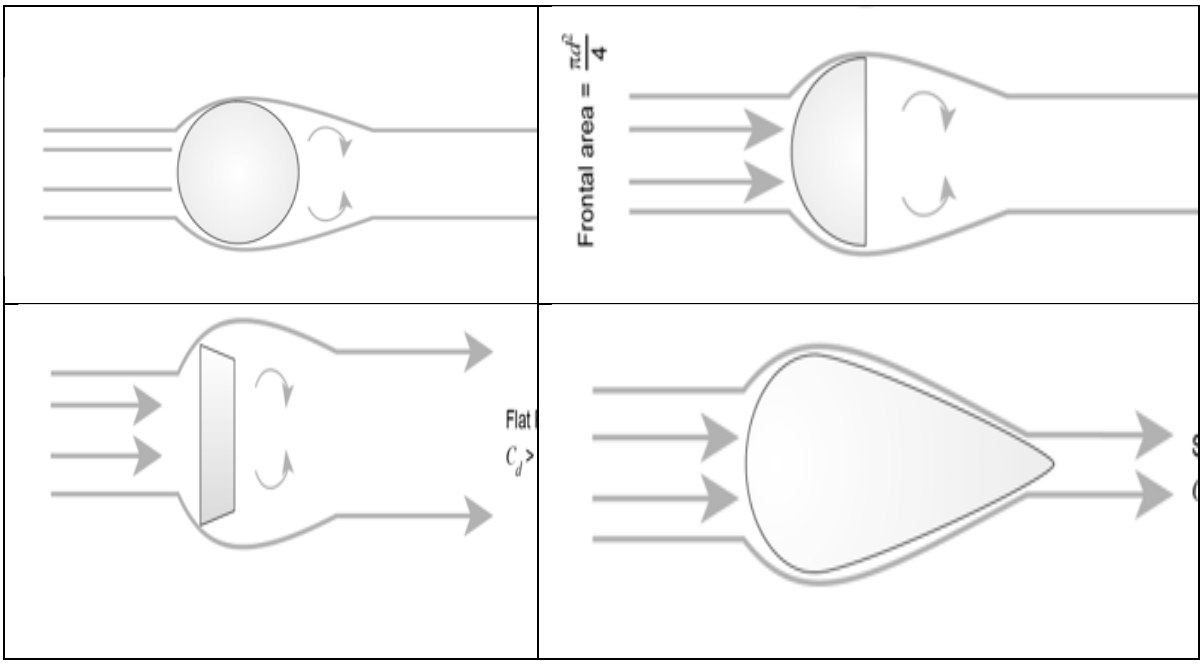

Figure 5. 48 : the different bodies

5.8.1 Aerodynamic Forces on the Curve Structure

The drag value (sometimes called air resistance) on the model is simply the force acting on it in the direction of an applied airflow. Generally, in the direction of flow, more aerodynamic shapes and shapes with a small area give lower drag coefficient values.

The drag coefficient is a dimensionless value that helps to quantify drag, but in relation to an object. Dimensions and velocity of the fluid (air) that passes around it. It allows the trail of objects of different sizes to be compared, allowing the results to be adapted.

As expected, the streamlined shape has the lowest Co compared to the rest with the flat plate.

5.8.2 Moment

Note that a honeycomb sphere has a lower drag coefficient than a simple sphere. This is due to the way the dimples work to allow the airflow to remain attached to its surface, resulting in a smaller wake.

5.8.3 Interpretation of Results

Not All results are for illustrative purposes only, actual results may differ slightly.

5.8.4 Convergence criteria

In most of the cases studied, the convergence criterion imposed by default in (ANSYSR1) is sufficient. This means that the wake (flow pattern behind the object) also affects the drag. A wide wake creates more drag than a narrow wake behind an object. Therefore, even the shape of the object behind the frontal area affects friction.

5.8.5 Aerodynamic coefficients

(Experimental and numerical) show good agreement for Reynolds number values ranging from *0.77x105 to 1.5x105. The two evolutions show a strong disparity from a Reynolds number of 1.5x105, they diverge as the velocity of the flow increases.*

This observation can be explained, in the experimental case, by the fact that friction tests are carried out during friction tests, which amply amplify the production of parasitic drag. Also, the presence of the control arm in the weighing of aerodynamic forces and pressure fields, may possibly be the cause of this error; Indeed, the flow around the sphere and the arm can modify the distribution of pressure fields downstream as well as upstream of the sphere by creating an asymmetric flow situation giving rise to a parasitic force.

By comparing the curve obtained numerically with that of the experimental, we notice that its intensity is strongly underestimated from the Reynolds number of *1.5x105, this is probably due to the idealist case considered in our simulations as well as to the qualities of the meshes generated.*

The results of the calculations summarized and compared to the data in the literature show an excellent agreement of the parameters listed., the force coefficients are defined by:

[= 0.05149. 10^5. (15,20.25.30) m/s.]

*(15-25) m/s -Laminar subcritical with street instabilities whirlwind

(150-300) $< R_e <$ (1-1,3) 10^5

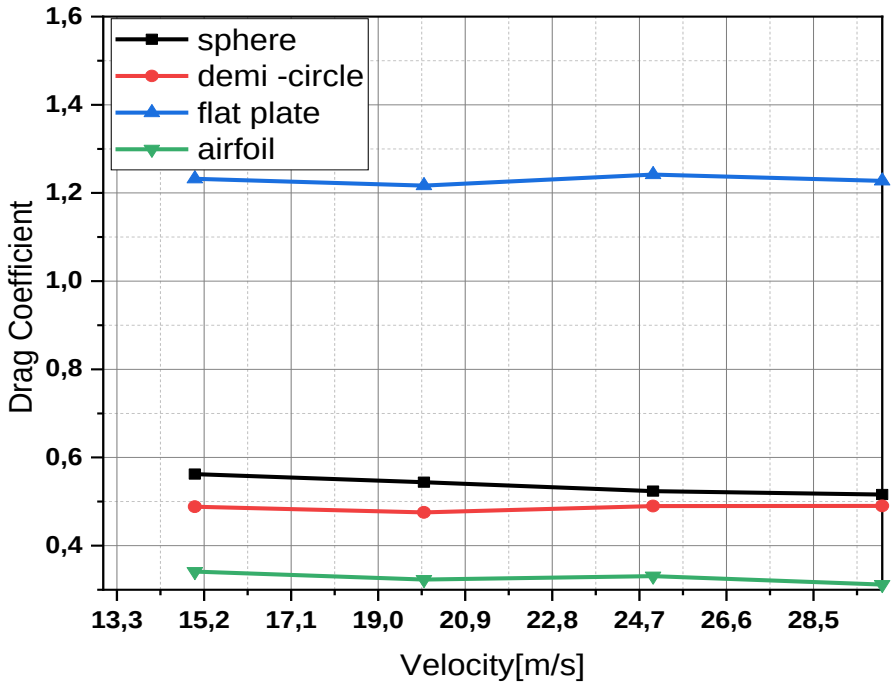

Figure 5. 49 : Typical results and conclusions.

5.8.6 Error absolute et relative

Theoretically, there should be no lift value. These models are only intended for drag experiments, so they are mounted directly in the line of the airflow, (at an incidence of 0 degrees) giving no lift value.

Scope of this guide. It is possible to experiment with lift on models, but it is beyond what is typical only. The drag coefficient varies with the Reynolds number and the flow velocity, so the results Theoretically, there should not be a lift value.

With:

a) Error absolute

$$\varepsilon = \left| v - v_{app} \right|$$

b) Relative error

$$\eta = \frac{|v - v_{app}|}{|v|}.$$

Table5. 5 The drag coefficient and Absolute and relative error for circle.

Vitesse (m/s)	15	20	25
Numerical Result	0,4839	0,4794	0,4832
Experimental Result	0,4732	0,4599	0,4763
Error absolute	0.0151	0.0157	0.0134
Relative error (%)	3.1910	3.4137	2.8133

Table5. 6 The drag coefficient and Absolute and relative error for flat plate.

Vitesse (m/s)	15	20	25
Numerical Result	1,2340	1,249	1,2046
Experimental Result	1,2285	1,2266	1,2696
Absolute error	0.0036	0.0099	0.028
Relative Error (%)	0.2930	0.8071	2.2054

Table5. 7 .: The drag coefficient and Absolute and relative error for the airfoil.

Vitesse (m/s)	15	20	25
Numerical Result	0,3438	0,3227	0,3355
Experimental Result	0,3480	0,3270	0,3330
Absolute error	0.0069	0.0038	0.0021
Relative error	1.9827	1.1620	0.6306

Table5. 8 The drag coefficient and Absolute and relative error for semi-circle.

Velocity (m/s)	15	20	25
Numerical Result	0,558	0,543	0,5191
Experimental Result	0,5536	0,5363	0,5144
Absolute error	0.0043	0.0061	0.0038
Relative error (%)	0.7767	1.1374	0.7387

5.8.7 Strouhal number

The Strouhal number is a dimensionless number that characterizes oscillating flow dynamics. It is defined as:

$St = (f * l)/V$

f is the vortex shedding frequency,
l is the characteristic length (e.g., diameter of the circle),
V is the flow velocity.

Table5. 6 .: The average of the Strouhal number.

The case	circle	Semi -circle	Flat Plate	NACA0040
St	0.2	0.178	0.15	0.12

CHAPTER 5 COMMENTS AND RESULTS

The relative and absolute errors are determined by the boundary conditions by ANSYS, a uniform velocity is imposed at the entrance of the domain and a pressure at the exit. The top and bottom walls, as well as the boundaries of the obstacle, were considered absolute and relative errors.

5.8.8. Strouhal number St and frequency

The frequency refers to the rate at which vortices are shed from the surface of a structure immersed in a fluid flow. It is typically measured in Hertz (Hz), representing the number of vortices shedding cycles per second. The vortex shedding frequency determines the oscillatory forces exerted on the structure, which can lead to vibrations if the frequency aligns with the structure's natural frequency.

For each shape and velocity, we use the formula:

$$f = (St * V)/D$$

Table5. 7 : Calculation of the frequency in each velocity

Shape	Velocity (m/s)	St	Frequency (Hz)
Circle	15	0.2	40
	20	0.2	53.33
	25	0.2	66.67
Semi circle	15	0.18	36
	20	0.18	48
	25	0.18	60
Flat Plate	15	0.15	30
	20	0.15	40
	25	0.15	50
NACA0040	15	0.12	24
	20	0.12	32
	25	0.12	40

When presenting tables of Strouhal numbers (St) and frequencies for different shapes in the context of Vortex-Induced Vibrations (VIV), it's important to highlight the following key points to provide context and clarity:

- The Strouhal number and the frequency have a direct relationship. As the number of Strouhal increases, the vibrations or the frequency increase with it, and this is what the frequency equation confirms.
- The vortex shedding frequency increases with the fluid velocity. This relationship is critical for designing structures to avoid resonance and potential structural damage.

- he characteristic length (e.g., diameter for a circle, chord length for an airfoil) is a crucial parameter in determining the Strouhal number and the resulting frequency.
- Different shapes are used based on the specific requirements of the application. For example, circles might be used in marine risers, while airfoils are common in aerodynamic applications. The choice of shape influences the VIV behavior and subsequent energy harvesting potential.
- Understanding the Strouhal number and frequency for different shapes aids in the design and optimization of structures to either harness VIV for energy generation or mitigate its effects to ensure structural integrity.

The provided Strouhal numbers are typically valid within a certain range of Reynolds numbers, which depend on the fluid velocity, characteristic length, and fluid properties. It's essential to ensure the operating conditions fall within this range for accurate predictions.

5.8.9 Conclusion

In this chapter, we have simulated the stationary and turbulent incompressible flow with the viscous fluid model and we have found very good results since they are closer than those indicated in the wind tunnel. The "ANSYS" software gave us complete satisfaction in the processing of numerical simulation on different geometric bodies.

The wind tunnel test campaign has led us to conclude that by making changes to the surface of the geometric shapes, we can reduce drag and improve aerodynamic performance. So, in terms of drag reduction, we have achieved an improvement of more than

The first part is for the comparison between the two results and the results of previous simulations demonstrate that the contact surface and the shape of the object have an important role in determining

The aerodynamic coefficients through which we have confirmed that the more aerodynamical shape is the give lower drag coefficient, and, if the shape is less aerodynamical shape we get higher drag coefficient, the only difference is changing one of the basic conditions, which is the initial speed.

If we talk about the field of power generation, for which Strouhal number is a fundamental factor, then the most important thing is basically the shape, and it does not matter if it is aerodynamic or not. The most important thing is to develop the shape so that it gives us more oscillations and thus greater energy production. The circuit won, which through simulations gave us the Strouhal number. It is acceptable, and in all cases, when calculating the number of frequencies, it gives us a larger number than the other shapes

General conclusion

In this work, through this modest work, we first understand the difficulties of simulating complex geometry in a fairly large area of study. We clearly understood the steps that need to be followed to perform the digital simulation. As a result, given the time allotted for this project and the means at our disposal, I achieved my goal.

Our primary goal was to use ANSYS 19.0 and OpenFOAM in all stages of the simulation: design, connection, simulation, and exploitation of the results. This program posed a problem for us during coupling because it requires a “surface” type liquid-structure interface in order to transfer data from the liquid to the structure and vice versa, which can only be done if the problem is 3D. We have avoided moving towards 3D digital simulation on different geometric objects. We therefore preferred to remain in two dimensions and seek to perform this coupling in a wind tunnel.

Numerical simulations of flow around a smooth circle, semi-circle, rectangle, triangle, NACA4412 and profile (NACA 0040) showed results in good agreement with experimental values, and also made it possible to shed light on the coefficients of drag, lift, and the Strouhal number by different large and small (Raynolds)

According to the work presented in this thesis, we can say that the theory of steady and turbulent incompressible viscous flows in subcritical and critical systems can be used to study ideal flow around seven geometries, sphere, hemisphere and dinner plate (trapezoid). shape) and profile (NACA 0040). This theory provides important theoretical information that will help us understand the behavior of fluids moving around geometric objects. There is no doubt, not only in the field of aerodynamics, but even in the field of electricity production, which constitutes a major challenge in the future in light of the depletion of non-renewable energies.

Bibliographie

[1] A. Brima, « Mécanique des fluides et Aérodynamique », cours de Master I, Département Génie mécanique, Université de Biskra, 2012-2013.

[2] ANDRE Lallemand, « Ecoulements monodimensionnels des fluides compressibles », Université de Lyon, France.

[3]. ***Kaushik, Mrinal. Theoretical and Experimental Aerodynamics. Springer Singapore, 2019.***

[4] SAMIR Khene, « Mécanique des fluides»,publications de l' université Badji Mokhtar, Annaba, 2000.

[5] Fiacre Ahonguio, « Ecoulements de fluides à seuil autour d'obstacles », Thèse université Grenoble Alpes, Français, 2015.

[6]: Gad-el-Hak M., 1990, Control of Low-Speed Airfoil Aerodynamics, AIAA Journal 28, N° 9.

[7] RIADH Ben Hamouda, « Notions de mécanique des fluides », Centre de publication universitaire, Tunis, 2008.

[8] F. Meddane et al (2007).

[9] Madani et Abidat (2002) Etude numérique de l'écoulement d'un fluide visqueux incompressible autour de corps profilés par une méthode combinée d'ordre 0(h2) et 0(h4). International de Génie Mécanique. Sigma'02. E.N.S.E.T. Oran. 28 & 29AVRIL2002.

[10] S. BENSEDIRA, A. ABDELLAH EL-HADJ et D. SEMMAR, « ETUDE DYNAMIQUE DE L′ECOULEMENT AUTOUR D′UN CYLINDRE PLACÉ PROCHE D′ UNE PAROI », Third International Conference on Energy, Materials, Applied Energetics and Pollution, ICEMAEP2016, October 30-31, 2016, Constantine, Algeria.

[11]. ***Paraschivoiu, Ion. Aérodynamique subsonique. Presses inter Polytechnique, 1998.***

[12] : Bourgois S, Etude expérimentale du découlement sur profile d'aile : analyse et contrôle, thèse de doctorat, Université de Poitiers 2006.

[13] Eggleston B.,Poole R.J.D, Jones,D.J. and Khalid M., "Thick supercritical airfoil with low dragand natural laminar flow," Journal of Aircraft,Vol.24, No.6, 1987, pp.405-411.

[14] : Thèse présentée pour obtenir le grade de docteur de l'université de Bordeaux, école

doctorale de mathématiques et informatique, par YOANN EULALIE, thème : Etude aérodynamique et contrôle de la trainée sur un corps d'Ahmad culot droit.

[15] " **WORLD AIRCRAFT Recognition Handbook** " édité par Jane's et écrit par Derek Wood tiragede 1989.

[16] Didier Féminier, " Méchanique du vol " de A.C.Kermode, édité par Modulo Editeur tirage deJanvier 1984.

[17] RAYMOND Brun, « Manuel du Mécanicien et du Thermicien », Editions Techip, Paris, 1977.

[18] Ira H. Abbott et Albert E. " THEORY OF WING SECTIONS including a summary of airfoil data" de Von Doenhoff édité par Dover publications, Inc. New York en aout 1958.

[19] INGEL Ryhming, « Dynamique des fluides », Presses Polytechniques et universitaires Romandes, 2004.

[20] Coutu, D., Brailovski, V., Terriault, P., "Optimised design of an active structure for an experimental morphing laminar wing", submitted to the Journal of Aerospace Technology and Science, January 2009.

[21] Pag`es, L., Trifu, O., Paraschivoiu, I., "Optimized laminar flow control on an airfoil using theadaptable wall technique", Proc. of the CASI Aero 2007 symposium, June 2007.

[22] Schofield & Logan (1990), *"Turbulent Shear Flow over Surface Mounted Obstacles", Trans. ASME, vol.112, 376-385.*

[23] ION Paraschivoiu, « Aérodynamique subsonique », Editions de l'école polytechnique de Montréal (Québec), Canada, 1998.

[24]. G. S. Constantinescu and K. D. Squires, LES and DES Investigations of Turbulent Flow over a Sphere, AIAA Paper 2000‑0540 (AIAA Press, Washington, DC, 2000).

[25] White, Frank. Fluid Mechanics. *4th edition. McGraw-Hill Higher Education, 2002, ISBN: 0-07-228192-8.*

[26] ION Paraschivoiu, MICHEL Prud'homme, LUC Robillard et PARTICK Vasseur, « Mécanique des fluides », Presses internationales polytechnique, Ecole de Montréal, Canada, 2003.

[27] PIERRE Louis, « Mécanique des fluides à masse volumique variable », Presses de l'école nationale des ponts et chaussées, Paris, 1997.

[28] E.E. Michaelides, Particles, Bubbles and Drop, their motion, heat and mass transfer, World Scientific Publishing Co. Pte. Ltd, 2006, 107-116.

[29] Yunus A... Çengel, and John M... Cimbala. Fluid Mechanics: Fundamentals and Applications. McGraw-Hill Higher Education, 2010.

[30] V.M. Voloshuk, J.S. Sedunow, The processes of coagulation in dispersed systems, Nauka, Moscow, 1971.

[31] uepar LJ Clancy Publié dans 1991 ***Utile Livres, AF1600j Tridimensionnel Glisser Des modèles, Utilisateur Guide TECOUIPMNT.*** Aérodynamiq par Longman Scientifique &Technique ISBN 0582 988802.

32. Gao D, Chen W, Li H, Huc H (2017) flow around a circular circle with slit. J Exp Therm Fluid

Sci 82: 287−301 http://dx.doi.org/10.1016/j.expthermflusci.2016.11.025

33. Rahimi H, Tang X, Esmaeeli Y, Li M, Pourbakhtiar A (2020) Numerical simulation of flow around

two side-by-side circular circles at high Reynolds number. Int J Heat Technol 38(1): 77-91 https://doi.org/10.18280/ijht.380109

34. Zdravkovich MM (1987) The effect of interference between circular circles in cross flow. J

Fluids Struct 1(2): 239−261 https://doi.org/10.1016/S0889-9746(87)90355-0

35. Bensedira S, Abdellah el-hadj A, Semmar D, Ait-Messaoudene N (2018) Dynamic analysis of flow

around two side-by-side circles near a wall. J Sci Eng 43 (9): 4531−4540

https://doi.org/10.1007/s13369-017-2932-1

36. An B, Bergada JM, Mellibovsky F, Sang, WM, Xi C (2020) Numerical investigation on the flow

around a square circle with an upstream splitter plate at low reynolds numbers. J Meccanica 1037-1059 https://doi.org/10.1007/s11012-020-01148-8

37. Sohankar A, Rangraz E, Khodadadi M, Alam MM (2020) Fluid flow and heat transfer around single

38.INTERNATIONAL JOURNAL FOR NUMERICAL METHODS IN FLUIDS
Int. J. Numer. Meth. Fluids 2006; 52:801–821
Published online 15 March 2006 in Wiley InterScience (www.interscience.wiley.com). DOI: 10.1002/

39. Simulation of three-dimensional flow around a square circle at moderate Reynolds numbers

40. THE EFFECTS OF VORTEX SHEDDING ON THE AERODYNAMICPERFORMANCE OF AIRFOILS

41. Marouane Salhi article about simulation of a circle with slit

Sites internet :

http://www.lavionnaire.fr/AerodynDifProfils.php
http://tpeaerodynamisme.free.fr/analyse.htm
http://aerodynamique.chez.com/profil.html
http://www.tecquipment.com